LA-3774

LOS ALAMOS SCIENTIFIC LABORATORY
of the
University of California
LOS ALAMOS • NEW MEXICO

Symmetric Fission of a Two-Parameter Liquid Drop

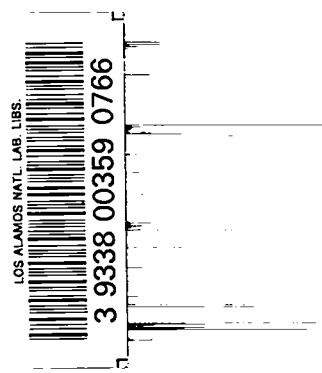

UNITED STATES
ATOMIC ENERGY COMMISSION
CONTRACT W-7405-ENG. 36

This report expresses the opinions of the author or authors and does not necessarily reflect the opinions or views of the Los Alamos Scientific Laboratory.

Printed in the United States of America. Available from Clearinghouse for Federal Scientific and Technical Information National Bureau of Standards, U. S. Department of Commerce Springfield, Virginia 22151

Price: Printed Copy $3.00; Microfiche $0.65

LA-3774
UC-34, PHYSICS
TID-4500

LOS ALAMOS SCIENTIFIC LABORATORY
of the
University of California
LOS ALAMOS • NEW MEXICO

Report written: August 1967
Report distributed: October 4, 1967

Symmetric Fission of a Two-Parameter Liquid Drop*

by

James N. P. Lawrence

*Also submitted as a thesis to the Faculty of the Graduate School of Vanderbilt University in partial fulfillment of the requirements for the degree of Doctor of Philosophy in Physics.

ACKNOWLEDGEMENTS

To Professor James J. Griffin (now with the University of Maryland) I express my deepest gratitude. While a staff member at Los Alamos Scientific Laboratory he suggested this study. His invaluable advice and constructive criticism over the past five years is greatly appreciated.

The continued interest and encouragement expressed by Professor William T. Pinkston of Vanderbilt University is also very much appreciated.

To my group leaders, Dean D. Meyer and Leo G. Chelius, for their consideration and understanding, my gratitude is expressed.

ABSTRACT

A review of fission theory is presented with attention focused on the liquid drop model. The contour of the liquid drop is described by a two-parameter equation in order that dynamic calculations could be performed. To obtain an indication of the accuracy to be expected in the dynamics, calculations of the fission-barrier energy and other saddle-point properties were made and compared with other studies. The equations of motion were derived under the assumptions of incompressibility and irrotational fluid flow. With the time dependent coordinates being the two shape parameters, a velocity potential is defined as a sum of terms, each of which satisfies Laplace's equation. The coefficients of each term are fixed by the boundary conditions and are seen to be functions of the shape parameters and their first derivatives. Lagrangian mechanics furnish the basis for the equations of motion. Tests of the theory are proposed and evaluated numerically using a two-term "velocity potential."

LIST OF TABLES

LIST OF ILLUSTRATIONS

Figure

Page

INTRODUCTION

This paper is divided into three major sections. The first section is a review of fission theory with emphasis on the applications of the liquid drop model. The remaining parts describe new work. By limiting the number of parameters which specify the surface shape of the drop, it becomes feasible to treat the fissioning liquid drop on a dynamic basis. This is considered in the third section. The second section deals with the static or potential energy aspect of symmetric fission. Comparisons are drawn with other more exact formulations to give an idea of the accuracies to be expected in the dynamic treatment.

I. REVIEW OF FISSION THEORY

The ideal way to theoretically treat nuclear fission, and for that matter all the problems of nuclear theory, would be to write an exact nuclear Hamiltonian, and solve the equations of motions. Such a Hamiltonian could be expressed as

$$H = \sum_{i=1}^{A} \frac{-\hbar^2}{2m_i} \nabla_i^2 + \frac{1}{2} \sum_{\substack{i \neq j \\ i=1 \\ j=1}}^{A} V_{i,j}$$

where the first term represents the kinetic energy of all A particles in the nucleus and the second term the potential energy of interaction. In this expression two body forces are implied, although there is no evidence to rule out the possibility of many body forces.

However, this approach is impractical, because the many body problem is incapable of exact solution at present and the two body potentials are not fully understood. One approach has been to simplify the problem by proposing to treat "nuclear matter".[1] By definition "nuclear matter" consists of a very large number of nucleons, so that surface effects can be ignored. Since such a large system of nucleons, half of which are protons and half neutrons, would be unstable because of Coulomb repulsion, these Coulomb forces are assumed to be turned off.

---

[1] J.S. Bell and E. J. Squires, Adv. in Physics, 10, 211 (1961).

Brueckner and Gammel[2] have performed calculations on such nuclear matter subjected to the two body potential which best conforms to the present state of knowledge. This potential consists of a hard core to a radius of 0.4 Fermi. Outside of the hard core it included an attractive central potential acting on even orbital angular momentum states (a Serber force), a tensor potential (designed to fit the quadrupole moment of the deuteron), and a spin-orbital angular momentum term (to account for high and low energy scattering data). The inclusion of the hard core prevented the use of ordinary perturbation techniques and tremendously increased the computational difficulties. However, their results, which should be applicable to the central region of naturally occurring heavy nuclei, were very close to the experimentally observed values of energy per nucleon and nuclear density.

These calculations demonstrate that, although the nucleons are subjected to strong two body forces, they behave dynamically as free particles in a degenerate Fermi gas. Weisskopf[3] recognized that this property is related to the operation of the exclusion principle for fermions. In a review article Eden[4] has indicated how the further developments in the many body problem have supplied the bases for the assumption of the independent particle shell and optical models, which have been so successful in accounting for nuclear data.

Historically, two models have been discussed in connection with the process of nuclear fission. These are the

---

[2]K. A. Brueckner and J. L. Gammel, Phys. Rev., 109, 1023 (1958).

[3]V. F. Weisskopf, Science, 113, 101 (1957).

[4]R. J. Eden, Nuclear Reactions,North Holland Pub. Co., Amsterdam, 1959.

independent particle shell model and the liquid drop model.

The Shell Model

The basic assumption of the shell model is that each nucleon moves in an average potential, which depends only on the coordinates of that nucleon. For a nucleus of A nucleons, this potential is considered to be the resultant of the effects of the other "A-1" nucleons. How such a potential, which seems at first sight to require a weak interaction between individual nucleons, can be compatible with the known strong interactions is a problem which only recently has been resolved in the manner indicated above. Upon inclusion of spin-orbit coupling properties, the shell model theory has accounted for the especially stable "magic number" nuclei with 2, 8, 20 , 28, 50, 82, 126 protons or neutrons.

One of the unexplained features of low energy nuclear fission of ^{235}U and ^{239}Pu is the well known asymmetry in mass division. Instead of the nucleus dividing into two equal parts, the mass and charge divide in about a 2 to 3 ratio in most cases. Mayer,[5] Wick,[6] and Meitner[7] observed that the number of neutrons in the fragments were near the "magic numbers" of 50 and 82, and suggested that shell effects might play a part in the explanation of asymmetric fission. However, Hill and Wheeler[8] contended that a nucleus in the process of fissioning could not "feel any

---

[5]M.G. Mayer, Phys. Rev., 74, 235 (1948).

[6]G. C. Wick, Phys. Rev., 76, 181 (1949).

[7]L. Meitner, Nature, 165, 561 (1950).

[8]D. L. Hill and J. A. Wheeler, Phys. Rev., 89, 1102 (1953).

potential shell structures in the not yet formed products", and thereby discount shell effects as an explanation of asymmetric fission. This observation of potential shell effects has arisen periodically whenever new experimental data on fission seem to indicate "magic number" tendencies. In any event, probably because of the enormous difficulties and lack of understanding, there have been no shell model calculations of the fission process.

The Nuclear Liquid Drop Model

In contrast with the shell model the description of fission falls quite naturally in the framework of the nuclear liquid drop model. However, even these calculations are extremely difficult, as is borne out by the lack of a complete treatment of the process.

The three primary assumptions which underlie the nuclear liquid drop model are:

1) The charge distribution is constant throughout the nucleus and has a sharp surface boundary.

2) The mass distribution is also uniform with a sharp surface.

3) The nuclear surface is characterized by uniform surface tension regardless of the distortion.

When the model was introduced, these assumptions were reasonable and made the model mathematically tractable. Hill[9] has summarized some of the experimental and theoretical data which now support these assumptions.

---

[9]D. L. Hill, Handbuch der Physik, 39, 178 (1957).

The most convincing evidence of uniform electrification is furnished by Hofstadter's[10] electron scattering experiments. It was demonstrated over a wide range of nuclei that the mean radius of the nuclear surface can be represented by the relation $R = r_0 A^{\frac{1}{3}}$. In these experiments $r_0 = 1.07$ Fermi and corresponds to the radius at which the charge density is 50% of that at the center of the nucleus. For nuclei with $A \geq 40$ the central region was found to be quite uniform. The thickness of the nuclear surface, as defined by the fall-off distance from 90% to 10% of the central charge density, was approximately constant at 2.4 Fermi from nucleus to nucleus. Other support of the first assumption is furnished by analyses of x-rays from mu mesonic atoms, x-ray and optical-spectra fine structure in isotopic shift, and the Coulomb energy differences in mirror nuclei.[9] All of these approaches confirm that the nuclear radius is proportional to $A^{\frac{1}{3}}$, but they give no indication of the diffuseness of the surface.

In contrast to the case of electron scattering, the experimental support of the second assumption is furnished primarily by scattering data on particles which interact appreciably with the nuclear constituents. Above 10 MeV the de Broglie wave length of the neutron is small compared to the nuclear dimensions, and the scattering cross section may reasonably be defined as the geometrical cross section $2\pi R^2$, where R is the nuclear radius. Early experiments[11] indicated that $R = 1.4A^{\frac{1}{3}}$ Fermi. More refined analyses must take into account nuclear transparency when the neutron energy exceeds

---

[10] R. Hofstadter, Science, 136, 1013 (1962).

[11] E. Amaldi, et al, Nuovo. Cim., 15, 203 (1946) and R. Sherr, Phys. Rev., 68, 240 (1945).

50 MeV. One such analysis[12] based on the "optical model", which assumes both a real and an imaginary nuclear potential, gave the nuclear radius as $R = (0.8 + 1.23A^{\frac{1}{3}})$ Fermi. High energy proton scattering has also been analyzed on the basis of the optical model with a special potential which has the surface thickness of the nucleus as a parameter.[13] The data was fitted to an $A^{\frac{1}{3}}$ radial dependence, and the nuclear "skin" thickness was found to be approximately the same as that indicated by the high energy electron scattering data. Further support for the $A^{\frac{1}{3}}$ radial dependence is obtained from alpha particle scattering and alpha decay data, although the constant of proportionality is somewhat larger.[9] In all these cases the radius measured is the nuclear force radius, which is assumed to be essentially the same as the mass radius.

The final assumption of constant uniform surface tension is reasonably supported for nearly spherical nuclei. The experimental findings of constant volume per nucleon and constant binding energy per nucleon (A>20) support the concept of saturation of nuclear forces. By analogy to molecular fluids the surface nucleons would experience unsaturated bonds, the manifestation of which would be a surface tension and sharply defined surface. For highly deformed nuclei, since experimental evidence is lacking, this remains the weakest assumption.

One of the early applications of the liquid drop model

---

[12]T. B. Taylor, Nuclear Scattering of High Energy Neutrons and the Optical Model, Thesis, Cornell University, 1954, AECU-2916.

[13]M. A. Malkenoff, et al. Phys. Rev., 106 793 (1957).

to the general field of nuclear theory was through the semi-empirical mass formula.[14] This formula accounts for the binding energy of nuclei in terms of saturated exchange forces whose effects are reduced by 1) incomplete saturation near the surface, 2) the Coulomb repulsion, 3) symmetry properties embodied in the exclusion principle, and 4) finite pairing energy differences between odd and even A nuclei.

The resulting formula with five empirically determined constants is useful for predicting mass and binding energies of any nucleus with $A \geq 40$, the Q value (energy release) of nuclear reactions involving changes in the mass number A, the energy considerations in alpha decay, and the energy release in nuclear fission. For example, in the case of symmetric fission, neglecting the small contribution from the pairing energy term, the energy release is

$$Q = M(Z,A) - 2M\left(\frac{Z}{2}, \frac{A}{2}\right) \simeq a_s A^{\frac{2}{3}} \left(1-2^{\frac{1}{3}}\right) + a_c \frac{Z^2}{A^{\frac{1}{3}}}\left(1-(\tfrac{1}{2})^{\frac{2}{3}}\right)$$

where $a_s = 17.97$ MeV and $a_c = 0.7183$ MeV.[15]
Using this result for thermal neutron fission of ^{235}U an energy release of about 185 MeV is obtained. Applying the Weizsäcker formula to asymmetric fission of this same isotope results in a smaller energy release, indicating that on an energy release basis symmetric fission would be expected.

---

[14] C. F. Weizsäcker, Z. Physik, 96, 431 (1935).

[15] A. E. S. Green, Rev. Mod. Phys., 30, 569 (1958).

The Classical Uniformly Charged Liquid Drop

Since the assumptions made about the nuclear liquid drop model are only approximately fulfilled, and since no quantum mechanical effects were included, the problem actually under consideration is that of fissioning of a uniformly charged liquid drop obeying the laws of classical hydrodynamics. An understanding of the physics of this relatively simple concept is by no means trivial (since no analytic solution is possible), but rather requires long and involved numerical calculations. Most of the treatments of the liquid drop model have considered just this classical problem, and as yet no complete solution has been obtained.

In order to discuss and treat the hydrodynamic motions of the classical charged liquid drop, several additional assumptions are made:

1) The fluid is taken to be absolutely incompressible. This does not actually constitute a new assumption, as it is embodied in the assumption of uniform mass distribution. However, the statement of incompressibility simplifies the equations of motion.

2) Irrotational flow is assumed. This assumption implies that all surface motions of the liquid drop will be perpendicular to the surface of the drop. Lord Kelvin first showed that "the irrotational motion of a liquid occupying a simply-connected region has less kinetic energy than any other motion consistent with the same boundary motion."[16] Since it is the

---

[16] H. Lamb, Hydrodynamics, Dover Publications, N. Y., 1945, p. 47.

intention of these studies to consider the lowest energy fission in a classical hydrodynamic sense, there would be no energy available for any other type of motion, such as rotation of the nuclear fluid.

3) The fluid is assumed to be nonviscous. By this assumption and that of incompressibility it is assured that no rotational or vortex motion will arise during the sequence of motion preceding fission.[17] For nuclear matter this assumption is not unwarranted, as multiple and random momentum transfers between the particles of a viscous liquid are largely prevented by the Pauli exclusion principle for nucleons.

4) For simplification of the computations it is further assumed that the motions of the fluid and the shapes of its surface are cylindrically symmetrical. A drop lacking azimuthal symmetry would be expected to require higher excitation for fission than a cylindrically symmetric drop.

Thus, the study of the nuclear liquid drop model is actually a study of a classical, incompressible, inviscid, uniformly charged liquid drop with a sharp surface and constant uniform surface tension, which is restricted to irrotational flow with cylindrical symmetry.

Since the fluid is incompressible, the mass density σ_m is constant. By definition of the divergence of mass flow, we have

$$\nabla \cdot \sigma_m \underline{v} = \sigma_m \nabla \cdot \underline{v} = 0$$

Since the flow is irrotational, curl $\underline{v} = 0$, and the velocity $\underline{v}$ is derivable from a scalar potential, as $\underline{v} = -\text{grad } \varphi$, and φ satisfies Laplace's equation, $\nabla^2 \varphi = 0$.

---

[17] L. M. Milne-Thomson, Theoretical Hydrodynamics, The Macmillan Co., N. Y. 1960, p. 82-85.

The kinetic energy (K.E.) of the liquid drop may be expressed as

$$T = \frac{\sigma_m}{2}\int_{Vol.} \underline{v} \cdot \underline{v}\, d\tau = \frac{\sigma_m}{2}\int_{Vol.} (-\nabla\varphi)^2\, d\tau$$

By the relation $\nabla \cdot \varphi\nabla\varphi = (\nabla\varphi)^2 + \varphi\nabla^2\varphi$, the K.E. can be converted to a surface integral,

$$T = \frac{\sigma_m}{2}\int_{Vol.} \nabla \cdot \varphi\nabla\varphi d\tau = \frac{\sigma_m}{2}\int_{S} \varphi\nabla\varphi \cdot \underline{dS}$$

Thus, if the velocity potential subject to the necessary boundary conditions can be found, an expression for the K. E. can be determined as a double integration.

Other investigators have not found such an attack to be convenient and Hill[18] has used a slightly different approach. He assumed that he knew the surface shape and velocities of each point on the surface at an initial time. Using the Eulerian equation of motion for a nonviscous fluid with mass density σ_m, subject to body forces $\underline{\chi}$ per unit volume and an external pressure p, he writes for the acceleration

$$\frac{d\underline{v}}{dt} = \frac{1}{\sigma_m}\left(\underline{\chi} - \text{grad } p\right)$$

Since the body forces are purely Coulombic, they are the negative gradient of the electrostatic potential V. Thus, the acceleration becomes

$$\frac{d\underline{v}}{dt} = -\frac{1}{\sigma_m}\nabla(V+p)$$

---

[18] D.L. Hill, Dynamical Analysis of Nuclear Fission, Doctorate Dissertation, Princeton University, 1951.

Upon taking the divergence of this equation, and using the assumptions of incompressibility ($\nabla \cdot \underline{v} = 0$) and irrotationality ($\nabla \times \underline{v} = 0$), the result may be expressed as

$$\nabla^2 \left(V + p + \tfrac{1}{2}\sigma_m v^2\right) = \nabla^2 H = 0$$

The functional qualtity H is expandable in a series expansion in solid harmonics. At an arbitrary point P on the surface, $H = H_s$ is determined from the calculable electrostatic potential V, the pressure $p = \vartheta\kappa$, and the known velocity, where ϑ is the surface energy (tension) and κ is the curvature of the surface at P. By minimizing the intergal $\int (H-H_s)^2 dS$ over the surface, the coefficients of the solid harmonic expansion of H can be obtained. This solution for H is substituted in the equation

$$\frac{d\underline{v}}{dt} = -\frac{1}{\sigma_m} \nabla \left(H - \tfrac{1}{2}\sigma_m v^2\right)$$

to obtain the acceleration. Having determined the acceleration and knowing the initial velocity, the velocity and position of the surface a short time later can be calculated. By this iterative procedure the surface shapes and kinetic energies can be calculated for incremental increases in time.

Previous investigations of the liquid drop model have primarily dealt with calculations of the potential energy for different values of Z^2/A. Supplementary to these calculations have been a few studies of the dynamics and kinetic energy. Some calculations of the spontaneous fission half life have also been performed.

Potential Energy Studies

The potential energy of a uniformly charged liquid drop consists of two classical terms: the surface energy (E_s) and

the Coulomb or electrostatic energy (E_c). By definition, the surface energy is simply

$$E_s = \vartheta \int_S dS$$

where ϑ is the surface energy (tension) per unit area, which is assumed constant, and whose numerical value is obtained from the semiempirical mass formula. The Coulomb energy is given by the integral

$$E_c = \tfrac{1}{2} \int_{Vol.} \sigma^2 \frac{d_{\tau_1} d_{\tau_2}}{r_{12}}$$

where σ is the charge density and r_{12} is distance between the two volume elements, d_{τ_1} and d_{τ_2}.

For a spherical configuration with a total charge Ze and radius $R_0 = r_0 A^{\frac{1}{3}}$, it is readily shown that $E_s^0 = 4\pi\vartheta r_0^2 A^{\frac{2}{3}}$ and $E_c^0 = \frac{3}{5} e^2 Z^2 / r_0 A^{\frac{1}{3}}$. Bohr and Wheeler[19] introduced the dimensionless fissionability parameter X, defined to be the charge squared over the product of ten times the surface tension and the volume of the sphere, that is

$$X = \frac{Z^2 e^2}{10\vartheta \frac{4}{3}\pi r_0^3 A} = \frac{E_c^0}{2E_s^0} = \frac{(Z^2/A)}{(Z^2/A)_{LIMITING}}$$

where $(Z^2/A)_{LIMITING} = \dfrac{40\pi\vartheta r_0^3}{3e^2}$.

Based on the ^{201}Tl fission threshold measurements,[20] the best value of $(Z^2/A)_{LIMITING} = 48.4$. This value is somewhat smaller than that obtained from Green's[15] values of r_0 and ϑ, but

---

[19] N. Bohr and J. A. Wheeler, Phys. Rev., 56, 426 (1939).

[20] D. S. Burnett, et al, Phys. Rev., 134, 5B B952 (1964).

should be more appropriate in that it is based on an isotope near the fission region, rather than on an average of properties throughout the range of nuclides.

Previous calculations of the potential energy have described the surface contour of the drop as a surface of revolution, the generator being expressed in terms of a radius as a function of the angular displacement θ from the z-axis. The most commonly used form has been

$$R(\theta) = \frac{R_0}{\lambda}\left(1 + \sum_{N=1}^{N} \alpha_N P_N(\cos\theta)\right) \qquad (1)$$

where R_0 is the radius of the spherical drop, λ is a constant to insure volume conservation, and α_N are the shape defining parameters. For shapes with reflection symmetry about the z=0 plane, only the even order Legendre polynomials are required. When asymmetric shapes are allowed, one of the odd parameters (usually α_1) may be eliminated (by expressing it in terms of the remaining N-1 parameters) in order to restrict movement of the center of mass of the drop.[21]

Small symmetric deviations from spherical may be specified by retaining only the second order term, i.e., $R = \mathcal{R}\left(1 + \alpha_2 P_2(\cos\theta)\right)$, where $\mathcal{R}$ is determined by the condition of constant volume, and α_2 is much less than unity. In Appendix I the surface and Coulomb energies for this case are

---

[21] W. J. Swiatecki, P/651, Proceedings of the Second United Nations International Conference on the Peaceful Uses of Atomic Energy, Geneva, 1958 (United Nations, Geneva, 1958).

shown to be

$$E_s = E_s^0 (1 + \tfrac{2}{5} \alpha_2^2 + \text{terms of higher power in } \alpha_2) \text{ and}$$

$$E_c = E_c^0 (1 - \tfrac{1}{5} \alpha_2^2 + \text{terms of higher power in } \alpha_2).$$

Thus, the deformation energy $\Delta E = (E_s - E_s^0) + (E_c - E_c^0)$ is

$$\Delta E \simeq \tfrac{1}{5} \alpha_2^2 \ (2E_s^0 - E_c^0) = \tfrac{2}{5} \alpha_2^2 E_s^0 (1 - X).$$

When $X<1$, the drop would be in a stable configuration requiring additional energy to cause fission. When $X>1$, the drop would be absolutely unstable, and fission would follow in the order of the period of a nuclear motion. In the case when $X=1$, the drop would be in a condition of unstable equilibrium, and any dynamical motion, such as the zero order quantum mechanical oscillations, could be sufficient impetus to initiate fission. By extrapolating the ratio of Z^2/A for naturally occuring and man-made isotopes to $(Z^2/A)_{LIMITING}$, the hypothetical element (for which $X=1$) would have $Z \simeq 130$ and $A \simeq 340$.[18] Heavy nuclei such as ^{239}Pu and ^{248}Cf have X values of 0.74 and 0.77, well below the value for unstable equilibrium. Thus, applications of the liquid drop model to actual nuclei require the use of fissionability parameters less than unity.

From the equation for ΔE given above, it is seen that the deformation energy increases as the distortion (α_2) increases. However, it was observed earlier through use of the semiempirical mass formula that energy is released in nuclear fission, implying a lower potential energy for the fission products than that possessed by the parent nucleus. Thus, as a fissioning drop or nucleus becomes more distorted, the potential energy must pass through a maximum value.

In order to consider the more distorted shapes on the

path to fission, one could retain more terms of equation (1). The electrostatic (E_c) and surface (E_s) energies have been calculated[21] explicitly by similar but more complicated techniques than those used in Appendix I.

Frankel and Metropolis[22] introduced the convention of expressing the surface and Coulomb energies in multiples of their respective energies for a spherical configuration. They also defined the total deformation energy (ξ) as a multiple of the surface energy of the sphere, i.e.,

$$\xi = \frac{\Delta E}{E_s{}^0} = B_s - 1 + 2X(B_c - 1)$$

where $B_s = E_s/E_s{}^0$ and $B_c = E_c/E_c{}^0$.

In Fig. 1 the Frankel-Metropolis graphical representation of ξ versus α_2, α_4 is reproduced. In this figure the saddle point of the deformation energy is readily visible. Mathematically, a saddle point is defined[23] to be a point for which the two first partial derivatives of a function f(x,y) are zero, but which is not a local maximum or a local minimum. If the second partial derivatives are continuous in a neighborhood of "p",

$\frac{\partial f}{\partial x} = \frac{\partial f}{\partial y} = 0$, and $\left(\frac{\partial^2 f}{\partial x \partial y}\right)^2 - \frac{\partial^2 f}{\partial x^2}\frac{\partial^2 f}{\partial y^2} > 0$ at "p", then "p" is a saddle point. For a hyperspace of more dimensions, the requirement that the first partial derivatives all equal zero

---

[22] S. Frankel and N. Metropolis, Phys. Rev., 72, 914 (1947).

[23] G. James and R. C. James, editors, Mathematical Dictionary, D. Van Nostrand Co., Princeton, N. J., 1959.

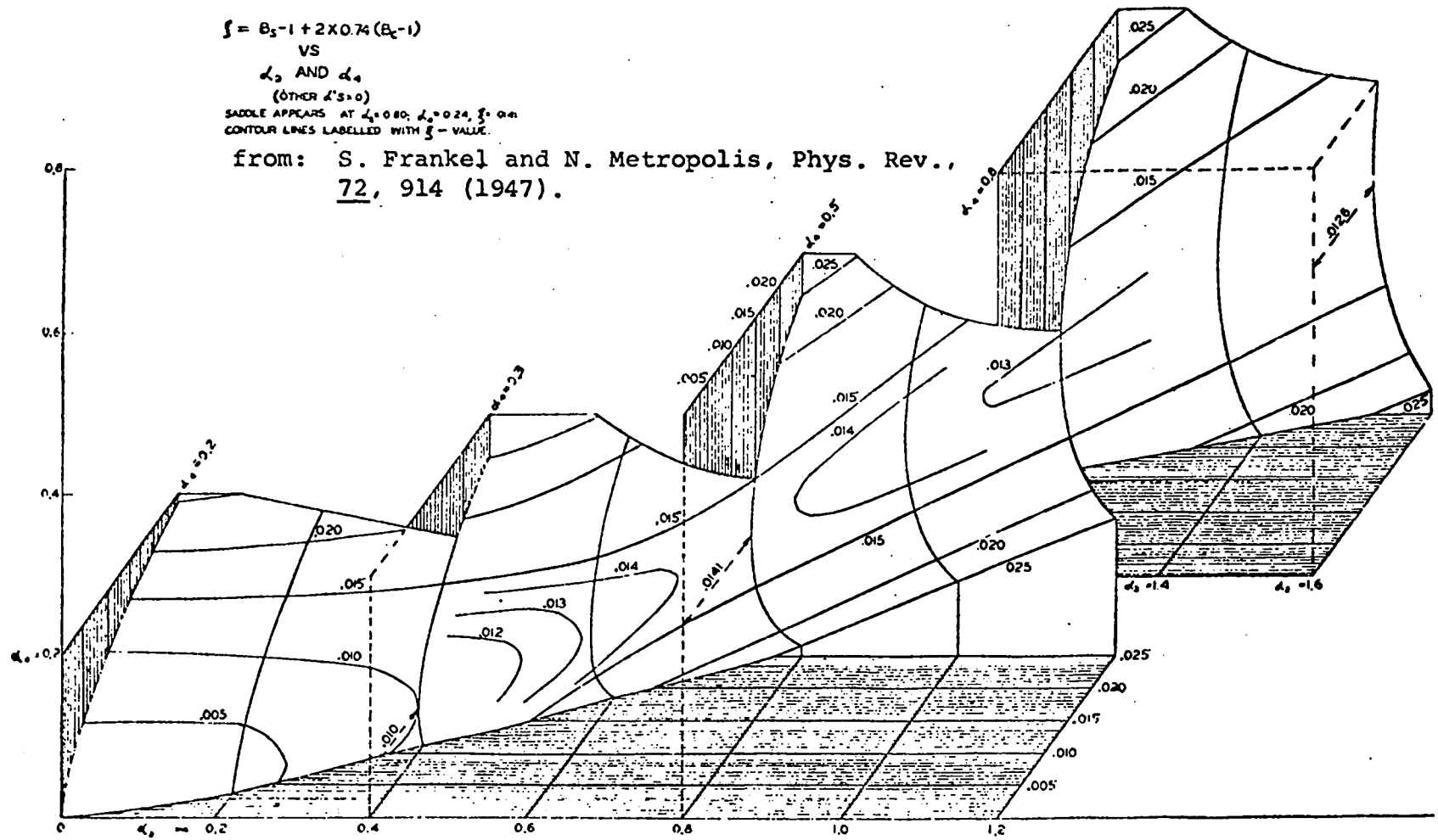

Fig. 1. Relative deformation energies as functions of α_2, α_4 for X=0.74

must still be met. A criteria for determining that such points do not represent a local maximum or a local minimum is given in Appendix II.

The physical significance of the saddle point is that it represents a condition of unstable equilibrium. A nucleus or drop could not remain at such a point, because the zero point quantum oscillations would force the nucleus to a more stable configuration on either side of the saddle point. In a simple case, to one side of the saddle would lie the spherical configuration and to the other, the path to binary fission, although Cohen and Swiatecki (C and S)[24] discussed other possible situations.

The interest in locating the saddle point is that the deformation energy at that point (for the simple case usually treated) is the minimum energy which must be supplied to the drop to induce fission with a high probability. Thus, the deformation energy at the saddle point is the classical fission threshold energy, a quantity which can be compared with experimental data.

Regardless of the number of parameters used to describe the surface of the liquid drop, the technique for locating the saddle point is the same in all cases. As indicated by the definition, such points are theoretically found by the solution of the simultaneous equations resulting from equating to zero the partial derivatives of the deformation energy with respect to each of the shape parameters. In the close neighborhood of the saddle point the contour of the deformation energy

---

[24]S. Cohen and W. J. Swiatecki, Ann. Phys., 19, 67 (1962).

hypersurface is approximated by a quadratic expression of the parameters. The quadratic approximation of a two parameter surface is simply a hyperbolic-paraboloid, for which the saddle is obvious. In practice, the saddle point is obtained by computing the deformation energy in a grid of points near the saddle and mathematically fitting the "best" quadratic approximation to these energies.

The most extensive calculations on the static aspects of fission have been performed by Swiatecki[25,26,21] and C and S[24,27] in a series of papers entitled "The Deformation Energy of a Charged Drop." In the latest of these papers,[27] α_N parameters through order 18 have been included. For fissionability parameter X from 0.30 to 1.0 (in steps of 0.02 units), the symmetric saddle shapes and the corresponding energies (total ξ, surface B_s, and Coulomb B_c), the moments of inertia about the two perpendicular axes, and the quadrupole moments were calculated. The instability of these saddle shapes for asymmetric as well as for symmetric distortions were investigated with the finding that asymmetric distortions did not become energetically favored for any X values larger than 0.39. It was also shown that for actual nuclei having low fission thresholds (i.e., nuclei for which $X \geq 0.7$) only two parameters, α_2 and α_4, had any appreciable effect on the fission threshold energy. C and S's saddle shapes[27] have been reproduced as Fig. 2. It can be seen that for $X \leq 0.7$ the saddle shapes were

---

[25] W. J. Swiatecki, Phys. Rev., 101, 651 (1956).

[26] W. J. Swiatecki, Phys., Rev., 104, 993 (1956).

[27] S. Cohen and W. J. Swiatecki, Ann. Phys., 22, 406 (1963).

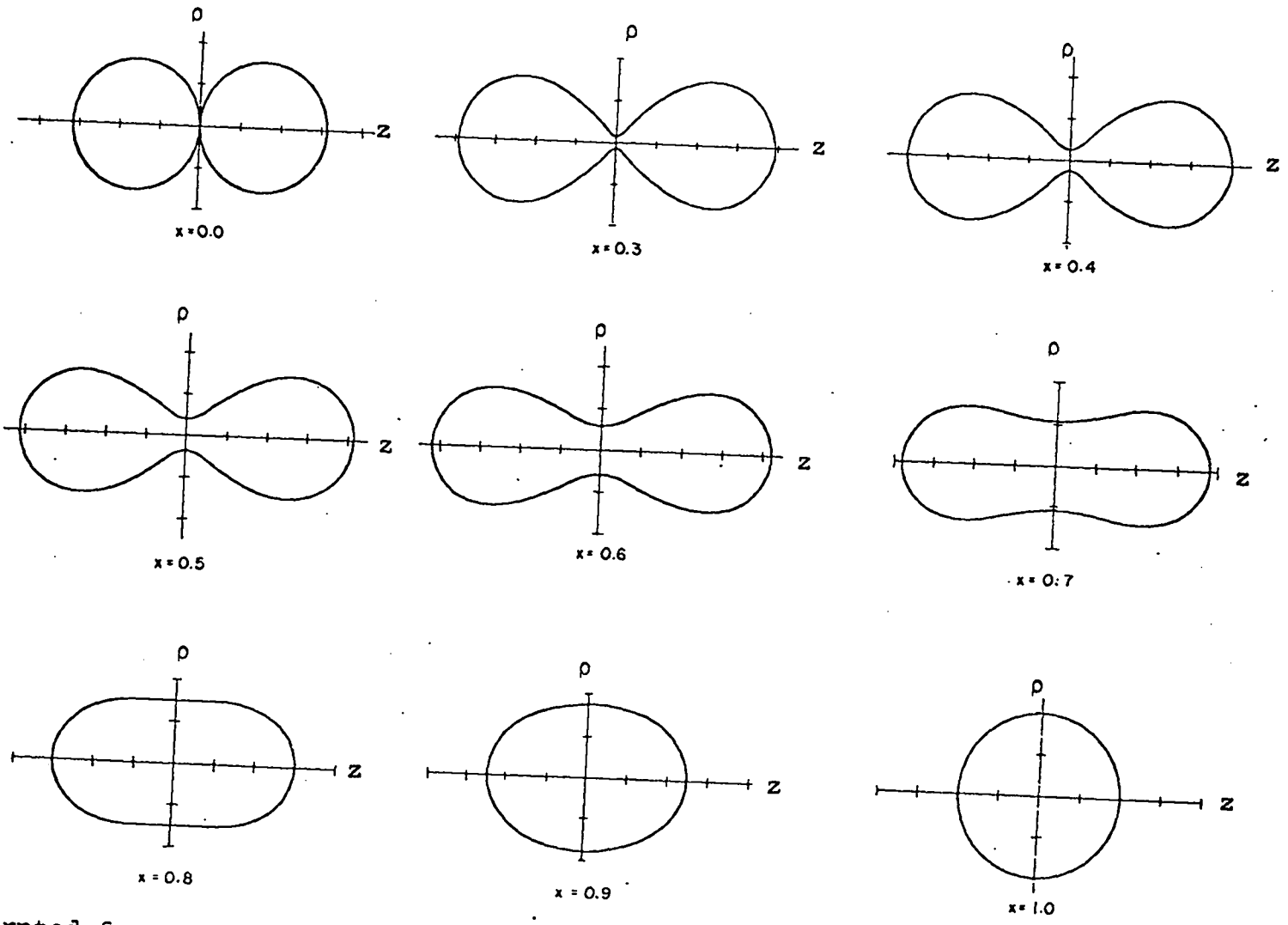

Excerpted from: S. Cohen and W. J. Swiatecki, Ann. Phys., 22, 406 (1963).

MUB-1222

Fig. 2. Saddle point shapes for various values of X

of the "dumbbell" variety and for larger values of X, they exhibited no necking-in, but were of the "cylindrical" form. The isotope ^{210}Po would have a fissionability parameter X=0.67, and would require fairly large excitation energies to be induced to fission. It was stressed that for actual nuclei, which have low fission threshold energies (i.e., when X>0.7), it "becomes impossible to predict with any confidence, on the basis of the properties of the saddle shapes, the relative sizes or even the number of fragments to be expected in the division".[27] C and S[27] concluded that to understand the fission process for X≥0.67 the dynamics of the process must be treated.

Work on the potential energy aspect of the liquid drop model was also pursued in the USSR by Struntinskii, et al,[28,29,30] Using a different approach requiring the solution of an integro-differential equation, he found the symmetric equilibrium (saddle point) shapes to have the same properties as those found by C and S.[27] In the last referenced paper[30] corrections for non-uniform surface tension and compressibility of the drop were included, but had small effects. Strutinskii also found that asymmetric saddle shapes had higher potential energy in accordance with earlier investigations. Concurring with Hill[18] and C and S,[27] Strutinskii also recognized that the problem of

---

[28]V. M. Strutinskii, JETP(USSR), 42, 1571 (1962).

[29]V. M. Strutinskii, N. Ya. Lyashchenko, and N. A. Popov, JETP(USSR), 43, 584 (1962).

[30]V. M. Strutinskii, Results of Calculations Based on the Liquid Drop Model of Nuclear Fission, Order of Lenin, Institute of Atomic Energy, Moscow, 1963.

They found significant corrections to the binding energy for spherical nuclei lighter than A=100, but negligible changes for nuclei with low fission thresholds (i.e., nuclei with A≥230). Hill and Wheeler[8] also discussed the possibility that nuclear polarizability and compressibility could split the symmetric saddle point into two asymmetric ones, but for a fissionability parameter near 0.7, they argue that the effect "does not offhand seem greater enough to lead to asymmetric critical forms for uranium." Since these refinements appear to lead only to minor corrections, further consideration of them is not planned in the present investigation.

Hill and Wheeler[8] did propose two mechanisms to account for the asymmetry of low energy fission. The first was attributed to a division of the individual particle states into "gerade" (wave function does not change sign on reflection in a plane perpendicular to the z-axis) and "ungerade" (wave function does change sign) classes. For approximately spherical shapes both classes of states are evenly filled. However, for large deformations the gerade states fill more rapidly, since "the one kind of wave function feels the pinch of the necking-off process more than the other". Thus, the total energy of the system could be lowered, and fission facilitated by "slippage" from gerade to ungerade states. For a completely symmetric system these slippages cannot occur, but could readily take place as an asymmetry develops. The second mechanism suggested was that the zero point asymmetric quantum oscillations would be amplified as the liquid drop system passed on toward the scission point after surmounting the symmetric fission barrier.

Dynamics of the Liquid Drop Model

In support of their second mechanism, Hill and Wheeler[8] attempted to follow the motion of a liquid drop at successive intervals of time by high speed computer techniques Even though the largest and fastest computer available at the time (1950) was used, they were forced to describe the surface of the drop by an eleven-point mesh, which proved too coarse for following the motion to the scission point. Nevertheless, they did find an amplification of the asymmetric oscillations and concluded that this might lead to a division into droplets of different mass.

A series of rather crude dynamical calculations were carried out by Inglis,[35] using a cylindrical approximation to the liquid drop shape. This work supported the previously mentioned result that small asymmetries become magnified. However, Inglis concluded that this effect was too small to account for asymmetric fission.

Nix[36,37,38] has undertaken a series of studies in the dynamical aspects of fission theory. In an extensive effort, he idealized the liquid drop as two spheroids, overlapping prior to and separated after fission.[36,37] He concluded from a consideration of the saddle point energies and shapes that this model would be most useful for discussing the fission of elements

---

[35]D. R. Inglis, Ann. Phys., 5, 106 (1958).

[36]J. R. Nix, "Estimates of Fission Fragment Kinetic Energy Distribution on the Basis of the Liquid Drop Model," UCRL-10695, (1963), unpublished.

[37]J. R. Nix, Nucl. Phys, 71, 1 (1965).

[38]J. R. Nix, "The Normal Modes of Oscillation of a Uniformly Charged Drop About its Saddle-Point Shape." UCRL-16786, (1966), unpublished.

lighter than radium.[37] In contrast to Hill's calculations, where the motion was followed from the saddle point shapes, Nix began his dynamic calculations at the scission point and traced the motion. He also calculated probability distributions for the total translation kinetic energies, mass, individual kinetic energies and individual angular momenta on the basis of this model. For the elements lighter than radium, the theory accounted for the magnitudes of the most probable values and widths of the experimental distributions of the total kinetic energy and fragment mass. He concluded that the limitation of the liquid drop model in his simplification of shapes (for the elements lighter than radium) were not yet in evidence to a severe degree. Taking a different approach, Nix[38] treated the subject where the drop shape was defined by equation (1). In the harmonic approximation he considered the normal modes of oscillation of such a drop about its saddle point shape, and calculated the frequencies and eigenvectors of these modes as functions of the fissionability parameter X. This study, he felt, was more applicable to the heavier elements in contrast to the aforementioned work . In general, experimental data concerning these modes of oscillation were not available for comparison.

A method of dynamic calculation of fission of an axially symmetric liquid drop was outlined by Kelson.[39] The basic assumption (accredited to Wheeler) is that the drop can be visualized as divided into a series of disks, and that the fluid initially in a disk always remains in that disk. When

---

[39]I. Kelson, Phys. Rev., 136, B1667 (1964).

the shape of the drop changes, the disk's expansion (or contraction) in radius is accompanied by a decrease (or increase respectively) in thickness in such a way that volume is preserved. Kelson's application of the technique was to the lighter elements where the saddle points shape exhibits a necking-in at the midpoint.

The problem of dynamics of the liquid drop model was further investigated with increased precision by Hill.[40] Retaining the assumptions outlined earlier in this paper, he considered only the single case of uranium-235 which has fissionability parameter X=0.72. Starting with a spherically shaped drop, and imposing only symmetric zero point harmonic oscillations (in the form of a second order Legendre polynomial, P_2), timewise integrations followed the motion of the model surface to the scission point. Just prior to symmetric division, a long neck developed, indicating that the fragments would possess considerable excitation energy.

Although this work was not continued, Hill[40] outlined a plan of attack, which he thought might account for asymmetric fission. He suggested superposing surface oscillations of the lowest symmetric and asymmetric orders (i.e., P_2 and P_3 oscillations) on the saddle point shapes, and restricting the motion such that the drop would proceed towards fission rather than towards the stable spherical configuration. This restriction of motion was merely to prevent excessive calculations on non-fissioning cases. The imposed oscillations were to be performed for different phase relations between the P_2 and P_3 modes to

---

[40]D. L. Hill, P/660, Proceedings of the Second United Nations International Conference on the Peaceful Uses of Atomic Energy, Geneva, 1958, United Nations, Geneva, 1958.

obtain a sampling of the possible division ratios. By a suitable averaging of a random selection of phase relations, Hill hoped to produce the experimentally observed fission fragment distribution. A by-product of these calculations would be the capability of computing the excitation energy of the fragments. Using this excitation energy in combination with the statistical model for evaporation of neutrons, he suggested that the neutron multiplicities could be predicted for comparison with experiment.

Spontaneous Fission

One of the possible decay modes for nuclei of $A \gtrsim 230$ is spontaneous fission, where the nucleus fissions in the absence of external excitations. Bohr and Wheeler[19] suggested that spontaneous fission was a quantum mechanical barrier penetration phenomena similar to alpha decay. By a natural extension of the alpha decay theory, they proposed[8] that the probability of spontaneous fission should be proportional to

$$\exp\left[-4\pi\int_{P_1}^{P_2}\left\{2\left(V(\alpha)-E\sum_i m_i\left(\frac{dx_i}{d\alpha}\right)^2\right\}^{\frac{1}{2}}d\alpha/h\right]\right.$$

$$= \exp\left[-\frac{\pi 2^{\frac{5}{2}}}{h}\int\left\{(\text{potential minus available energy})\right.\right.$$
$$\left.\left.\times\ (\text{effective mass})\right\}^{\frac{1}{2}}d(\text{distance})\right]$$

where x_i is the coordinate of each elementary particle, m_i, expressed in terms of the parameter α, which specifies the path of the system in configuration space. The integral extends from point P_1 of stable equilibrium over the fission saddle point and down on a path of steepest descent to the point P_2 where the classical value of kinetic energy, E - V,

is again zero. Bohr and Wheeler made a very crude estimate of the spontaneous fission half-life for an A=239 nucleus. The obtained value of 10^{22} years is considerably larger than measured half-lives for such nuclei which vary from 10^{12} to 10^{18} years.

Foland and Present[41] have used a modification of the formula given above to calculate the penetration factor for spontaneous fission. The potential and kinetic energies of the liquid drop were calculated, using only the second order Legendre polynomial term in their expansions. From their expression for the kinetic energy a representation of the effective mass was obtained as a function of the single parameter describing the surface of the drop. It was realized that the use of such a low-order approximation would preclude the possibility of an accurate half-life determination. However, they did find from their calculation that an increase of 1.0 Mev in the barrier height would correspond to a $10^{3.7}$ increase in half-life. This was thought significant, since it agreed well with the empirical deduction of Swiatecki.[42]

Nix[38] has applied his study of the normal modes of oscillation to the penetration of the fission barrier. However, he obtained only order of magnitude agreement and stated that "the data (experimental) are at present not sufficiently accurate to provide a sensitive test of the theory."

---

[41]W. D. Foland and R. D. Present, Phys. Rev., 113, 613 (1959).

[42]W J. Swiatecki, Phys Rev., 100, 937 (1955).

II. STATICS AND POTENTIAL ENERGY CONSIDERATIONS

Choice of Units

For computational simplicity, it is desirable to use dimensionless quantities. This is accomplished by adopting a "natural" set of physical units and expressing all normally dimensioned quantities as multiples thereof.

Considering the liquid drop to consist of A nucleons, of which Z are protons, the fundamental mass unit M_0 is taken to be: $M_0 = m_0 A$, where $m_0 = 1.66 \times 10^{-24}$ (reciprocal of Avogadro's number) grams/nucleon.

Consistent with the Frankel and Metropolis' convention for defining the relative deformation energy, the fundamental unit of energy is chosen to be the surface energy of the spherical nucleus, i.e., $E_s^0 = \alpha_s A^{\frac{2}{3}}$ where $\alpha_s = 17.97$ MeV.[15]

The radius of the spherical nucleus, R_0, is selected as the fundamental unit of length, and is proportional to the cube root of the number of nucleons, i.e., $R_0 = r_0 A^{\frac{1}{3}}$. The value of r_0 is determined through the definition of the fissionability parameter X, consistent with the value of $(Z^2/A)_{LIMITING}$ as found by Burnett, et al,[20] from a measurement of the fission barrier of ^{201}Tl. The merit of this method of defining r_0 is its direct relation to the fission process.

The fissionability parameter X has previously been defined as: 1) the ratio of the Coulomb energy E_c^0 of a spherical, uniformly charged liquid drop divided by twice the surface energy E_s^0 of that drop, and 2) the ratio of Z^2/A for the drop under consideration divided by $(Z^2/A)_{LIMITING} = 48.4$.[20] The spherical

Coulomb energy is $E_c^0 = \frac{3}{5}e^2Z^2/R_0$, where e is the electrostatic charge of the electron. Manipulation of these relations gives: $r_0 = 1.16_3 \times 10^{-13}$ cm.

Having defined the fundamental units of mass, length, and energy, time is no longer a fundamental unit. However, it becomes convenient to define a "basic" time unit, T_0, such that the kinetic energy is normally expressed in multiples of E_s^0. This is accomplished by setting:

$$T_0 = r_0\sqrt{\frac{3m_0A}{\alpha_s}} = 0.482_4 \times 10^{-22}A^{\frac{1}{2}} \text{ seconds.}$$

Parameter Choice

The surface of the symmetric liquid drop in the present study is to be designated by only two free parameters. While such a system would probably not provide as accurate results as a more numerous set of parameters, the choice of a two-parameter set should facilitate calculations.

If one examines C and S's saddle shapes[27] in Fig. 2 (discounting the case for X=0, which is uninteresting for application to nuclear fission since it corresponds to a droplet with no electric charge), three features emerge. All of the indicated shapes have 1) at most two lobes, 2) zero slopes at the median plane (z=0), and, 3) infinite slopes at the extreme values of z. These general properties which C and S obtained with a ten-parameter expansion can be reproduced by a simple three-parameter description of the surface. One such three-parameter description is given by the dimensionless equation

$$\rho_0^2 = c + a_2z^2 + a_4z^4 \qquad (2)$$

where z is the distance from the median plane and ρ_0 is the

distance from the z-axis. While the variables in equation (2) are dimensionless, the dimensionality problems are treated Appendix III. To describe the surface of the drop, this equation is rotated about the z-axis. The shapes obtained are necessarily symmetric about the z=0 plane. Of the three parameters a_2, a_4 and c, only c has an obvious graphical interpretation, i.e., the $\sqrt{c}$ is the distance of the surface from the z-axis at the median plane.

The assumption of an incompressible fluid requires that, regardless of the distortion undergone, the volume of the liquid drop must remain constant. This restraint serves to fix one of the three parameters, leaving only two parameters free for designating the shape of the drop. C and S[27] used the same restraint to obtain their nine free-parameter system.

In the computer calculations the parameter c was chosen to be fixed by the condition of volume preservation. A subroutine, CALCZO, was prepared for determining the value of the parameter c and the intercept, z_0, of the surface along the positive z-axis. The intercept, z_0, applies only to prescission shapes and is used as the limit of integration in computing the Coulomb and surface energies and other saddle point properties. One equation relating c and z_0 is equation (2) when $\rho_0=0$. The second equation is obtained by setting the volume of the surface of revolution from $-z_0$ to z_0 equal to the volume of a unit sphere. These equations combine to give:

$$f(z_0) = a_2 z_0^3 + \tfrac{6}{5} a_4 z_0^5 + 1 = 0 \qquad (3)$$

Because of the physical interpretation of z_0, only the smallest positive real roots of equation (3) are acceptable. If one wished to examine this model after scission, then the integrated

volume must be modified, and two values of the intercept must be determined.

At the scission point the value of ρ becomes zero for $z=0$, but the integration from $-z_0$ to z_0 does not extend over any imaginary values of ρ. Setting $c=0$ (which represents scission) in the two relations used to determine equation (3), and eliminating z_0 between them, the scission line in a_2-a_4 space is seen to be

$$a_4 = -\sqrt[3]{.04a_2^5} \qquad (4)$$

This expression was used to limit the range of the parameters a_2 and a_4 to prescission values.

Cross sections of some of the shapes obtainable with the chosen parameter set under the condition of constant volume are shown in Fig. 3. While no shapes with $a_2<-1.0$ or for $a_4>0$ are shown, search programs for the saddle point in a_2-a_4 space did include the possibility of such values.

Surface and Coulomb Energies

The Frankel and Metropolis[22] convention of using the relative surface and Coulomb energies was adopted. In addition, these energies were further normalized to a sphere of unit radius. These procedures made possible direct comparisons not only with their work but also with that of C and S.[27]

For the shapes described by equation (2), the relative surface energy is given by the integral

$$B_s = \frac{E_s}{E_{s0}} = z_0 \int_0^1 \left\{ 4a_4 z_0^6 x^6 + (4a_4 a_2 + a_4) z_0^4 x^4 + (a_2^2 + a_2) z_0^2 x^2 + c \right\}^{\frac{1}{2}} dx \qquad (5)$$

This equation is developed in Appendix IV. With arbitrary values of a_2 and a_4, equation (5) belongs to a class of integrals

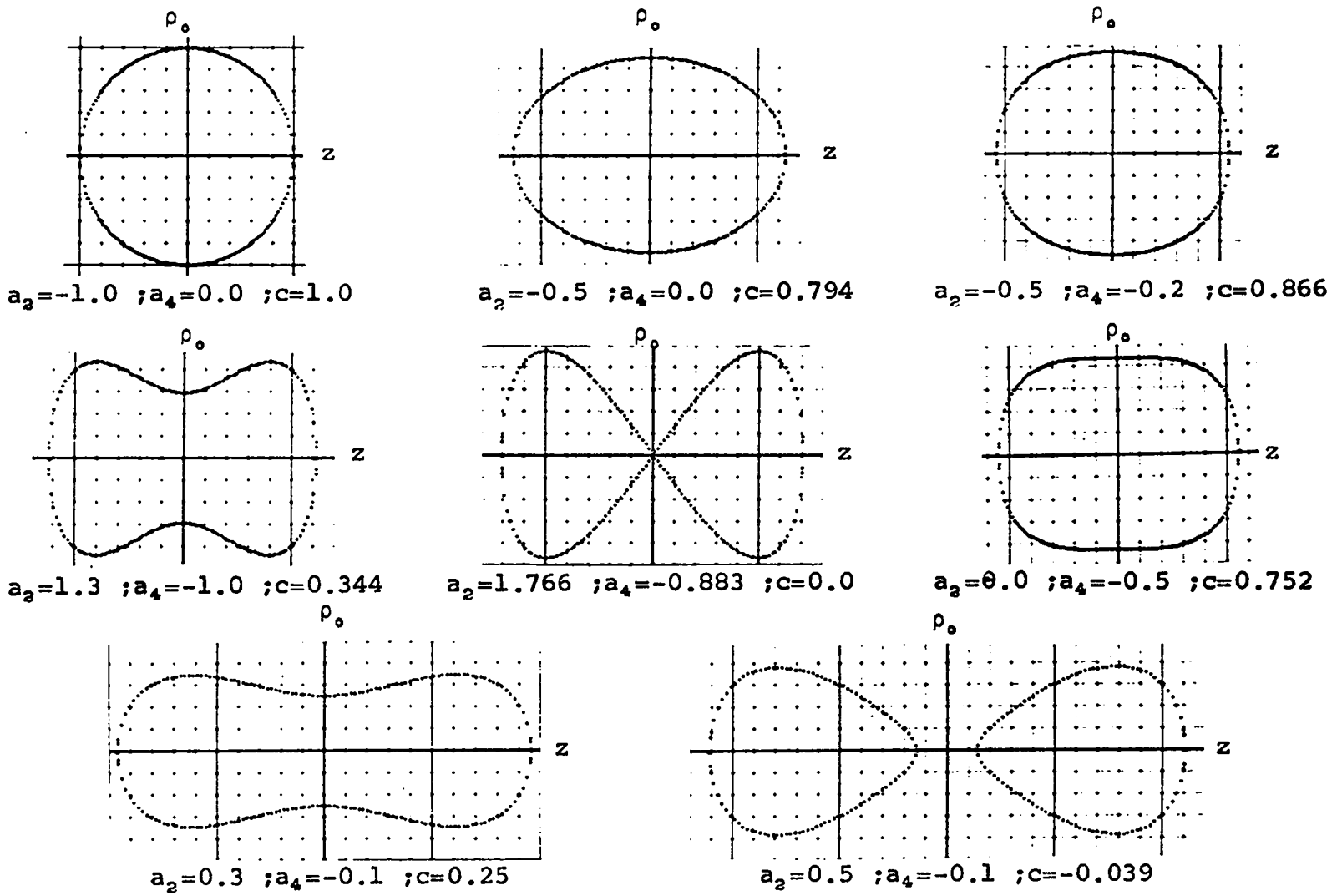

Fig. 3. Drop contours described by the function $\rho_0^2 = c + a_2 z^2 + a_4 z^4$ with volume preservation.

which cannot be evaluated in closed form in terms of ordinary functions.[43] Therefore, it was necessary to perform the integration numerically by computer techniques.

In Appendix V the relative Coulomb energy of the uniformly charged volume of revolution is shown to be

$$B_c = 120 z_0^5 \int_0^1 \rho_1^2 dz \int_0^1 z \rho_2^2 dy \int_0^1 \frac{\sin^2 \pi x dx}{z(1-y)+\sqrt{z^2(1-y)^2+\rho_1^2+\rho_2^2-2\rho_1\rho_2\cos\pi x}} \quad (6)$$

where

$$\rho_1^2 = 4a_4 z_0^2 z^4 - 8a_4 z_0^2 z^3 + (6a_4 z_0^2+a_2) z^2 - (2a_4 z_0^2+a_2) z$$

$$\rho_2^2 = 4a_4 z_0^2 z^4 y^4 - 8a_4 z_0^2 z^3 y^3 + (6a_4 z_0^2+a_2) z^2 y^2 - (2a_4 z_0^2+a_2) zy.$$

This integral was also evaluated on a computer.

Assuming that the integration technique suitable for the triple integral B_c would be more than adequate for B_s, consideration was given to the numerical integration of equation (6). Attempts on an IBM 7090 computer to integrate equation (6) by breaking each integral into evenly spaced intervals failed to give satisfactory results for a sphere.

Other integration techniques were investigated and Gauss quadrature was chosen when it was found to have a theoretical accuracy of 2N evaluation points when only N points were used. Since the three integrals of equation (6) have unit weighting functions, Legendre Gauss quadrature proved the most appropriate.

In Gauss quadrature the integrand is evaluated at each of the zeros of an nth-order Legendre polynomial (normalized to the interval of integration), multiplied by weighting factors which depend only on the particular zero of the Legendre polynomial,

---

[43] R. Courant, Differential and Integral Calculus, 2nd ed. Vol. 1, (Interscience Publishers, Inc., New York, 1937) p. 242.

and the result is summed for all "n" zeros. In effect, this procedure expands the integrand in terms of Legendre polynomials of order n-1. Thus, the higher the order used in the numerical integration, the more accurate the results; but also the more time required for the calculation.

After modifying the zeros and weights for order 2 through 16 Legendre polynomials[44] to correspond to the appropriate interval of integration, equation (6) was programmed for the IBM 7090. For a sphere the exact relative Coulomb energy is unity, and for spheroids the exact energy is also calculable. These shapes provide a check on the absolute accuracy of the Gauss quadrature calculations. The Gauss quadrature results were also compared with those obtained by C and S[27] and with those of Beringer[45] who claimed to have calculated the Coulomb self-energy of axial figures "accurate enough for studies in liquid-drop nuclear fission."

These comparisons are included in Table I, where it is seen that the absolute accuracy is correct to about 1 part in 10^5. While this is about a factor of 10 better than Beringer's results, it is less accurate than C and S's results.

The inaccuracies noted could arise in two ways: 1) they could be the result of too low an order Gauss quadrature, or 2) they could be accumulative results of the inherent inaccuracies during the summation in the Gauss quadrature. On the IBM 7090, sines, cosines, and square roots are computed only to five units in the eighth significant digit, and the summation of some 4000 terms could result in errors in the fifth significant digit.

---

[44]A. N. Lowan, N. Davids, and A. Levenson, Bulletin of Am. Math. Soc., 48, 739 (1942).

[45]R. Beringer, Phys. Rev., 131, 1402 (1963).

TABLE I. CALCULATED VALUES OF RELATIVE COULOMB AND SURFACE ENERGIES OF A SPHERE AND TWO SPHEROIDS, WITH COMPARABLE FIGURES FOR OTHER INVESTIGATORS.

Machine or Author	Gauss Order or Number of Grid Points	Sphere	Spheroid Major axis = 1 Minor axis = .7	Spheroid Major axis = 1 Minor axis = .5
		Relative Coulomb Energy B_c		
STRETCH	Exact[a]	1.000 000 000	0.988 678 870	0.957 975 926
7090	16	0.999 990 396	0.988 669 217	0.957 967 214
STRETCH	16	0.999 999 708	0.988 678 578	0.957 975 557
STRETCH	96	0.999 999 999	0.988 678 869	0.957 975 925
C and S[b]	41	0.999 998 2	0.988 676 6	- -
C and S[b]	61	0.999 999 3	0.988 678 4	- -
C and S[b]	81	- -	0.988 678 6	- -
Beringer[c]	40	0.999 828	- -	0.957 662
		Relative Surface Energy B_s		
STRETCH	Exact[a]	1.000 000 000	1.021 383 583	1.076 728 262
STRETCH	16	1.000 000 000	1.021 383 583	1.076 728 262
STRETCH	96	1.000 000 000	1.021 383 583	1.076 728 262

[a] "Exact means that the closed algebraic expressions for the energies were evaluated, while the numbers designate numerical integrations.

[b] Reference 27

[c] Reference 40

The second possible source of error was reduced by performing the calculation on the STRETCH (IBM 7030) computer. On this computer, sines, cosines, and square roots are calculated accurately to 14 decimal digits. Thus, even with a 10,000-fold accumulative error, the final results of 16th order Gauss quadrature should be accurate to the ninth decimal digit.

Zeros and weighting coefficients for 96 order Gauss quadrature were found,[46] and programmed for STRETCH. The results for 16th order Gauss quadrature on STRETCH were now slightly improved over C and S's values. Ninety-six order Gauss quadrature also showed significant improvement over the 16th order Gauss quadrature. However, each 96 order triple integral required about five minutes computer time, which is prohibitive for the many calculations required to determine the saddle points. Sixteen order Gauss required only a few seconds computer time.

Since the Coulomb energy calculations by 16 order Gauss quadrature were slightly more accurate than any known to be reported in the literature, it was decided to use 16 order Gauss quadrature on the STRETCH computer for all integrations. Use of a CDC 6600 computer which has since proved more readily available has given the same results as those quoted for STRETCH. The computations of B_s were also of acceptable accuracy. The results for B_c and B_s for the sphere and two spheroids are given in Table I.

---

[46] P. Davis and P. Rabinowitz, J. of Research on N.B.S., 60, 613 (1958).

Deformation Energy Saddle Point Calculations

The relative deformation energy (ξ) by the Frankel-Metropolis[32] convention is

$$\xi = (B_s - 1) + 2X(B_c - 1) \qquad (7)$$

where X is the fissionability parameter. The saddle point is represented by a pair of values (a_{2_s}, a_{4_s}) of the parameters which define the shape of the liquid drop.

For X=1 no true "saddle" exists. In the parameter space of this study the spherical configuration is given by the parameter point (-1,0). A change in "a_2" to a less negative value leads to a prolate spheroid deformation and a decrease in the deformation energy. A change in "a_2" to a more negative value or any change in "a_4" results in an increase in deformation energy. Numerical calculations have established the validity of these statements. Thus, for X=1 there is a zero classical fission threshold, but the point representing the sphere is only an unstable point, not a saddle point.

The C and S[37] calculations determined several liquid drop properties of the saddle points for X=0.98 to X=0.30 for differences in X of 0.02. This investigation covered the same range of X.

Prior to beginning the computer search for the saddle points, a model was constructed of the relative deformation energy for X=0.7. The approximate saddle point (a_{2_s}= 0.25, a_{4_s}= 0.10) observed from this model served as a verification of later computer calculations. It was also seen from the model that for similar changes in deformation energy the variations in the "a_4" parameter should be less than those in "a_2". It was arbitrarily decided that the magnitude of the "a_4" variations would be one-tenth of the "a_2" variations in the computer search.

The computational method of locating a saddle point is outlined in Part I. For a two-parameter space, the deformation energy in the vicinity of the saddle point may be expressed as:

$$\xi(a_2, a_4) = c_1 + c_2 a_4 + c_3 a_2 + c_4 a_4^2 + c_5 a_2 a_4 + c_6 a_2^2 \quad (8)$$

where the pair (a_2, a_4) represents a point in the parameter space and $(c_j, j=1,6)$ are the coefficients defining the hyperbolic paraboloid. The partial derivatives with respect to "a_2" and "a_4" are taken and equated to zero. The solution of these two simultaneous equations for "a_2" and "a_4" in terms of the c_j's is the critical point:

$$\left.\begin{aligned} a_{2s} &= \frac{c_2 c_5 - 2c_3 c_4}{4c_4 c_6 - c_5^2} \\ a_{4s} &= \frac{c_3 c_5 - 2c_2 c_6}{4c_4 c_6 - c_5^2} \end{aligned}\right\} \quad (9)$$

This point is a saddle point, if $c_5^2 - 4c_4 c_6 > 0$. Thus, the problem simply becomes one of approximating the actual function ξ by equation (8) to a sufficient degree of accuracy.

An initial estimate (a_2, a_4) is made of the saddle point. For X=0.98 an initial estimate corresponding to the spherical shape was attempted. This converged on itself, and indicated a minimum rather than a saddle point. A second initial estimate, equal to one-fifteenth the distance (from spherical) of the approximate saddle found for X=0.7, was successful in locating a saddle for X=0.98. As X was reduced by increments of 0.02, initial estimates for the saddle points were the actual saddle points for the next larger value of X.

A quantity defined as the original grid size (GRDSZO) was set at 0.04 units. For the first attempt to locate the

saddle point the grid size (GRDSZ) was set equal to the original grid size. A pentagonal array about the initial estimate provided the remaining five points needed to fit equation (8). The coordinates of these six-point sets were:

$A2(1) = a_{2_1}$	$A4(1) = a_{4_1}$
$A2(2) = a_{2_1} + 0.95$ GRDSZ	$A4(2) = a_{4_1} + 0.031$ GRDSZ
$A2(3) = a_{2_1} + 0.59$ GRDSZ	$A4(3) = a_{4_1} - 0.08$ GRDSZ
$A2(4) = a_{2_1} - 0.60$ GRDSZ	$A4(4) = a_{4_1} - 0.08$ GRDSZ
$A2(5) = a_{2_1} - 0.93$ GRDSZ	$A4(5) = a_{4_1} + 0.035$ GRDSZ
$A2(6) = a_{2_1}$	$A4(6) = a_{4_1} + 0.10$ GRDSZ

The deformation energy was calculated for each of these point sets. A matrix solution of the six simultaneous equations provided the coefficients ($c_j, j=1,6$) in equation (8), and the new estimate of the saddle ($a_{2_s}\, a_{4_s}$) was provided by equation (9).

Three convergence conditions were imposed:

$$\Delta a_2 = | a_{2_1} - a_{2_s} | \leq 0.0004$$

$$\Delta a_4 = | a_{4_1} - a_{4_s} | \leq 0.00004 \qquad (10)$$

$$\Delta \xi = | \xi_1 - \xi_s | \leq 0.00000005$$

where ξ_1 and ξ_s are the deformation energy of the point (a_{2_1}, a_{4_1}) and the point (a_{2_s}, a_{4_s}) respectively. If any of these conditions were not met, the results (a_{2_s}, a_{4_s}) just obtained were used as the new initial estimate (a_{2_1}, a_{4_1}) and the process repeated.

For a constant grid size the procedure detailed above can lead to erroneous results when deviations from the parabolic are large compared to the grid size. To eliminate this difficulty, a procedure was instituted to reduce the grid size, when

the current grid size (GRDSZ) exceeded the value:

$$DIST = \sqrt{100\ (\Delta a_4)^2 + (\Delta a_3)^2}$$

The grid was reduced by dividing the original grid size (GRDSZO=0.04) by successively larger Fibonacci numbers (F_k for $k \geq 2$). The Fibonacci sequence of numbers is defined as

$$F_o = F_1 = 1$$

$$F_k = F_{k-1} + F_{k-2} \qquad k = 2, 3 \ldots\ldots\ldots\ldots$$

Just how economical such a scheme is for reducing mesh size is not known; however, convergence to meet the requirements of equation (10) was accomplished in all cases by the tenth such reduction.

Grid size reductions were initiated by two other conditions. When any of the grid points exceeded the scission line, as defined by equation (4), a reduction was accomplished. This occurred only for original size grids (GRDSZ = GRDSZO = 0.04), since the first reduction was sufficient in all cases to correct this condition. The second condition came about when the convergence conditions [equation (10)] were met the <u>first</u> time for each value of X. In this case, a reduction by $1/F_{10} = 1/89$ was performed, and the surface refitted. If a reduction by F_{10} had already been performed, then the reduction was by the next larger Fibonacci number. The purpose of this procedure was to provide further assurance that the computational determination of the saddle point was correct, and not inaccurate because of too large a search grid.

Results of Saddle Point Calculation

The primary purpose of the saddle point calculations was

to determine how well the chosen two-parameter system would describe the actual liquid drop properties. Assuming that the nine-parameter work by C and S[27] comes the closest of any known studies to the actual physical situation, comparisons of the results of this two-parameter study with those of C and S appeared appropriate.

In addition to the properties already treated, C and S[27] made saddle point calculations of the moments of inertia about different axes and the quadrupole moment. For the (a_2, a_4) parameter space the moment of inertia (relative to a sphere of the same volume) about the axis of symmetry is:

$$I_{\parallel} = \frac{15}{8}\left\{\frac{a_4^2 z_0^9}{9} + \frac{2a_2 a_4 z_0^7}{7} + \frac{(a_2^2+a_4 c) z_0^5}{5} + \frac{2a_2 c z_0^3}{3} + c^2 z_0\right\}$$

The relative moment of inertia about an axis at right angles to the symmetry axis is:

$$I_{\perp} = \frac{15}{8}\left\{\frac{a_4^2 z_0^9}{18} + \frac{(2a_4+a_2 a_4) z_0^7}{7} + \frac{(4a_2+a_2^2+2a_4 c) z_0^5}{10} + \frac{(a_2 c+2c) z_0^3}{3} + \frac{c^2 z_0}{2}\right\}$$

C and S[27] also calculated the inverse of the effective moment of inertia which is defined as:

$$\tau = 1/I_{\parallel} - 1/I_{\perp}$$

Using the C and S[27] definition of the quadrupole moment one obtains:

$$Q = 4\pi\left\{\frac{-a_4^2 z_0^9}{36} + \frac{(2a_4-a_2 a_4) z_0^7}{14} + \frac{(4a_2-a_2^2-2a_4 c) z_0^5}{20} + \frac{(2c-a_2 c) z_0^3}{6} - \frac{c^2 z_0}{4}\right\}$$

The saddle point values of these properties are obtained by substituting the saddle point values of a_2, a_4, c, and z_0. The development of the expressions for $I_{\parallel}$, $I_{\perp}$ and Q is outlined in Appendix VI.

The saddle point values of "a_3" and "a_4" are given in Table II. This information is plotted in Fig. 4 along with the scission line. It is seen that the calculated saddle points approach the scission line as the fissionability parameter decreases below X = 0.60, but a significant separation still exists at X = 0.30 (the right most point plotted). Table III contains the calculated saddle point properties.

The results of this study have been graphically compared with C and S^{27} in Figs. 5 through 11. In all these figures the fissionability parameter X is plotted along the abscissa, and the various saddle point properties along the ordinate. The results of this study compare favorably from X = 0.98 to about 0.70. The reason for this is seen in Figs. 12 through 18 in which are plotted the contours of the saddle point configurations for selected values of X. The C and S^{27} contours are indicated at specific points, and to about X = 0.7 they fall extremely close to the shapes derived in this study.

TABLE II. SADDLE POINT VALUES OF THE PARAMETERS a_2 AND a_4

X	a_4	a_2
.98	-.00610	-.8643
.96	-.01933	-.7380
.94	-.03477	-.6211
.92	-.04988	-.5134
.90	-.06341	-.4142
.88	-.07483	-.3231
.86	-.08398	-.2393
.84	-.09093	-.1622
.82	-.09581	-.0912
.80	-.09881	-.0256
.78	-.10011	.0353
.76	-.09987	.0922
.74	-.09822	.1458
.72	-.09526	.1970
.70	-.09122	.2469
.68	-.08742	.2945
.66	-.08675	.3327
.64	-.08886	.3605
.62	-.09211	.3829
.60	-.09584	.4025
.58	-.09979	.4203
.56	-.10388	.4370
.54	-.10805	.4529
.52	-.11229	.4682
.50	-.11657	.4829
.48	-.12089	.4973
.46	-.12523	.5112
.44	-.12963	.5249
.42	-.13409	.5384
.40	-.13855	.5516
.38	-.14306	.5647
.36	-.14760	.5776
.34	-.15220	.5903
.32	-.15682	.6029
.30	-.16150	.6154

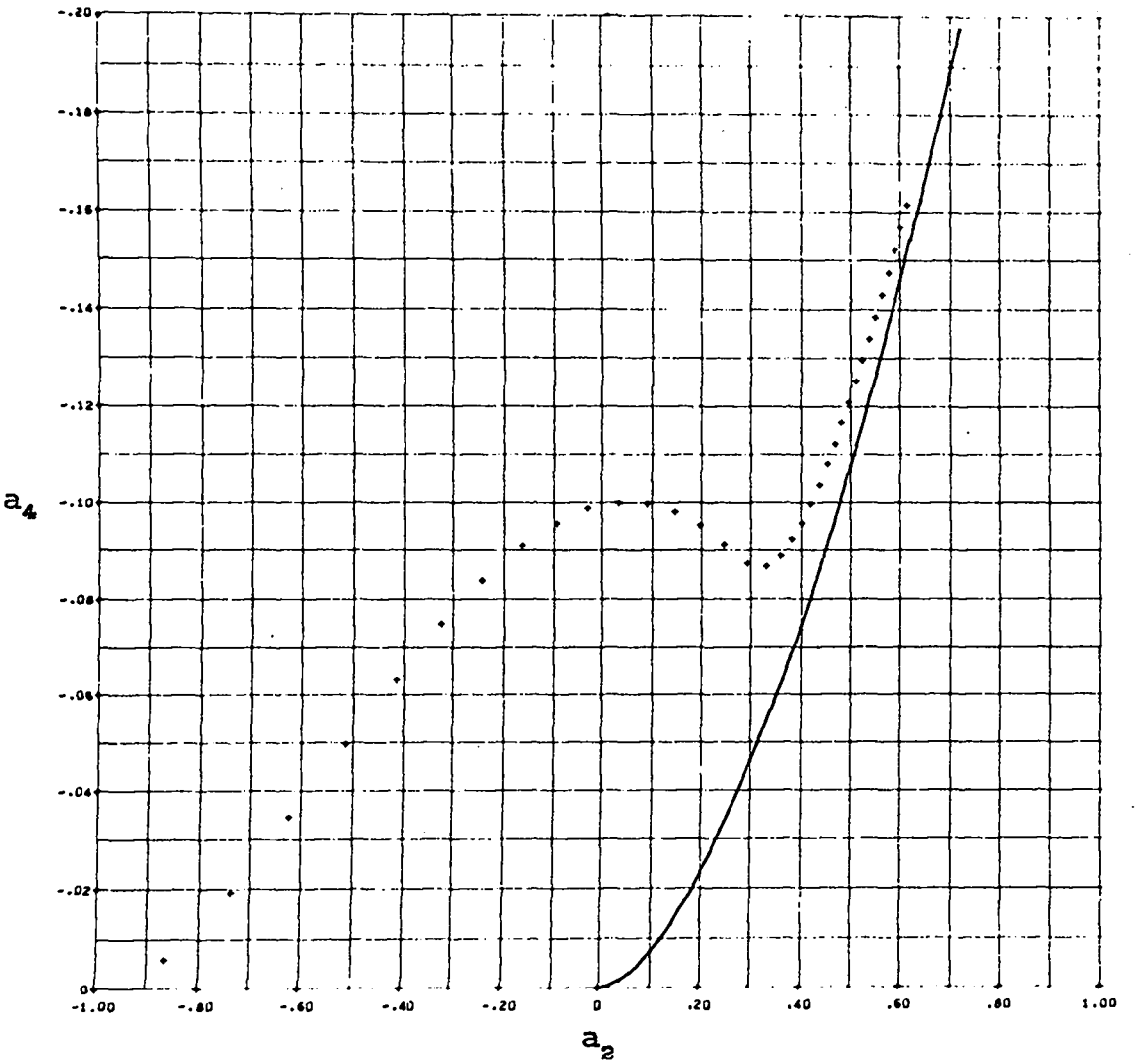

Fig. 4. Graph of the deformation energy saddle points and the scission line. The fissionability parameter X starts with the value 1.0 at the extreme left and decreases by 0.02 as the points move to the right.

TABLE III. CALCULATED SADDLE POINT PROPERTIES FOR THE RANGE OF FISSIONABILITY PARAMETERS 0.98 TO 0.30

X	F	B_3	B_e	$I_{\parallel}$	$I_{\perp}$	τ	Q
.98	.00001	1.00085	.99957	.9547	1.0259	.0728	.2389
.96	.00005	1.00334	.99828	.9117	1.0574	.1511	.4880
.94	.00015	1.00740	.99614	.8708	1.0949	.2351	.7511
.92	.00037	1.01302	.99312	.8314	1.1393	.3251	1.0318
.90	.00072	1.02022	.98917	.7934	1.1916	.4212	1.3346
.88	.00125	1.02903	.98422	.7566	1.2533	.5239	1.6646
.86	.00199	1.03953	.97818	.7208	1.3260	.6333	2.0281
.84	.00301	1.05183	.97094	.6859	1.4120	.7497	2.4332
.82	.00434	1.06608	.96235	.6519	1.5144	.8736	2.8901
.80	.00604	1.08248	.95222	.6187	1.6374	1.0054	3.4134
.78	.00818	1.10135	.94028	.5865	1.7871	1.1456	4.0235
.76	.01085	1.12312	.92614	.5551	1.9730	1.2946	4.7513
.74	.01413	1.14845	.90924	.5250	2.2099	1.4522	5.6460
.72	.01815	1.17832	.88878	.4969	2.5231	1.6161	6.7898
.70	.02309	1.21368	.86386	.4730	2.9531	1.7757	8.3111
.68	.02908	1.25137	.83655	.4594	3.5073	1.8916	10.2135
.66	.03605	1.27762	.81699	.4610	3.9796	1.9180	11.7911
.64	.04359	1.29019	.80734	.4692	4.2452	1.8957	12.6536
.62	.05140	1.29626	.80254	.4784	4.3875	1.8625	13.0998
.60	.05936	1.29942	.79995	.4872	4.4664	1.8286	13.3345
.58	.06739	1.30111	.79852	.4956	4.5098	1.7961	13.4517
.56	.07547	1.30199	.79775	.5035	4.5314	1.7656	13.4976
.54	.08357	1.30239	.79739	.5109	4.5388	1.7369	13.4974
.52	.09167	1.30248	.79730	.5180	4.5366	1.7100	13.4663
.50	.09978	1.30238	.79739	.5248	4.5276	1.6848	13.4135
.48	.10788	1.30217	.79762	.5312	4.5137	1.6609	13.3453
.46	.11597	1.30187	.79793	.5374	4.4963	1.6384	13.2664
.44	.12404	1.30153	.79831	.5434	4.4761	1.6170	13.1738
.42	.13210	1.30115	.79875	.5491	4.4536	1.5965	13.0841
.40	.14014	1.30077	.79922	.5547	4.4298	1.5771	12.9858
.38	.14816	1.30038	.79971	.5601	4.4049	1.5585	12.8841
.36	.15617	1.30000	.80023	.5653	4.3790	1.5407	12.7800
.34	.16415	1.29963	.80076	.5703	4.3524	1.5236	12.6738
.32	.17210	1.29927	.80131	.5753	4.3254	1.5072	12.5667
.30	.18004	1.29892	.80186	.5800	4.2979	1.4913	12.4587

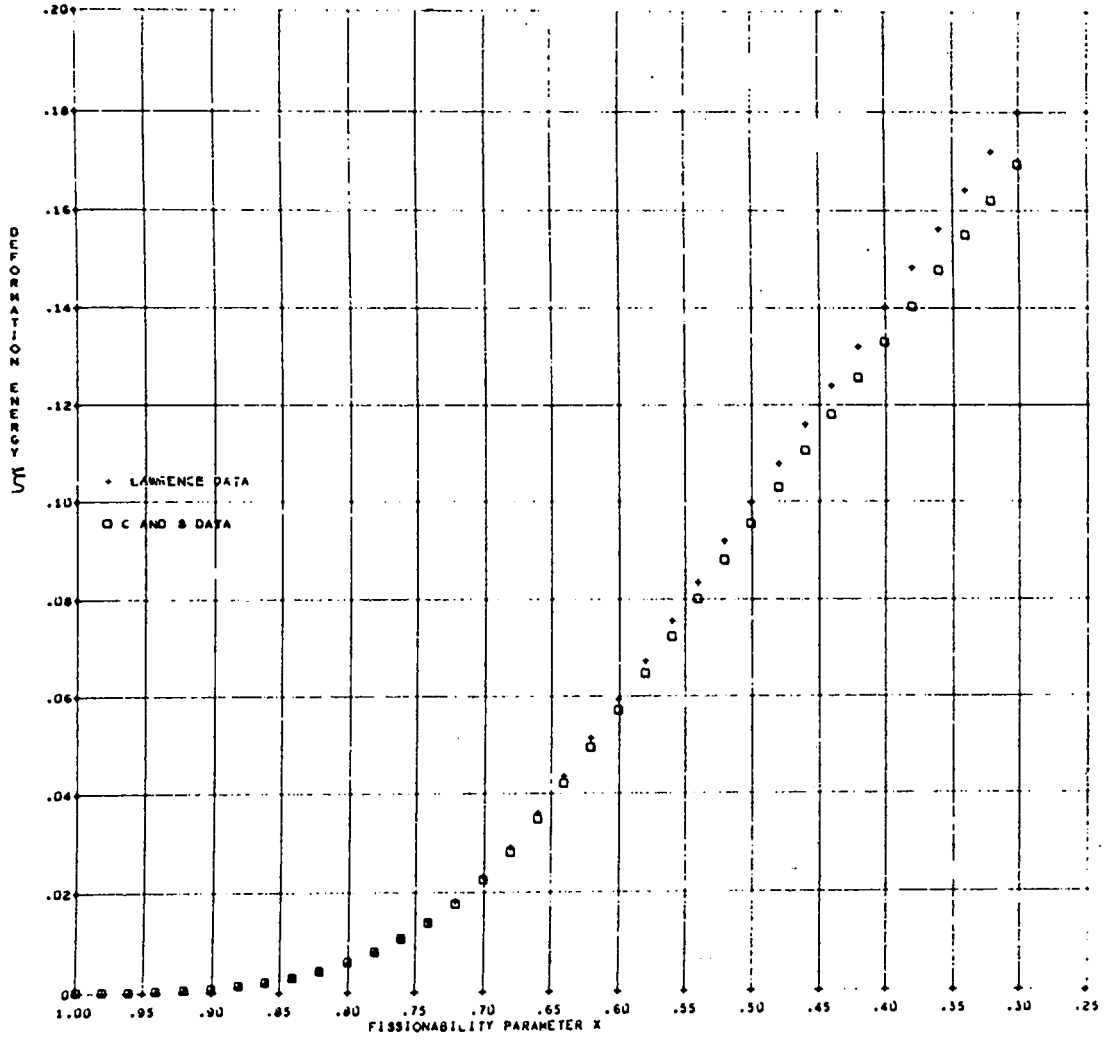

Fig. 5. Comparison of deformation energy ξ vs fissionability parameter X

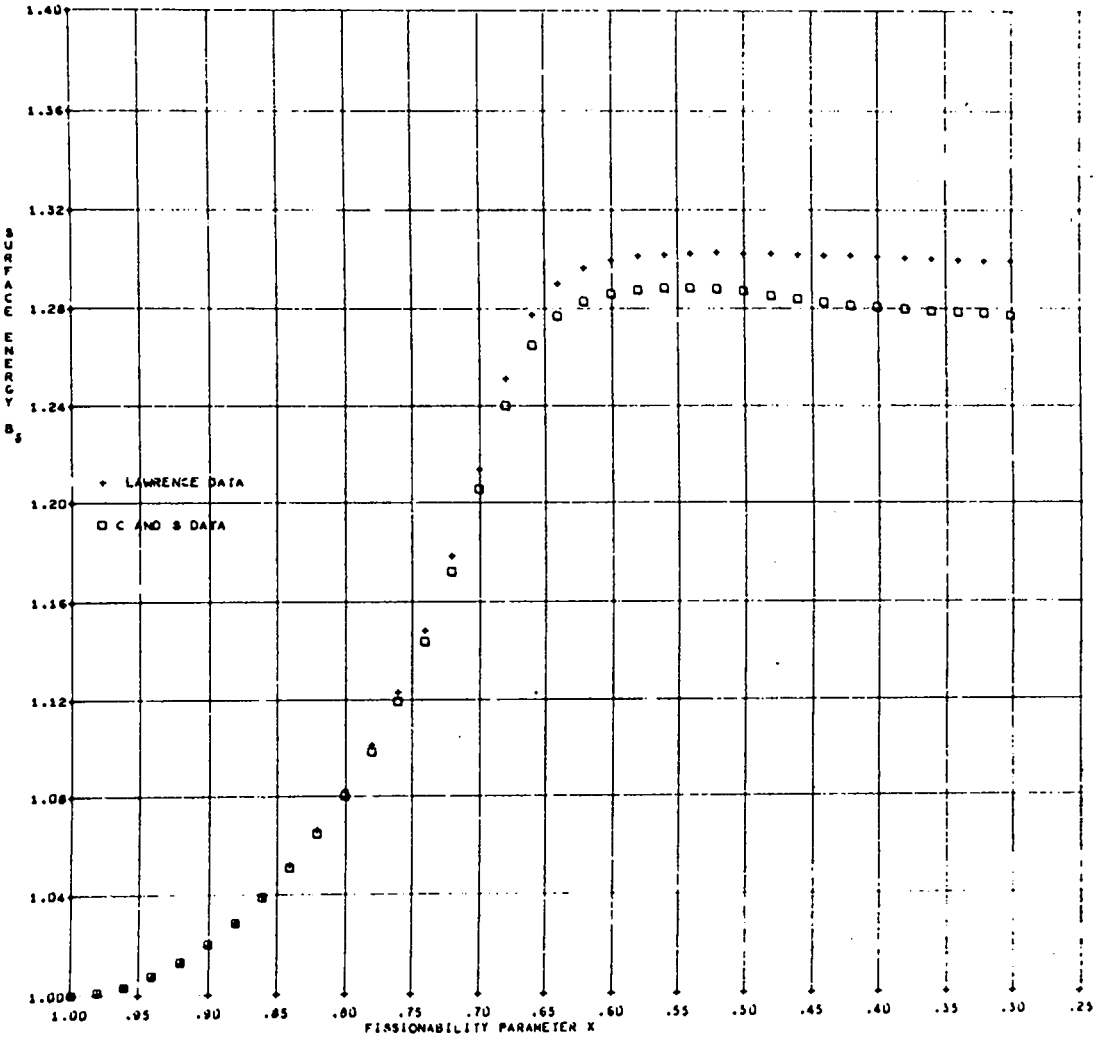

Fig. 6. Comparison of surface energy B_s vs fissionability parameter X

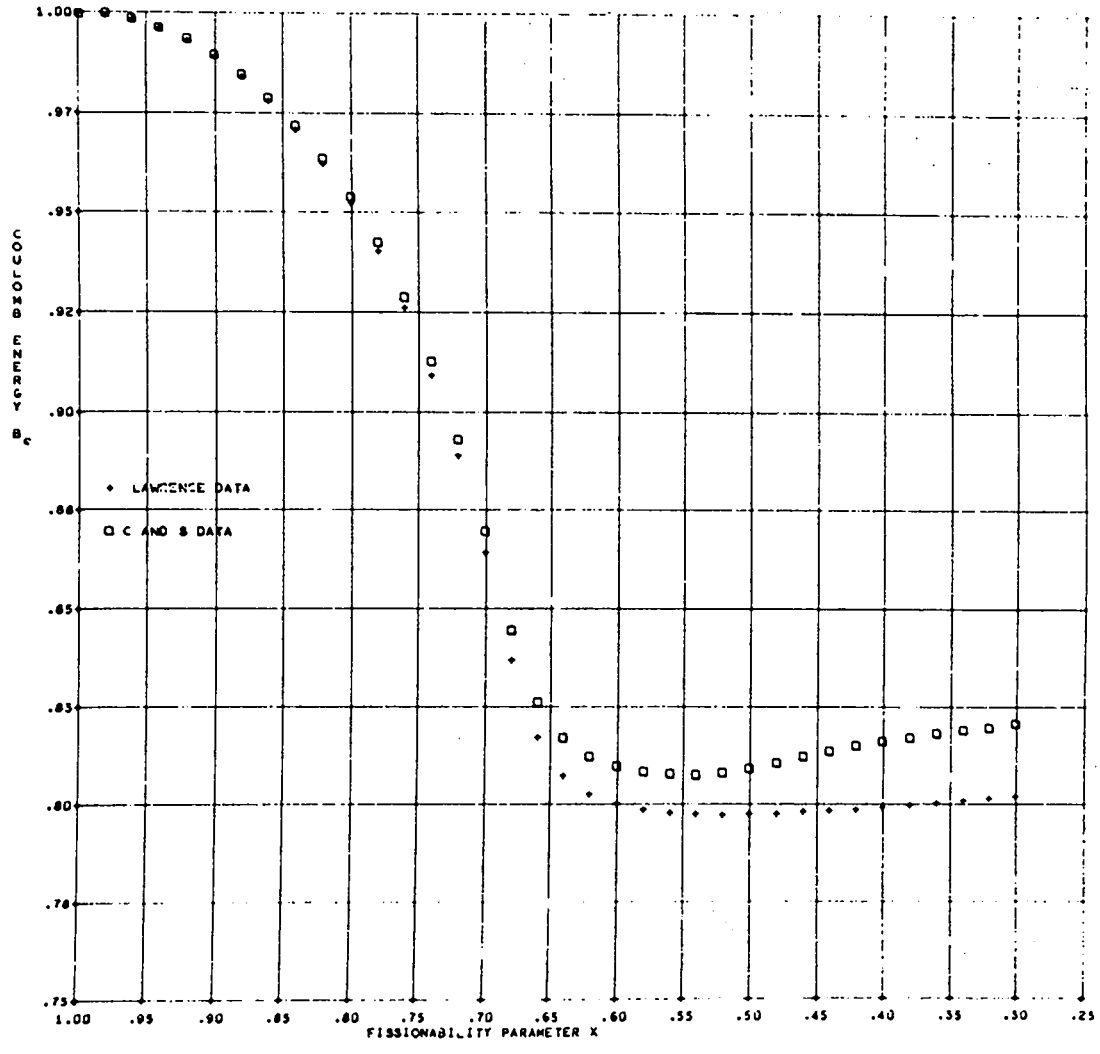

Fig. 7. Comparison of Coulomb energy B_c vs fissionability parameter X

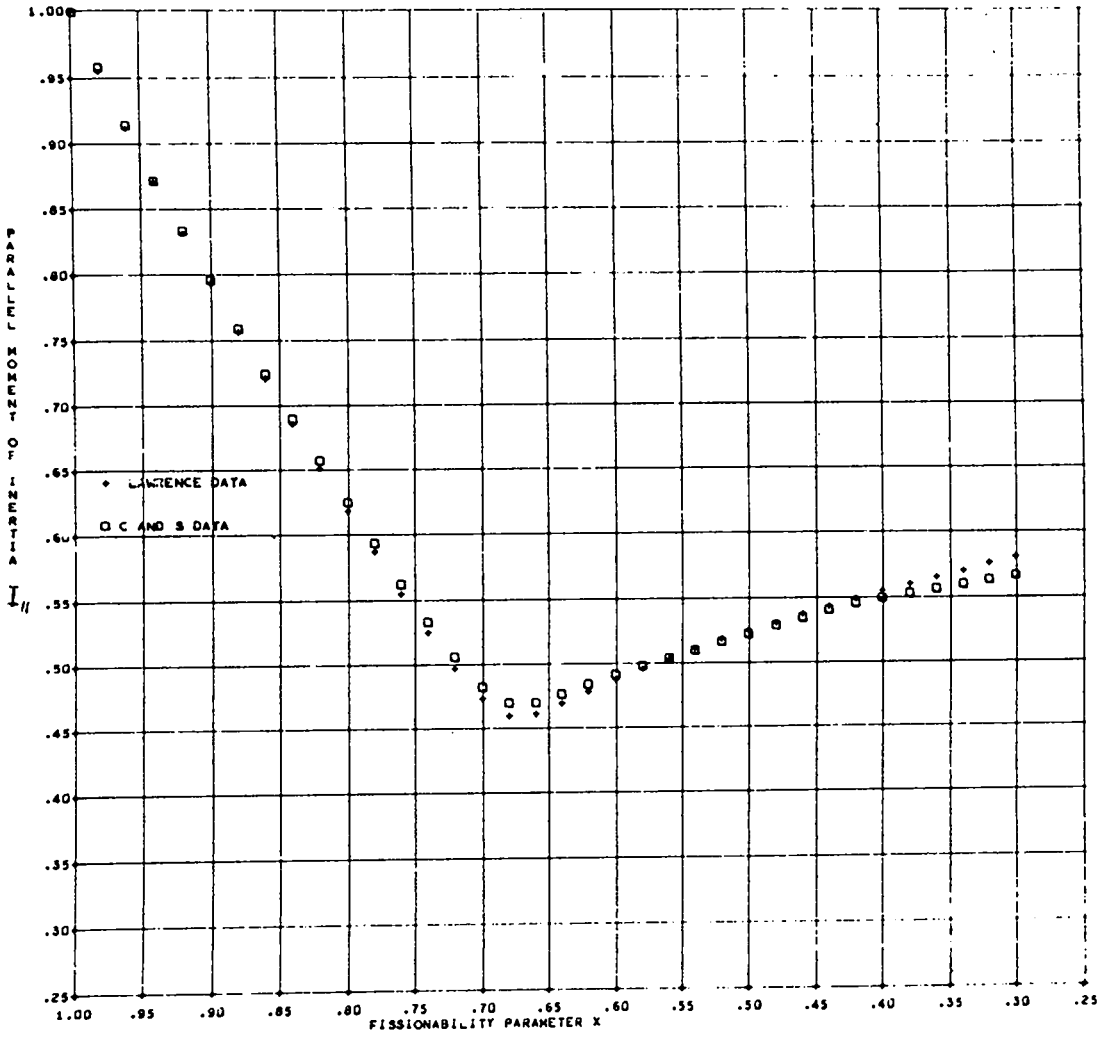

Fig. 8. Comparison of parallel moment of inertia $I_{\parallel}$ vs fissionability parameter X

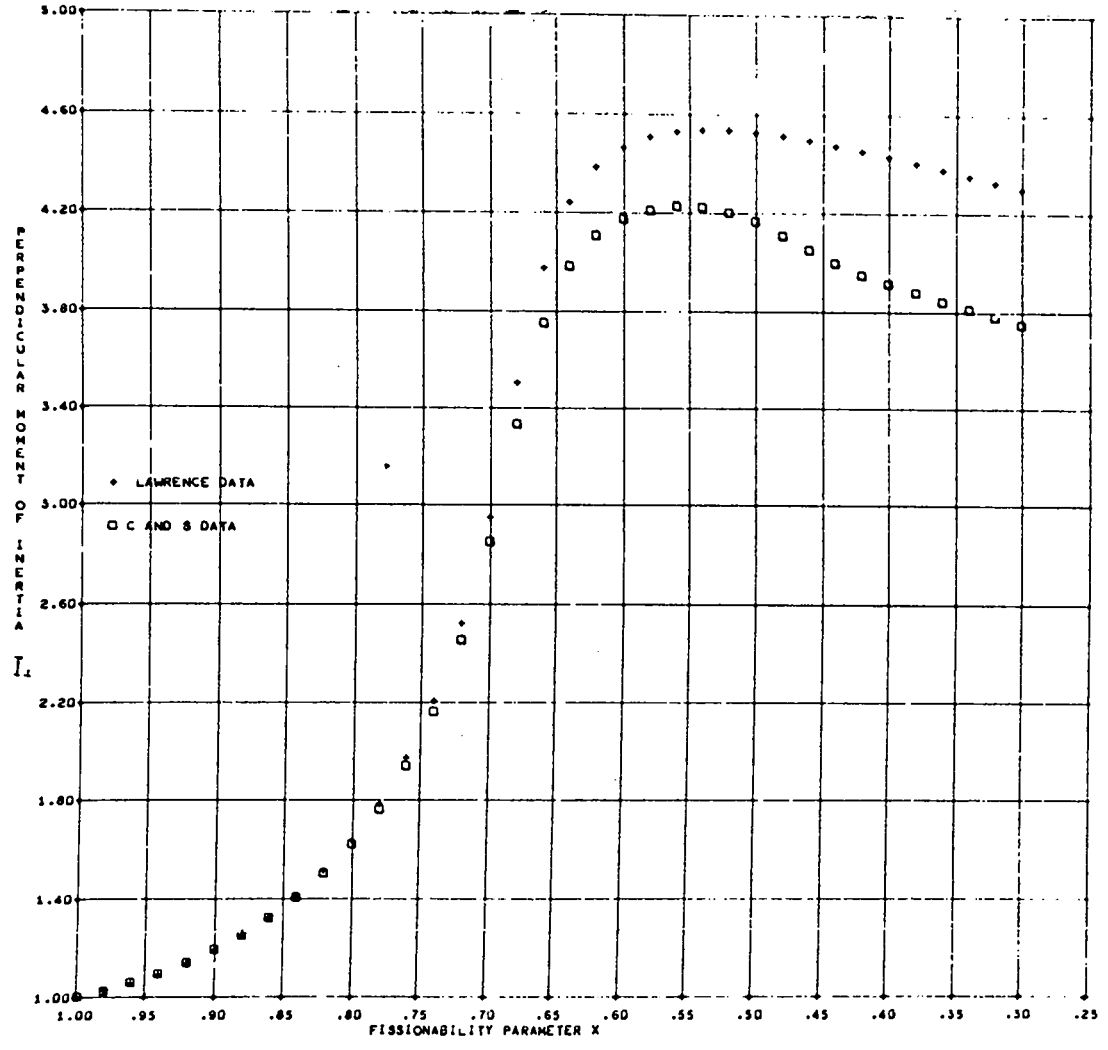

Fig. 9. Comparison of perpendicular moment of inertia $I_\perp$ vs fissionability parameter X

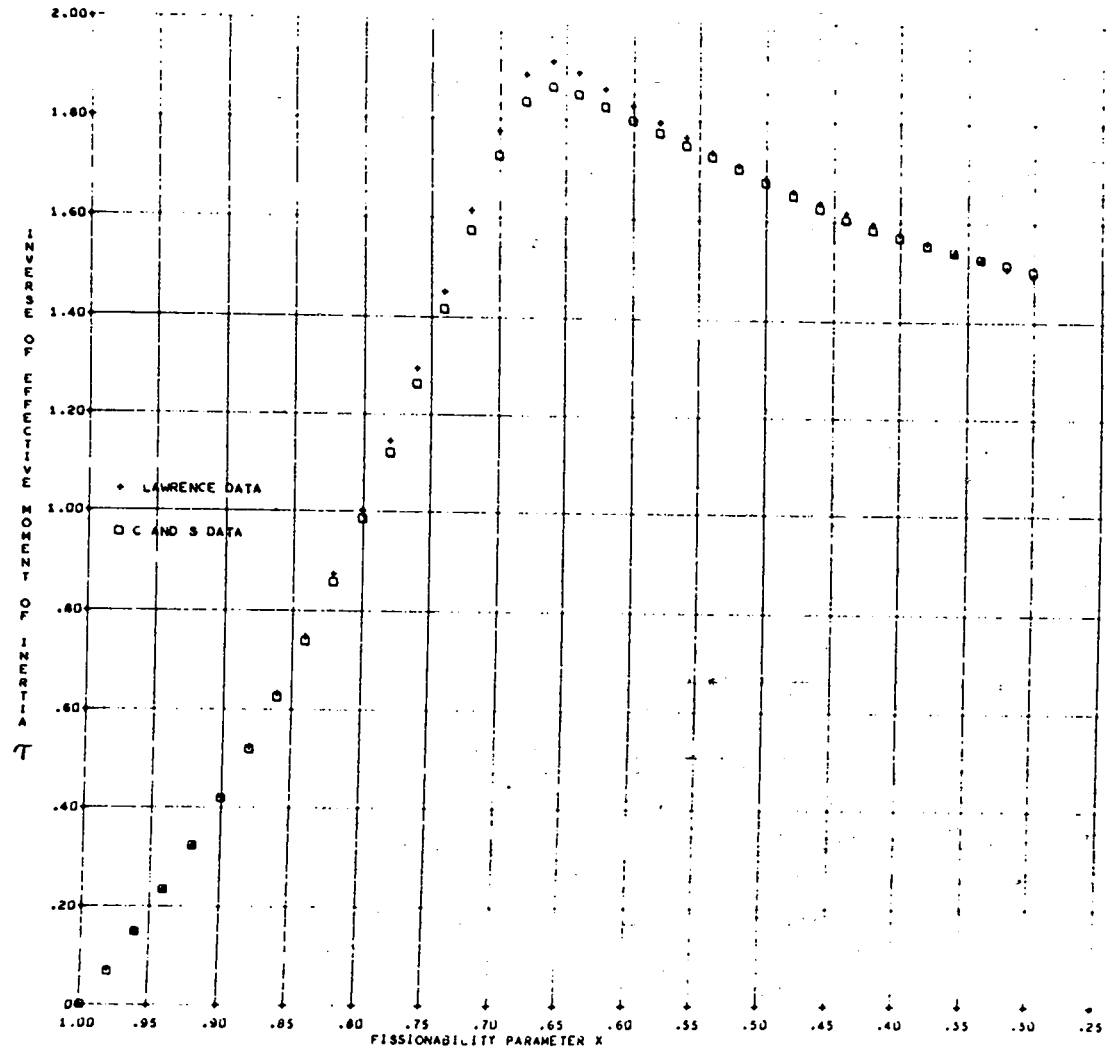

Fig. 10. Comparison of inverse of effective moment of inertia τ vs fissionability parameter X

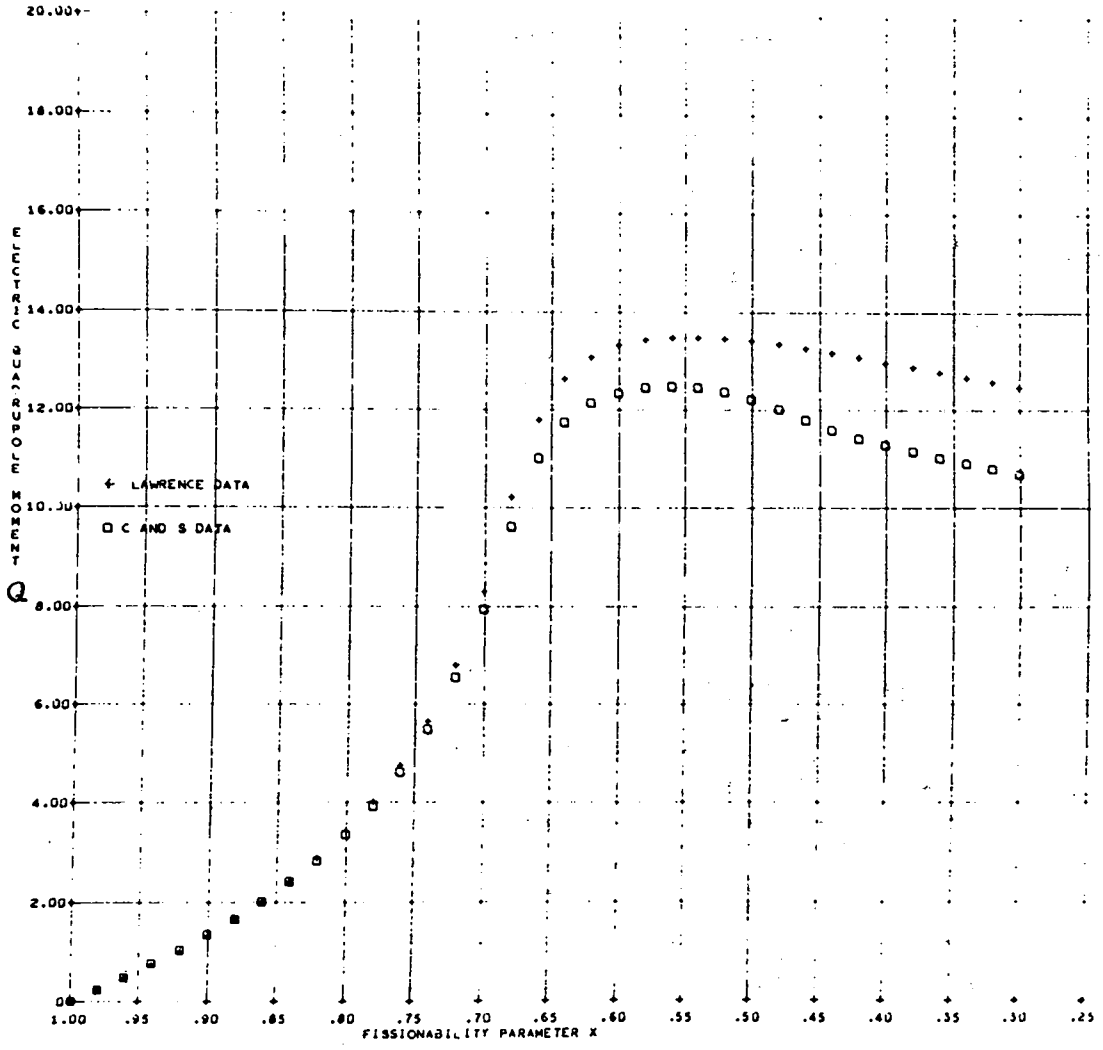

Fig. 11. Comparison of electric quadrupole moment Q vs fissionability parameter X

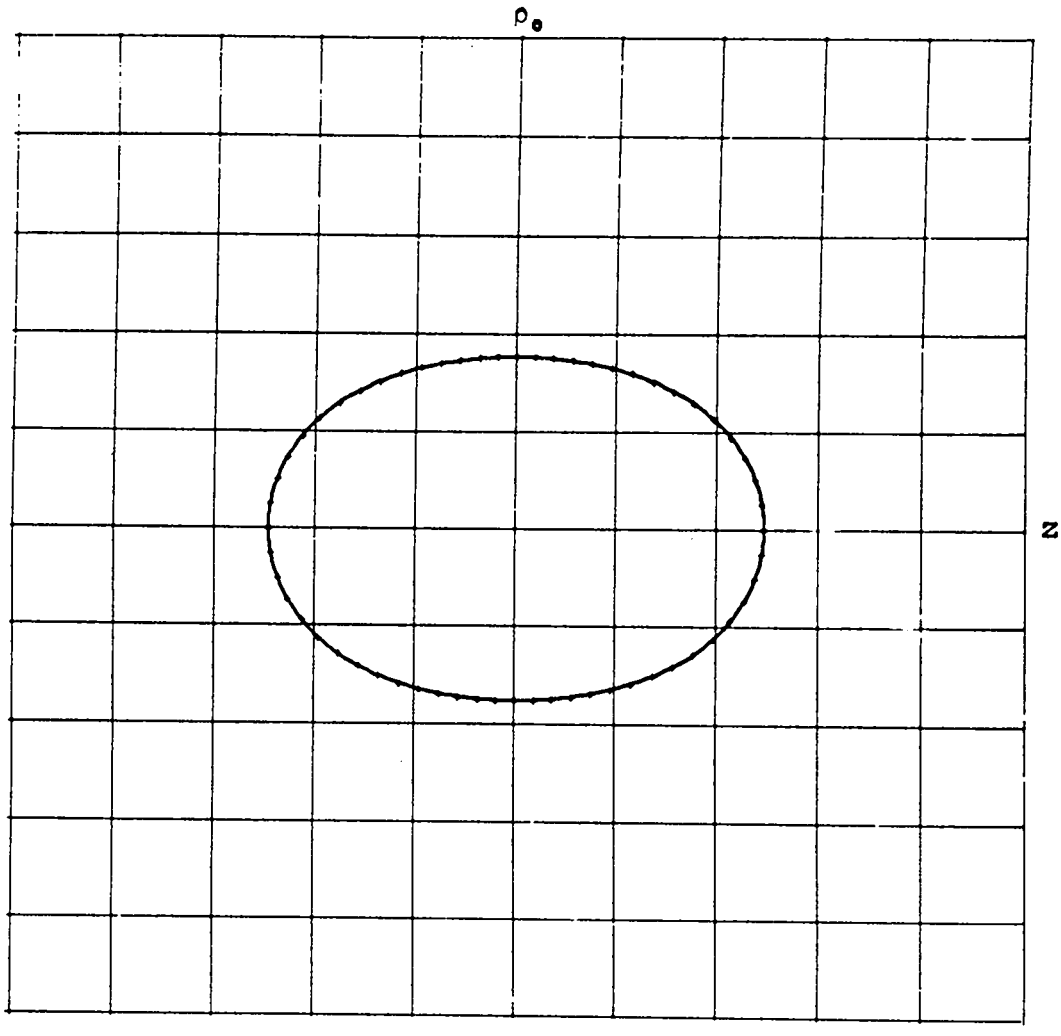

Fig. 12. Comparison of saddle point drop-contours for fissionability parameter X=0.9. Continuous line is the result of this investigation, while + signs are C and S data[27].

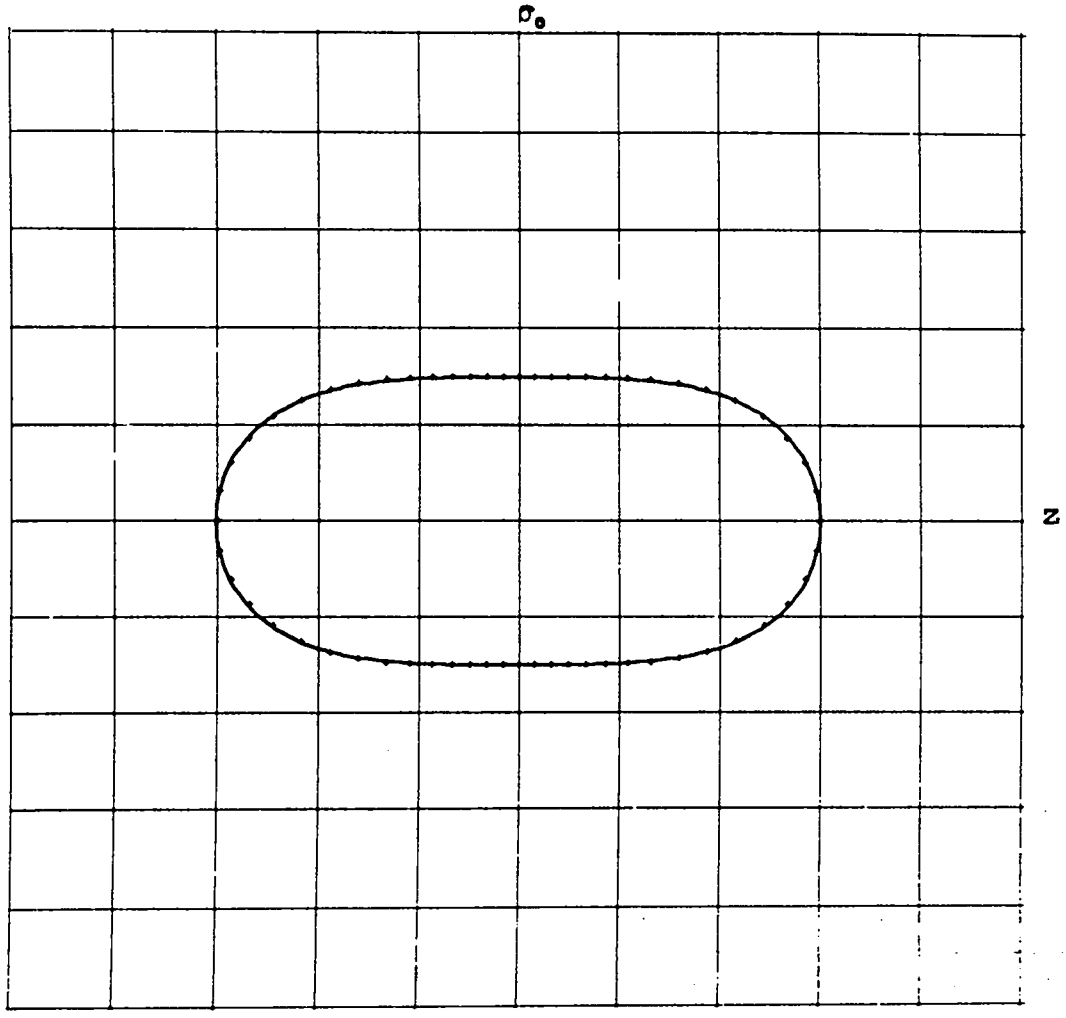

Fig. 13. Comparison of saddle point drop-contours for fissionability parameter X=0.8. Continuous line is the result of this investigation, while + signs are C and S data[27].

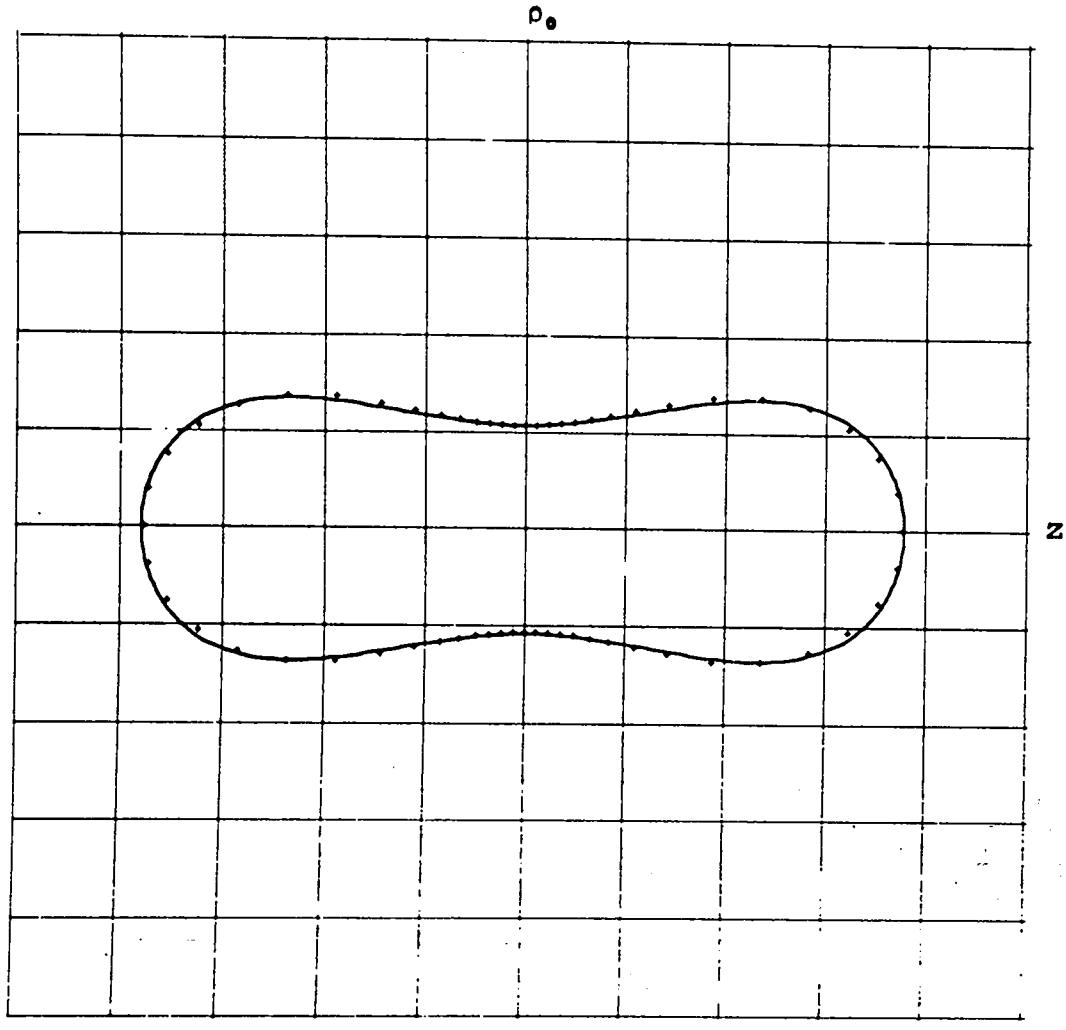

Fig. 14. Comparison of saddle point drop-contours for fissionability parameter X=0.7. Continuous line is the result of this investigation, while + signs are C and S data[27].

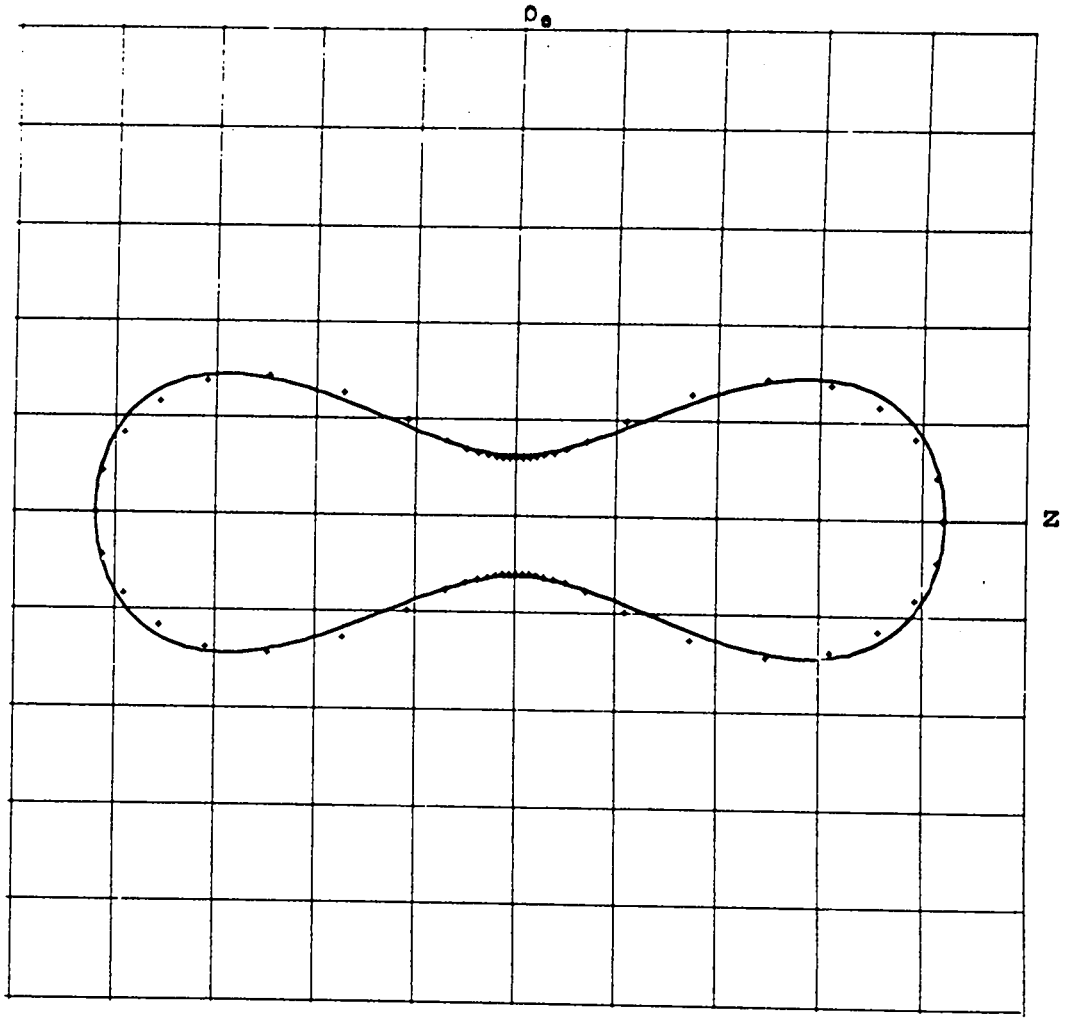

Fig. 15. Comparison of saddle point drop-contours for fissionability parameter X=0.6. Continuous line is the result of this investigation, while + signs are C and S data[27].

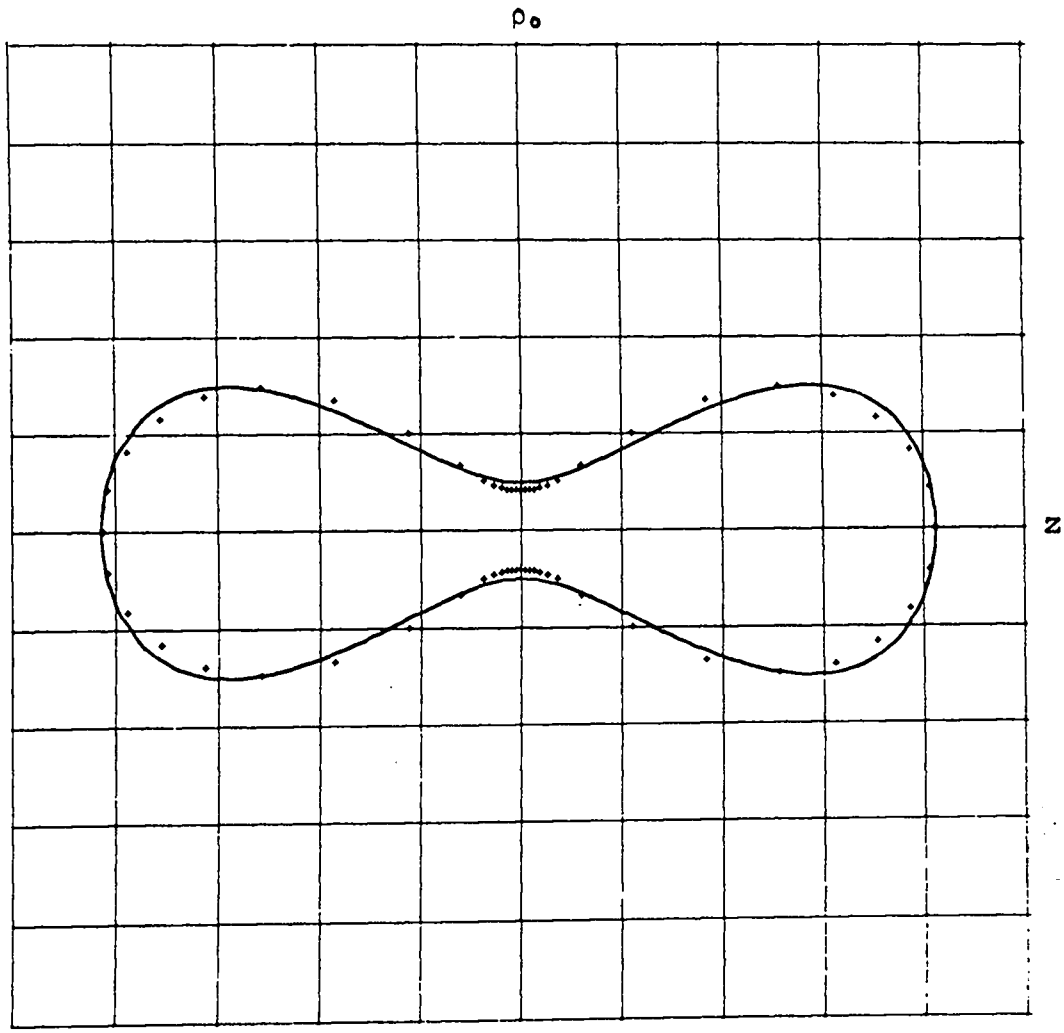

Fig. 16. Comparison of saddle point drop-contours for fissionability parameter X=0.5. Continuous line is the result of this investigation, while + signs are C and S data[27].

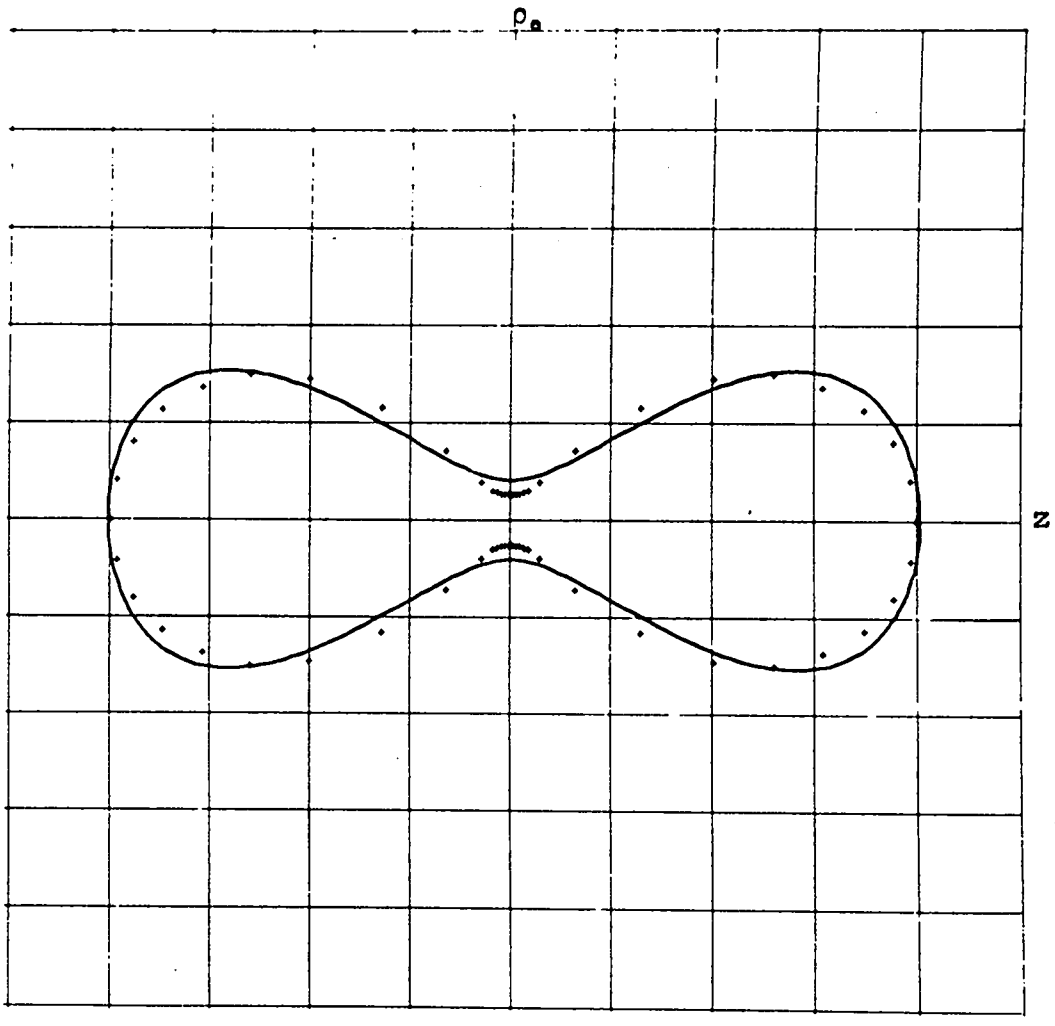

Fig. 17. Comparison of saddle point drop-contours for fissionability parameter X=0.4. Continuous line is the result of this investigation, while + signs are C and S data[27].

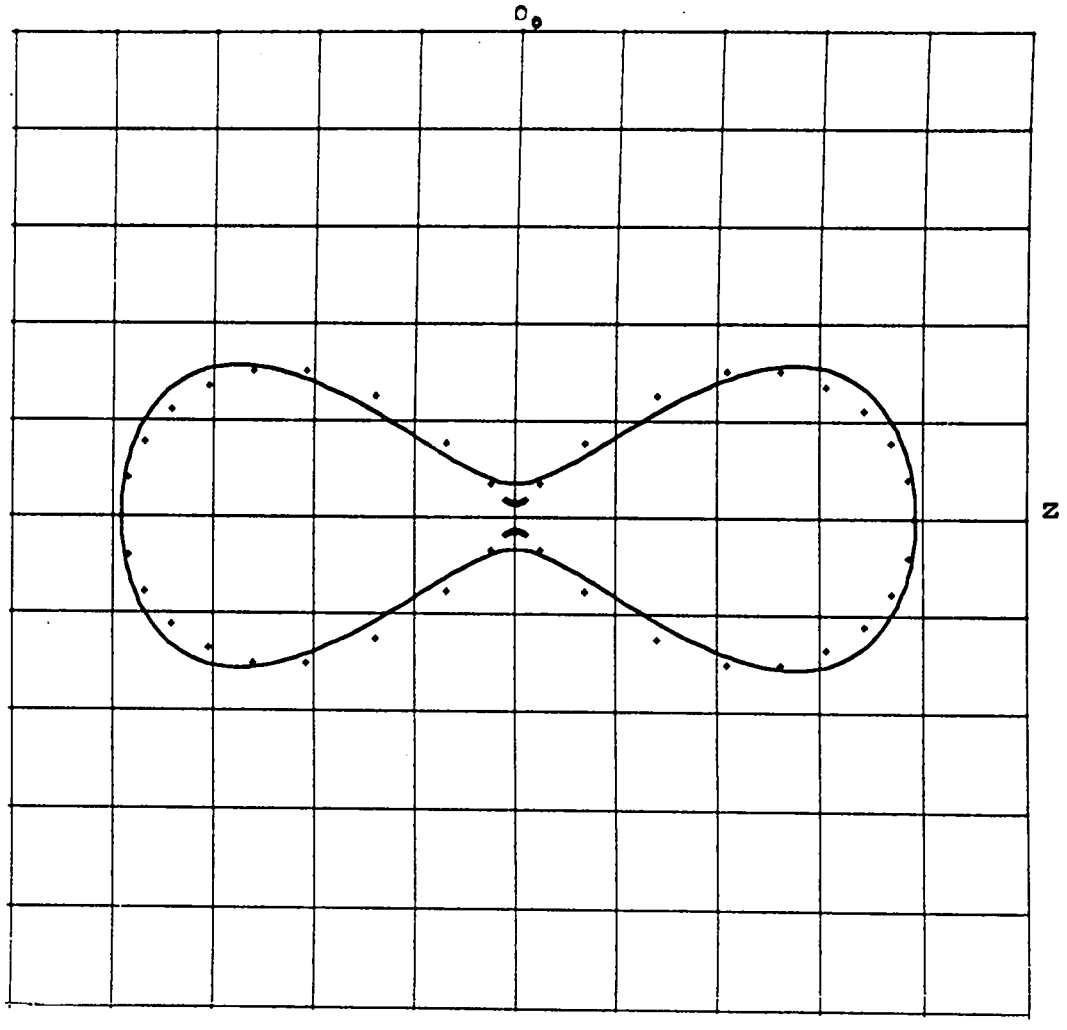

Fig. 18. Comparison of saddle point drop-contours for fissionability parameter X=0.3. Continuous line is the result of this investigation, while + signs are C and S data[27].

III. DYNAMICS AND KINETIC ENERGY CONSIDERATIONS

The treatment of the motion of the liquid drop differs from the usual motion studies in that there is no displacement of the center of mass. The entire motion consists of changes in the shape of the drop. Since in this work the shape of the drop is given by equation (2), the dynamic variables are taken to be a_2 and a_4 and their time derivatives. The approach adopted for this study differs from those discussed in the section REVIEW OF FISSION THEORY and is based on the Lagrangian formalism. The standard definition of the Lagrangian L is the difference in the kinetic energy B_K and the potential energy ξ, as

$$L = B_K - \xi \tag{11}$$

In this study both the kinetic energy and the potential (deformation) energy are expressed relative to the surface energy E_s° of the spherical configuration.

Since irrotational flow is assumed, the velocity of the fluid at any point in the liquid drop is derivable from a scalar velocity potential, i.e.,

$$\underline{v} = - \text{grad}\varphi$$

Requiring the fluid to obey the principle of the conservation of mass implies that within any volume element the rate of loss of mass must equal the flow of mass from that element. This is simply a statement of the equation of continuity for the fluid. If σ_m is the density of the fluid, then

$$\frac{\partial \sigma_m}{\partial t} = - \nabla \cdot \sigma_m \underline{v}$$

For an incompressible fluid (which is also assumed), σ_s is a constant and the equation of continuity reduces to Laplace's equation:

$$\nabla^2\varphi = 0$$

Thus for an incompressible fluid undergoing irrotational motion, the potential φ defining the velocity must obey Laplace's equation. It follows that an arbitrary potential (not satisfying Laplace's equation) would correspond to a compressible motion, and account must be taken of such compressions in the equations of motion.

Velocity Potential and Kinetic Energy

The solution of Laplace's equations in spherical coordinates is a convenient form of the velocity potential. Because of the assumed axial symmetry, only two of the three spherical coordinates enter this representation. These are "r", the radial distance from the origin to the point under consideration, and "Θ", the angle between "r" and the z-axis. In terms of these coordinates the velocity potential has the form:

$$-\varphi = \sum_{n=1}^{N} \theta_{2n}\, r^{2n}\, P_{2n}(\cos\Theta)$$

where P_{2n} is the Legendre polynomial of order "$2n$" and θ_{2n}'s are time dependent parameters (functions of a_2, a_4 and their first time derivatives). While readily recognizable as a solution to Laplace's equation, this form of the velocity potential is not suitable for application. By successive applications of the relation:

$$r\cos\Theta = z,$$

followed by:

$$r^2 = \rho^2 + z^2,$$

the velocity potential is re-expressed in cylindrical coordinates as:

$$-\varphi = \sum_{n=1}^{N} \beta_{2n} H_n(\rho, z) \tag{12}$$

While the functions $H_n(\rho, z)$ are not widely tabulated, they are easily derived from the well published Legendre polynomials.

In terms of equation (12) the vector velocity at any point in the liquid drop is

$$\underline{v} = -\text{grad}\varphi = \underline{i}_z \sum_{n=1}^{N} \beta_{2n} \frac{\partial H_n}{\partial z} + \underline{i}_\rho \sum_{n=1}^{N} \beta_{2n} \frac{\partial H_n}{\partial \rho} \tag{13}$$

where $\underline{i}_z$ and $\underline{i}_\rho$ are unit vectors in the z and ρ directions, respectively. In Appendix VII, treating the dimensionality aspects fully, the kinetic energy (relative to the surface energy of the sphere) is shown to be

$$B_K = \sum_{\substack{i=1 \\ j=1}}^{J} \sum^{J} B_{2i} B_{2j} I_{2i,2j} \tag{14}$$

where

$$I_{2i,2j} = \frac{1}{4} \int_{-z_o}^{z_o} dz \int_{o}^{\rho_o} \left\{ \frac{\partial H_i}{\partial z} \frac{\partial H_j}{\partial z} + \frac{\partial H_i}{\partial \rho} \frac{\partial H_j}{\partial \rho} \right\} \rho d\rho \tag{15}$$

Boundary Conditions and β_{2n} Determinations

For a fluid of finite extent the equation of continuity is replaced at the surface of the fluid by a special boundary condition[47]. This boundary condition is obtained from the requirement that the motion of a fluid point on the surface follows exactly the motion of the surface itself. If the implicit equation of the surface of the axially symmetric liquid drop is:

$$F(\rho, z; a_2, a_4) = \rho_o(z; a_2, a_4) - \rho = 0$$

then the special boundary condition becomes

$$\frac{DF}{Dt} = \frac{\partial F}{\partial t} + \underline{v} \cdot \nabla F = 0$$

or

$$G = \rho_o v_\rho - \rho_o \rho_o' v_z - \rho_o \dot{\rho}_o = 0 \qquad (16)$$

where v_ρ and v_z are the ρ and z velocity components evaluated on the surface and ρ_o' and $\dot{\rho}_o$ are the derivatives of ρ_o (equation (2)) with respect to "z" and time, respectively. Again dimensional considerations are discussed in Appendix VII.

In general for a finite number of terms in the velocity potential it is impossible to satisfy equation (16), because of contradictions in the determinations of the β_{2n}'s. A compromise was adopted which uniquely determines the β_{2n}'s, and which more nearly satisfies the boundary conditions as the number of terms in the velocity potential increases. By squaring equation (16) and integrating over the range of z spanned by the liquid drop,

---

[47] H. Lamb, Hydrodynamics, 6th Ed., Dover Publications, New York, p. 6.

i.e., from $-z_o$ to z_o, an expression quadratic in the β_{2n}'s is obtained as

$$GSI = \sum_{\substack{i=1 \\ j=1}}^{J} \beta_{2i}\beta_{2j}G_{ij} + \sum_{j=1}^{J} \beta_{2j}G_j + G_o \qquad (17)$$

where

$$G_{ij} = \int_{-z_o}^{z_o} \left\{ \rho_o^2 \frac{\partial H_i}{\partial \rho}\frac{\partial H_j}{\partial \rho} - 2\rho_o\left(a_2 z + 2a_4 z^3\right)\frac{\partial H_i}{\partial \rho}\frac{\partial H_j}{\partial z} + \left(a_2 z + 2a_4 z^3\right)^2 \frac{\partial H_i}{\partial z}\frac{\partial H_j}{\partial z}\right\} dz \qquad (18)$$

$$G_j = \int_{-z_o}^{z_o} \left\{ \dot{a}_4\left(z^4 + \frac{\partial c}{\partial a_4}\right) + \dot{a}_2\left(z^2 + \frac{\partial c}{\partial a_2}\right)\right\} \times \left\{-\rho_o\frac{\partial H_j}{\partial \rho} + \left(a_2 z + 2a_4 z^3\right)\frac{\partial H_j}{\partial z}\right\} dz \qquad (19)$$

$$G_o = \int_{-z_o}^{z_o} \left\{ \dot{a}_4\left(z^4 + \frac{\partial c}{\partial a_4}\right) + \dot{a}_2\left(z^2 + \frac{\partial c}{\partial a_2}\right)\right\}^2 dz \qquad (20)$$

GSI is minimized with respect to the β_{2n}'s by setting its partial derivative with respect to the β_{2n}'s equal to zero. The resulting set of N linear equations in the N β_{2n}'s is then solved for the β_{2n}'s. The β_{2n}'s so determined will be linear in $\dot{a}_2$ and $\dot{a}_4$.

The Equations of Motion

By inserting the β_{2n}'s found by the above procedure in equation (14), the kinetic energy B_K is seen to be a function of a_2 and a_4, quadradic in $\dot{a}_2$ and $\dot{a}_4$. In the section STATICS AND POTENTIAL ENERGY CONSIDERATION the functional dependence of the

deformation energy ξ is expressed by equations (5), (6), and (7). In Appendix VII application of the Euler-Lagrange operator:

$$\frac{d}{dt}\left(\frac{\partial}{\partial \dot{a}_\varkappa}\right) - \frac{\partial}{\partial a_\varkappa} = 0$$

to the Lagrangian, equation (11), provides the equations of motion as:

$$\sum_{\substack{i=1\\j=1\\\eta=2,4}}^{J\,J} \ddot{a}_\eta \frac{\partial \beta_{2i}}{\partial \dot{a}_\varkappa} \frac{\partial \beta_{2j}}{\partial \dot{a}_\eta} I_{2i,2j} + \sum_{\substack{i=1\\j=1\\\eta=2,4}}^{J\,J} \dot{a}_\eta \left\{ \left(\frac{\partial^2 \beta_{2i}}{\partial \dot{a}_\varkappa \partial a_\eta} \beta_{2j} + \frac{\partial \beta_{2i}}{\partial \dot{a}_\varkappa} \frac{\partial \beta_{2j}}{\partial a_\eta} \right) I_{2i,2j} + \frac{\partial \beta_{2i}}{\partial \dot{a}_\varkappa} \beta_{2j} \frac{\partial I_{2i,2j}}{\partial a_\eta} \right\}$$

$$- \sum_{\substack{i=1\\j=1}}^{J\,J} \left\{ \frac{\partial \beta_{2i}}{\partial a_\varkappa} \beta_{2j} I_{2i,2j} + \tfrac{1}{2} \beta_{2i} \beta_{2j} \frac{\partial I_{2i,2j}}{\partial a_\varkappa} \right\} + \tfrac{1}{2} \frac{\partial \xi}{\partial a_\varkappa} = 0 \qquad (21)$$

for $\varkappa = 2,4$

Equation (21) is a linear set of equations in $\ddot{a}_2$ and $\ddot{a}_4$. This set of equations may be numerically integrated to provide successive values of a_2, a_4, $\dot{a}_2$ and $\dot{a}_4$ after an initial set of values of these variables is specified. Because the set of equations is coupled, changes in a single one of the quantities a_2, a_4, $\dot{a}_2$ or $\dot{a}_4$ will affect both accelerations.

Tests Applicable to the Developed Theory

An obvious check on the theory is its prediction of the motion of small amplitude about the equilibrium configuration (spherical). Early investigations of the oscillations

of water droplets in jets by Rayleigh[48] were modified by Plesset[49] to treat a uniform electrical charge throughout the volume of the drop. Both Rayleigh and Plesset considered very small oscillations, such that for kinetic energy purposes the drop could be approximated by the undeformed sphere. Both of their treatments were to order α^2 (where α is a small quantity). In Appendix VIII somewhat larger motions are considered (to order α^4). To reduce the complexity the coordinate a_4 is not considered. It is shown that to the order α^2 the motion in the a_2 coordinate is simple harmonic, with a period:

$$\tau_{SHM} = \frac{2\pi T_o}{\sqrt{8(1-x)}} \qquad (22)$$

where X is the fissionability parameter and T_o is the "basic" time unit ($= 0.482_4 \times 10^{-22} A^{\frac{1}{2}}$ seconds). For a motion starting from spherical with a non-zero $\dot{a}_2$, the kinetic energy is

$$B_K = \frac{1}{180}\dot{a}_2^2 \qquad (23)$$

In considering the higher order approximations (i.e., to order α^4) an unusual property of the motion becomes apparent. This property is the existence of non-vanishing accelerations at the equilibrium configuration (spherical) whenever finite coordinate velocities are present. It is shown that this

---

[48] J. W. Strutt (Lord Rayleigh), Theory of Sound, ed.2, Vol. II, (Dover Publications, New York, 1945) pp. 371-375; Phil. Mag. 14, 184, (1882).

[49] M. S. Plesset, Am. J. of Physics, 9, 1 (1941).

property arises from the linear coordinate dependence of the "mass" in the kinetic energy expression. In the single coordinate treatment of Appendix VIII this acceleration was proportional to $\dot{a}_2^2$. However, in the complete two-coordinate theory where $\ddot{a}_2$ and $\ddot{a}_4$ are coupled, one should expect at spherical that a non-vanishing $\dot{a}_2$ ($\dot{a}_4$=0) would generate both $\ddot{a}_2$ and $\ddot{a}_4$.

Two other tests of the theory are suggested from the general description of the liquid drop (as given in the section REVIEW OF FISSION THEORY). One is to start the motion from the saddle point with a small velocity component in the direction of scission. The second is to start from spherical with sufficient kinetic energy to surpass the fission barrier (saddle point energy). In both cases an acceptable theory will produce a motion which goes to scission.

A final general check will be the behavior of the total energy of the system (i.e., $B_K+\xi$). Since the forces acting on the system are derived from the deformation energy, the system is conservative, and the total energy of the system should remain constant as the various test motions proceed.

The Deformation Energy Surface

The deformation energy ξ is a function of fissionability parameter X (see equation (7)) as well as of the coordinates a_2, a_4. While the individual appearance of the deformation energy surface as a function of a_2, a_4 will depend on the value of X, the general features will remain for the same for any $X < 1$. In Figs. 19 the calculated deformation energy contours are plotted in a_2-a_4 space for X = 0.74. While the selection of X = 0.74 was arbitrary, it does represent an easily fissionable nucleus (i.e., ^{239}Pu). To simplify the

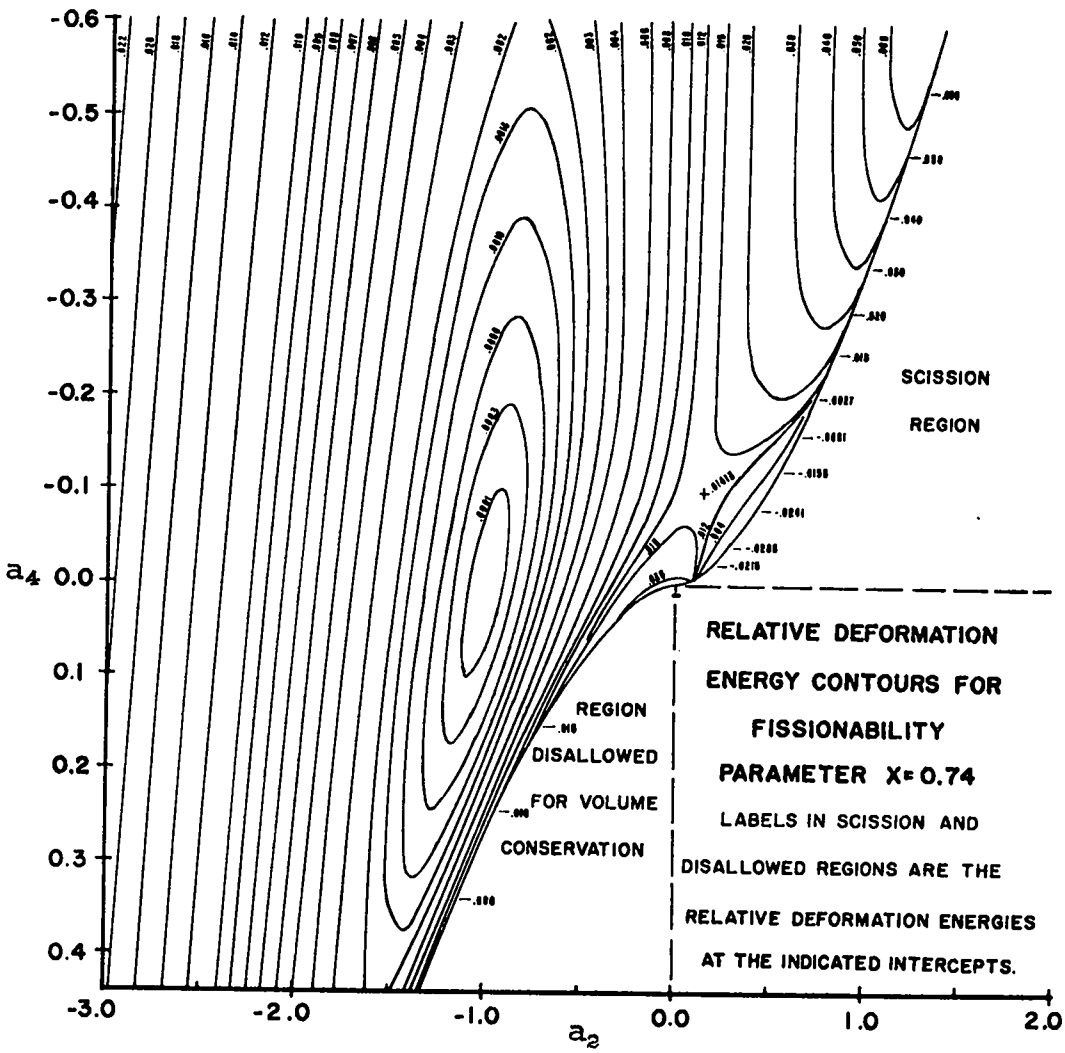

Fig. 19. Relative deformation energy contours for liquid drops, whose shape is defined by the equation:

$$\rho_0^2 = c + a_2 z^2 + a_4 z^4$$

discussion all numerical calculations of the dynamics will be done for X = 0.74.

A prominent feature is the saddle point at (a_2 = 0.1458, a_4 =-0.09822). At the point (0,0) the shape of the drop degenerates into an infinitely long line with infinite deformation energy. For shapes defined by equation (2) the region of positive a_4, labeled "Diasllowed Region for Volume Conservation", was not anticipated. It arose because of the inability to satisfy the volume conservation condition, equation (3), for positive real roots. The border of this region is defined for negative values of a_2 by the relation:

$$a_4 = \sqrt[3]{-0.02\ a_2^5}$$

In the vicinity of spherical (-1,0) the deformation energy could be represented by a paraboloid, which is slightly mis-aligned from the coordinate axes. This mis-alignment is an indication that the chosen parameter set (a_2, a_4) are not those which diagonalize the potential energy, even in the vicinity of spherical. This mis-alignment should contribute to some mixing of the a_2 and a_4 motions for small oscillations about spherical.

Numerical Calculations of the Motion

While a many term velocity potential (large "N" in equation (12)) would be capable of satisfying the boundary condition to a greater accuracy, the complications of the expressions involved (and increased computer time) dictated that a simple velocity potential be used to investigate the motion. The simplest velocity potential, which results in an independent set of simultaneous differential equations in $\ddot{a}_2$ and $\ddot{a}_4$, is for N=2 in equations (12). For this two term

velocity potential the specific expressions required for the kinetic energy, boundary condition integral,and equations of motion are developed in Appendix IX. Using these expressions and a suitable integration scheme the problem was programmed in FORTRAN for the CDC 6600 computer.

The first integration technique attempted used the relations:

$$\dot{a}_\kappa\,(t_{N+1}) = \dot{a}_\kappa\,(t_N) + \ddot{a}_\kappa(t_N)\,\Delta t$$

$$a_\kappa\,(t_{N+1}) = a_\kappa\,(t_N) + \dot{a}_\kappa(t_N)\,\Delta t$$

for $\kappa=2,4$

This failed to give simple harmonic motion about spherical, probably because of too large a value for Δt and the coupling of the a_2 and a_4 motions.

Successful integrations were obtained by the Runge-Kutta method. An excellent concise account of this method is given by Scarborough[50]. An available computer subroutine utilizing a dual pass 4th order Runge-Kutta was used. The interval determining and self testing features of the subroutine are described in Appendix X.

The motion experienced by the liquid drop in the present description depends only on the initial values of variables a_2, a_4, $\dot{a}_2$, and $\dot{a}_4$. For this set of initial values at time zero the corresponding values of the accelerations ($\ddot{a}_2$ and $\ddot{a}_4$), energies (B_κ, ξ, and total= $B_\kappa+\xi$),and GSI are calculated. By Runge-Kutta integration the values of

---

[50] J. B. Scarborough, Numerical Mathematical Analysis, (The Johns Hopkins Press, Baltimore, 1966) pp. 358-367.

a_2, a_4, $\dot{a}_2$, and $\dot{a}_4$ are computed to an accuracy of 5 decimal digits at a time of 0.1 T_0 seconds. For the value of the variables at 0.1 T_0 seconds the corresponding accelerations, energies, and GSI are calculated. Time is advanced by 0.1 T_0 seconds; and using the values of a_2, a_4, $\dot{a}_2$, and $\dot{a}_4$ from the integration just completed, the process is continued. Before each integration is begun, the values of time, the variables, the accelerations, the energies, and GSI are stored for eventual tabulation. The calculation is terminated by the completion of 100 time steps, the occurrence of scission, or the elapse of the alloted computer time. In general the 100 time steps for the 5 decimal digit accuracy required computer runs from 60 to 90 minutes.

To investigate the motion about spherical the initial conditions were always for $a_2 = -1.0$, $a_4 = 0.0$, and $\dot{a}_4 = 0$. The motions for three initial values of $\dot{a}_2$ are discussed. If the deformation energy surface had been aligned with the a_2-a_4 axes, these initial conditions would generate no motion in the a_4 direction. In such a case the period of oscillation in a_2 (or $\dot{a}_2$) would be 4.3566 T_0 for X=0.74 (from equation (22)). The kinetic and potential energies would oscillate with half that period, since B_K is proportional to $\dot{a}_2^2$ (from equation (23)). The total energy should remain constant at the value of the initial kinetic energy, since there is zero deformation (potential) energy at the spherical configuration.

In Table IV the initial values of $\dot{a}_2$ are listed along with the initially computed accelerations ($\ddot{a}_2$ and $\ddot{a}_4$) and kinetic energy. The calculated initial kinetic energy is in all three cases precisely that given by equation (23). As predicted the initial accelerations, both $\ddot{a}_2$ and $\ddot{a}_4$, are approximately proportional to the square of the initial input velocity.

From these properties the effects of increasing the energy to remove the motion from the class of "small oscillations" are not obvious.

TABLE IV

INITIAL VALUES OF THE ACCELERATIONS AND KINETIC ENERGY CAUSED BY THREE INITIAL VELOCITIES FOR MOTION ABOUT SPHERICAL

$\dot{a}_2$	$\ddot{a}_2$	$\ddot{a}_4$	B_K
0.01	-0.5046×10^{-3}	0.4454×10^{-3}	$0.5555^{\cdot}\times10^{-6}$
0.1	-0.3751×10^{-1}	0.3015×10^{-1}	$0.5555^{\cdot}\times10^{-4}$
1.0	$-0.3738\times10^{+1}$	$0.3000\times10^{+1}$	$0.5555^{\cdot}\times10^{-2}$

Fig. 20, 21, and 22 show the time variations of a_2, a_4, B_K and total energy for these three cases. The most consistent feature of all three motions is the constancy of the total energy. For the motion with the least energy (Fig. 20) the observed period of oscillation is 4.36 T_0. While not shown the ratio of the maximum excursions of $\dot{a}_4$ to $\dot{a}_2$ is approximately $\frac{1}{100}$; thus the contribution of the a_4 motion to the kinetic energy would be insignificant. For the next larger motion $\dot{a}_2=0.1$ (Fig.21) the ratio of the maxima of $\dot{a}_4$ to $\dot{a}_2$ is approximately $\frac{1}{10}$. Again since the kinetic energy is proportional to the square of the velocity components, the effect of $\dot{a}_4$ on the kinetic energy is indiscernible. However, the increased amplitude has affected the period of oscillation slightly, raising it to 4.37 T_0. When $\dot{a}_2=1.0$ (Fig.22), the coupling effect between the a_2 and a_4 motions is quite apparent. In this case $\dot{a}_2$ and $\dot{a}_4$ have about the same amplitude of variation, and the kinetic energy no longer has a true sinusoidal appearance.

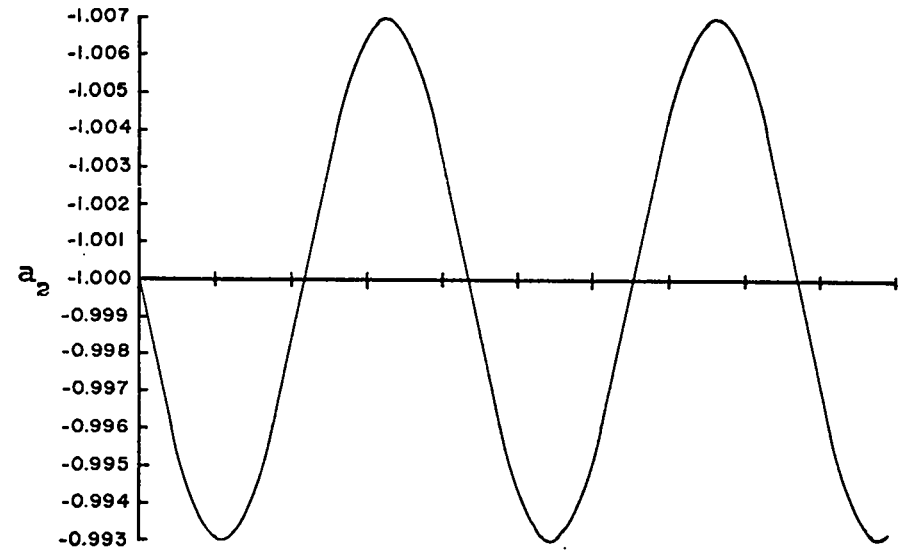

Note that the ordinate scale of a_2 is one hundred times that of a_4.

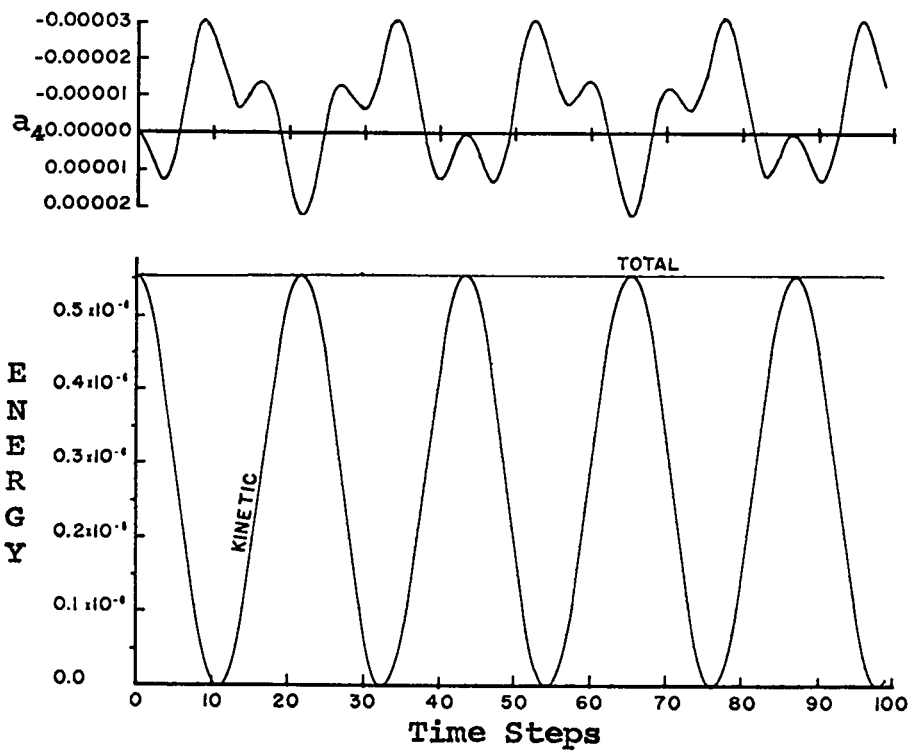

Fig. 20. Time variation of a_2, a_4, kinetic and total energies for small oscillations about spherical. Initial conditions were: $a_2=-1.0, a_4=0.0, \dot{a}_2=0.01, \dot{a}_4=0.0$

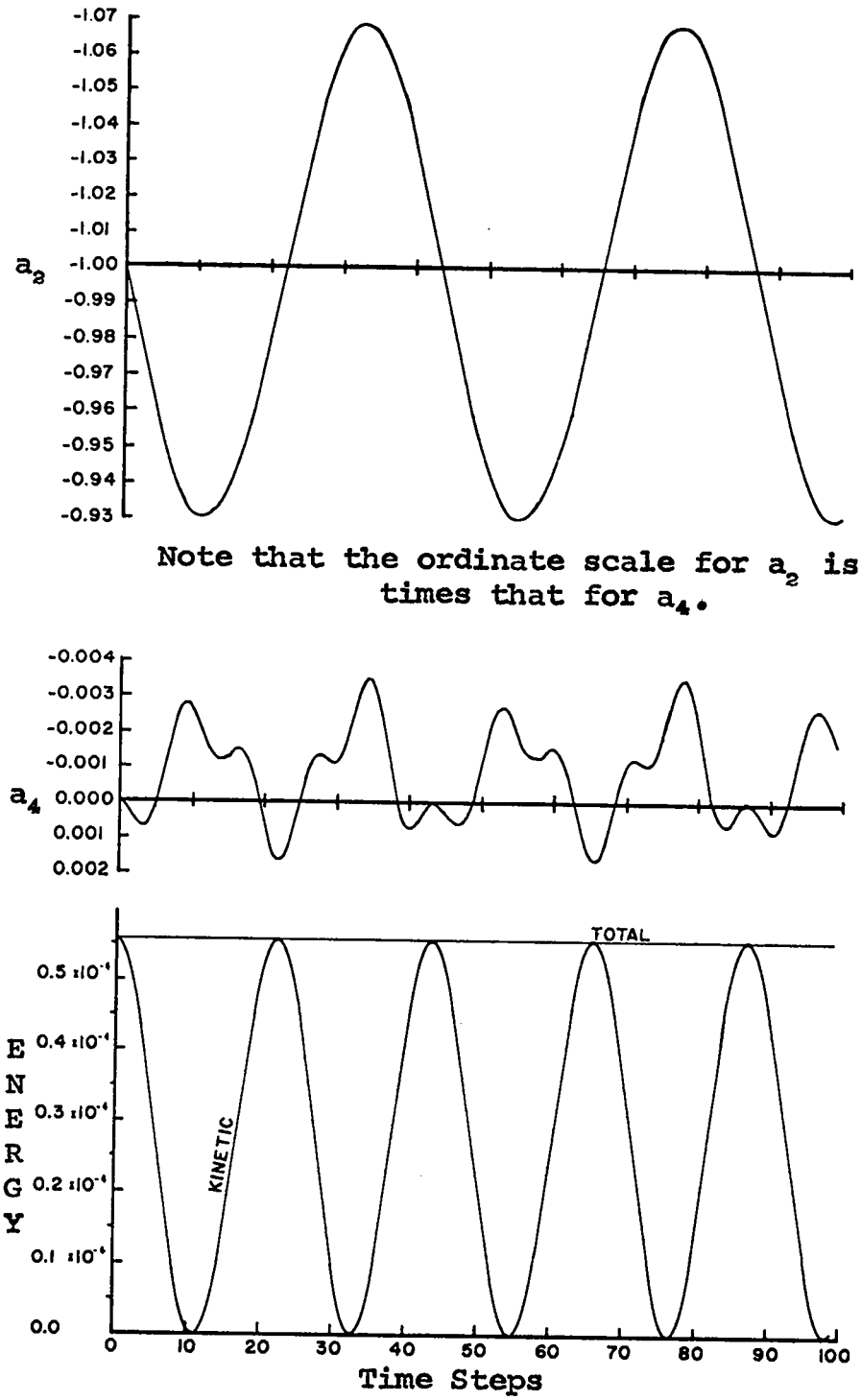

Fig. 21. Time variation of a_2, a_4, kinetic and total energies for oscillations about spherical. Initial conditions were:

$$a_2=-1.0, a_4=0.0, \dot{a}_2=0.1, \dot{a}_4=0.0$$

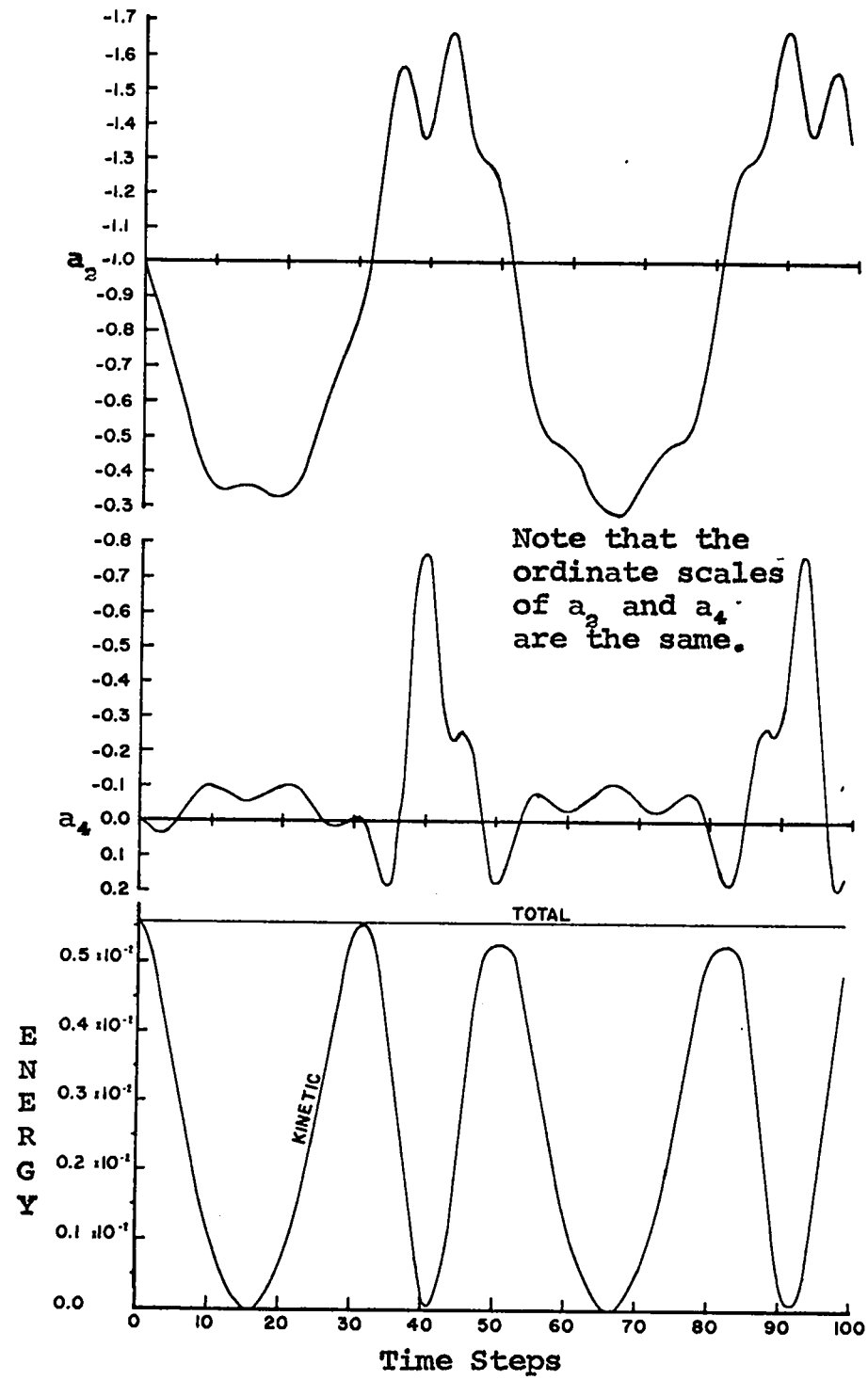

Fig. 22. Time variation of a_2, a_4, kinetic and total energies for oscillations about spherical. Initial conditions were:

$$a_2=-1.0, a_4=0.0, \dot{a}_2=1.0, \dot{a}_4=0.0$$

The single cycle in the variation of a_2 is about 5.2 T_0, a significant increase over that for the "small oscillations". In Fig. 23 the motion on the deformation (potential) energy surface is shown for $\dot{a}_2$ (initial) = 1.0. The small circled numbers indicate the number of time steps to reach that configuration. After the 66th time step the motion began backtracking its path. At the 40th, 50th and 66th time steps the shapes of the drops are shown.

An indication of how well the two term velocity potential is capable of satisfying the boundary condition integral (equation (17)) is supplied from these motion studies. In all three cases for the spherical configuration GSI=0. For the calculated motions the magnitude of GSI varies from configuration to configuration. However, the maximum value of GSI is $\sim 10^{-19}$, $\sim 10^{-13}$, and $\sim 10^{-5}$ for the motions induced by $\dot{a}_2$ (initial values) 0.01, 0.1, and 1.0, respectively.

In Fig. 24 is shown the motion induced by the initial conditions: a_2=0.25, a_4= -.09, $\dot{a}_2$=0, and $\dot{a}_4$=0. From a standing start on the scission side of the saddle point, 28 time steps (or 2.8 T_0 seconds) were required to accomplish scission. In Fig. 25 the motion was initiated at the saddle point with $\dot{a}_2$=.01 and $\dot{a}_4$=.00075 (initial kinetic energy = $.3425 \times 10^{-4}$), and scission occurred in 60 time steps. With a zero or near zero initial momentum one might naively expect the path to scission to be directly down the gradient of the potential energy surface. However, as Wilets[51] has remarked in discussing the qualitative

---

[51] L. Wilets, Theories of Nuclear Fission, (Clarendon Press, Oxford, 1964) pp. 46-47.

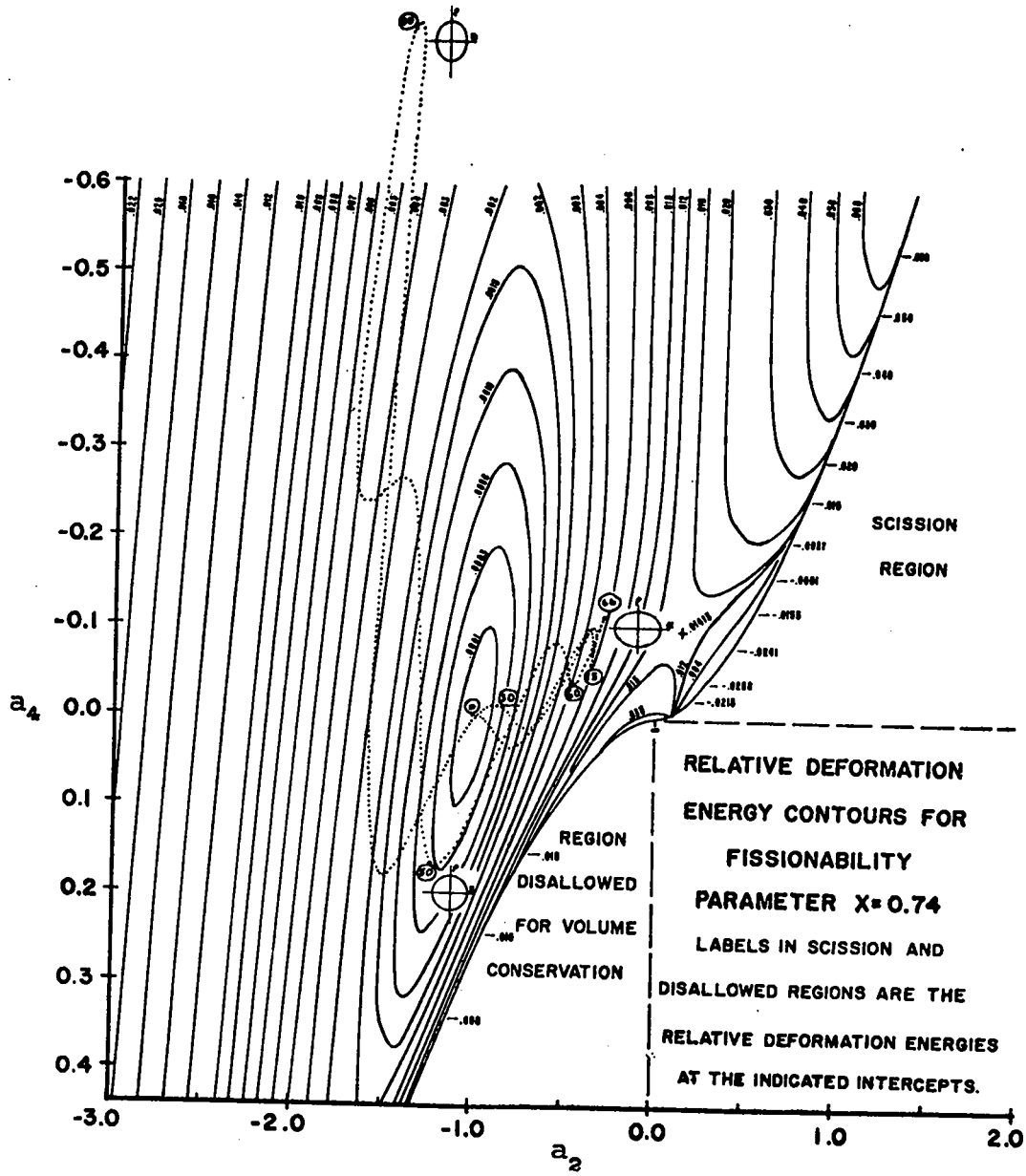

Fig. 23. Dotted curve traces the motion on the deformation energy surface from a spherical (a_2=-1.0, a_4=0.0) start with a_2=1.0 and a_4=0.0. Small circled numbers indicate the number of time steps required to reach that configuration. Inserts are the drop shapes at the 40th, 50th, and 66th time steps.

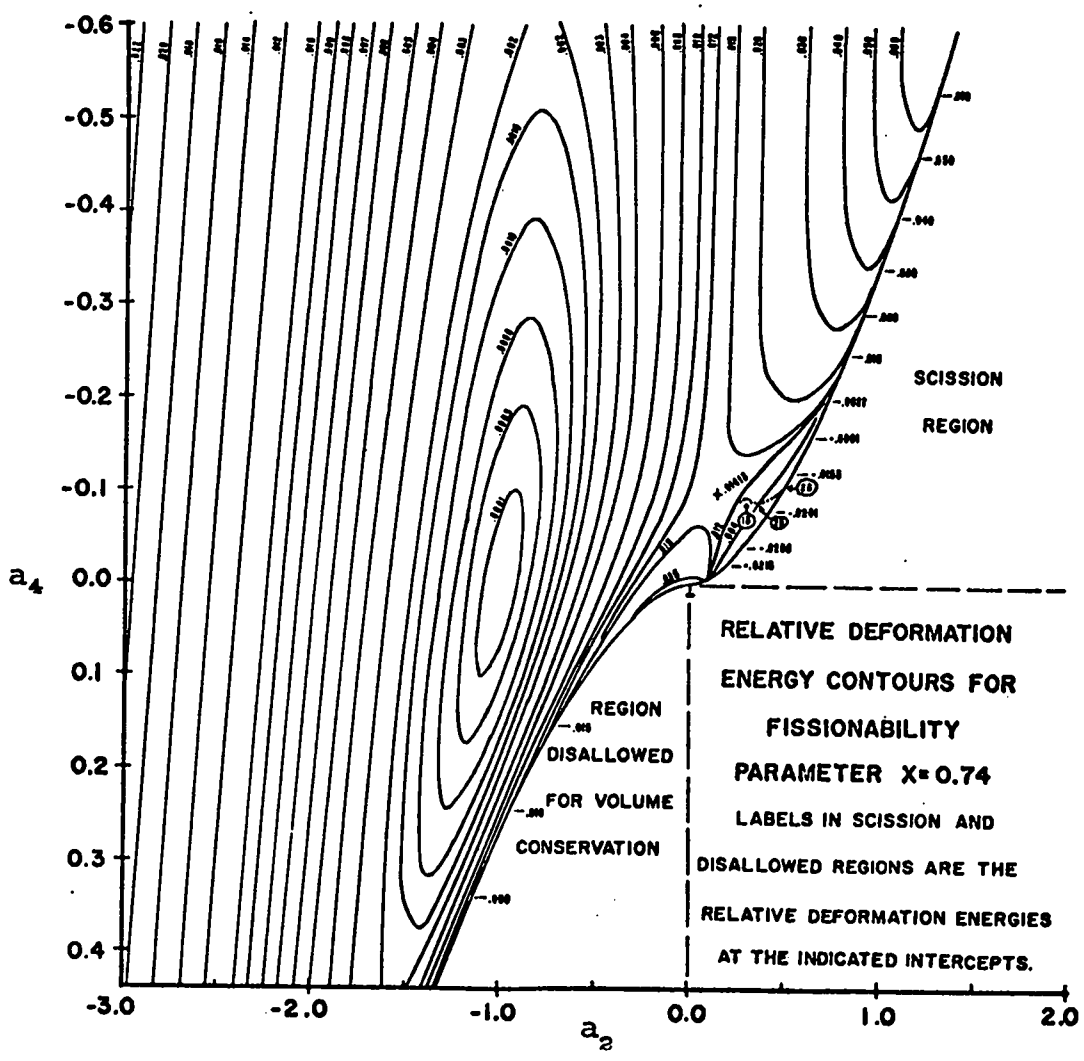

Fig. 24. Dotted curve traces the motion on the deformation energy surface from a stationary start on the scission side of the saddle point. Initial conditions were: $a_2=0.25, a_4=-0.09, \dot{a}_2=0.0; \dot{a}_4=0.0$. Small circled numbers indicate the number of time steps to reach that configuration. Scission was accomplished in 28 time steps.

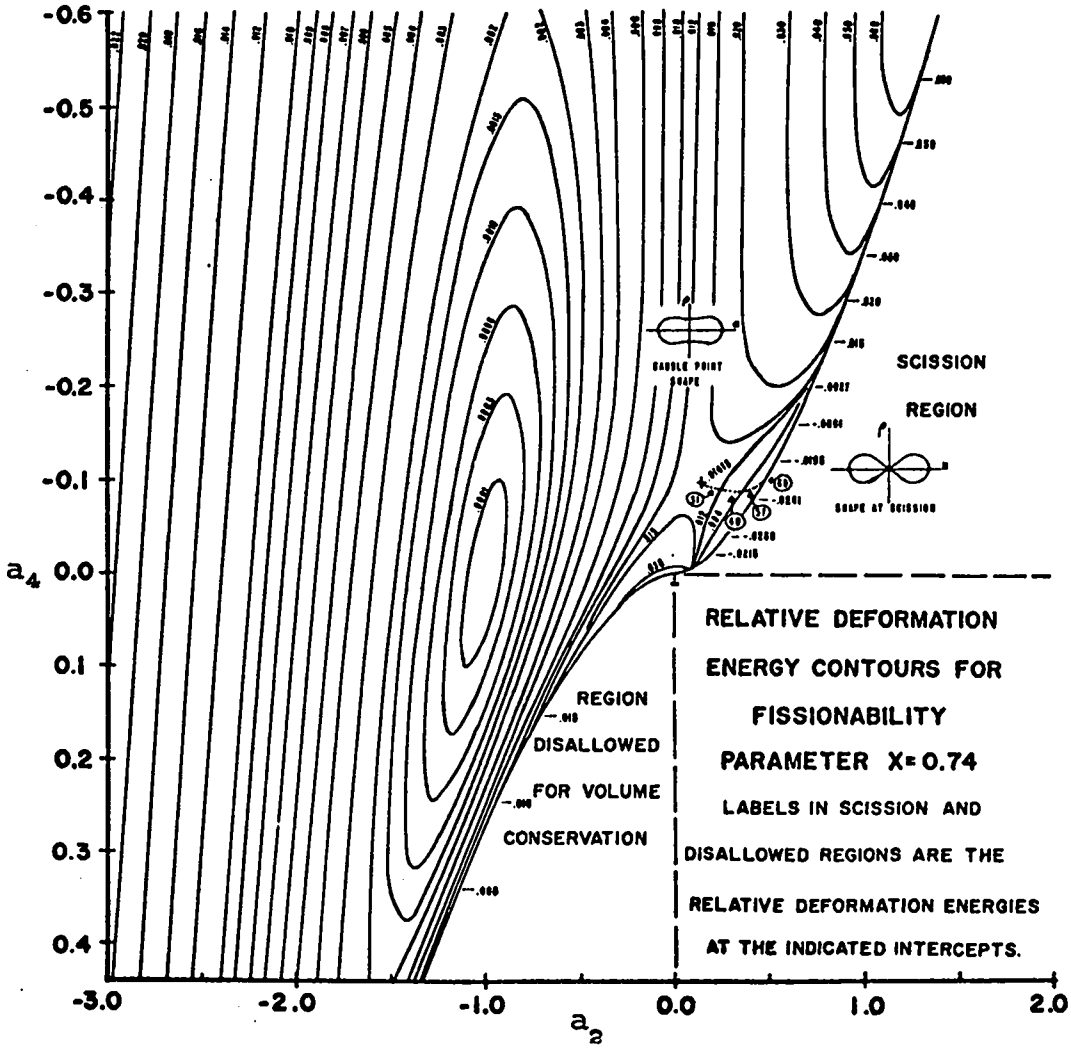

Fig. 25. Dotted curve traces the motion on the deformation energy surface from the saddle point with small initial velocities in the direction of scission. Initial conditions were: $a_2=0.1458, a_4=-0.09822, \dot{a}_2=0.01, \dot{a}_4=0.00075$. Small circled numbers indicate the number of time steps required to reach that configuration. Scission was accomplished in 60 time steps.

features of the deformation energy surface, such motion would occur when the kinetic energy was solely a function of the sum of the squares of the velocity components. He[51] implies that the motion cannot be arbitrarily predicted when the "mass" is coordinate dependent and mixed products of the velocities occur in the kinetic energy expression. Since the kinetic energy of this theoretical treatment (equation (14)) is of the latter form, the observed motion was to be expected.

Two cases of scission with the motion begun at the spherical configuration appear in Figs. 26 and 27. In Fig. 26 zero initial velocity was given in the a_4 direction and $\dot{a}_2=1.7$. The initial kinetic energy of 0.01606 well exceeded the saddle point energy of 0.01413, and scission occurred in 59 time steps. In Fig. 27 $\dot{a}_2$(initial) = 2.0 and $\dot{a}_4$(initial) = -0.45,corresponding to a kinetic energy of 0.01451. In this case the available energy exceeded the fission threshold (saddle point energy) by very little. Due to the oscillations about the saddle point this motion required 89 time steps to scission.

In Fig. 28 the motion was started from spherical with $\dot{a}_2=1.6$ and $\dot{a}_4=0$. The initial kinetic energy of 0.0142222 is in excess of the saddle point energy of 0.01413. However, scission did not occur. The saddle point was approached, but the motion oscillated "between the hills on two sides of the saddle". The maximum deformation energy attained was 0.0142189, when the kinetic energy reached a minimum of 0.0000033 at 50 time steps. The motion then proceeded to approximately retrace its path in the direction of the spherical configuration. Had the path of approach to the saddle been different and the component of motion in the a_2 direction been greater as the saddle was neared, the energy available was sufficient to lead to scission.

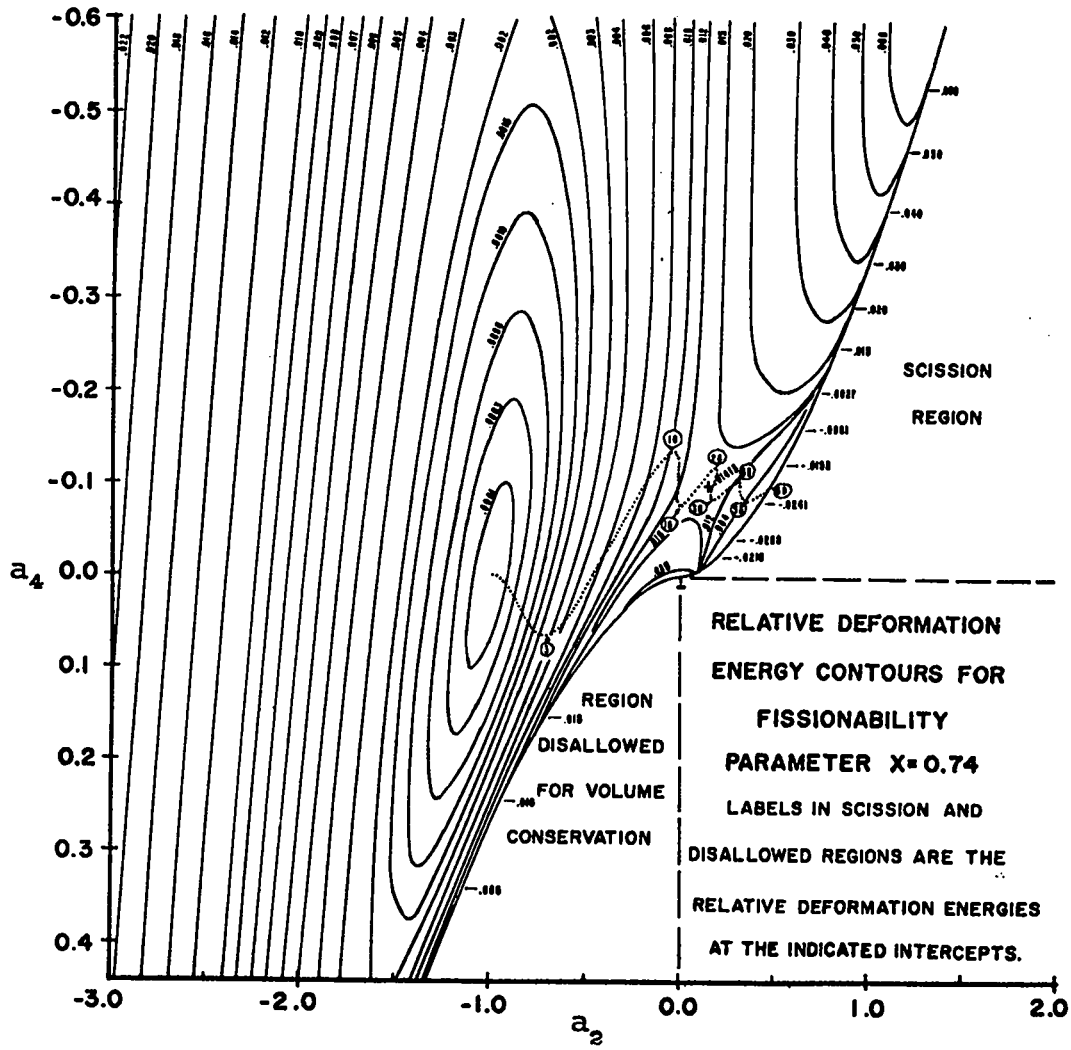

Fig. 26. Dotted curve traces the motion on the deformation energy surface from the spherical configuration with sufficient initial kinetic energy to pass over the fission barrier. Initial conditions were: $a_2=-1.0, a_4=0.0, \dot{a}_2=1.7, \dot{a}_4=0.0$. Initial kinetic energy was 0.01606. Saddle point energy was 0.01413. Small circled numbers indicate the number of time steps required to reach that configuration. Scission was accomplished in 59 time steps.

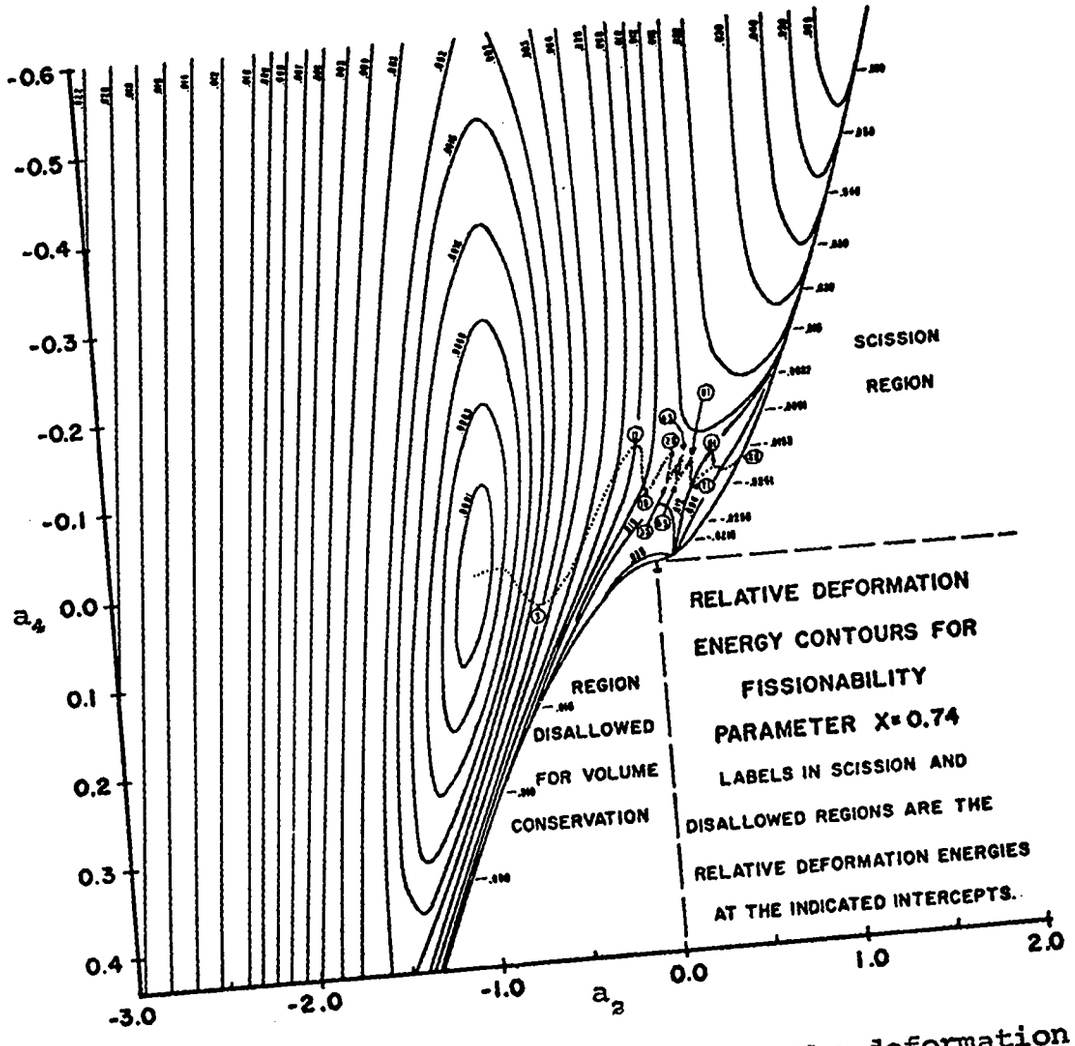

Fig. 27. Dotted curve traces the motion on the deformation energy surface from the spherical configuration with sufficient initial kinetic energy to pass over the fission barrier. Initial conditions were: a_2=-1.0, a_4=0.0, $\dot{a}_2$=2.0, $\dot{a}_4$=-0.45. Initial kinetic energy was 0.01451. Saddle point energy was 0.01413. Small circled numbers indicate the number of time steps required to reach that configuration. Scission was accomplished in 89 time steps.

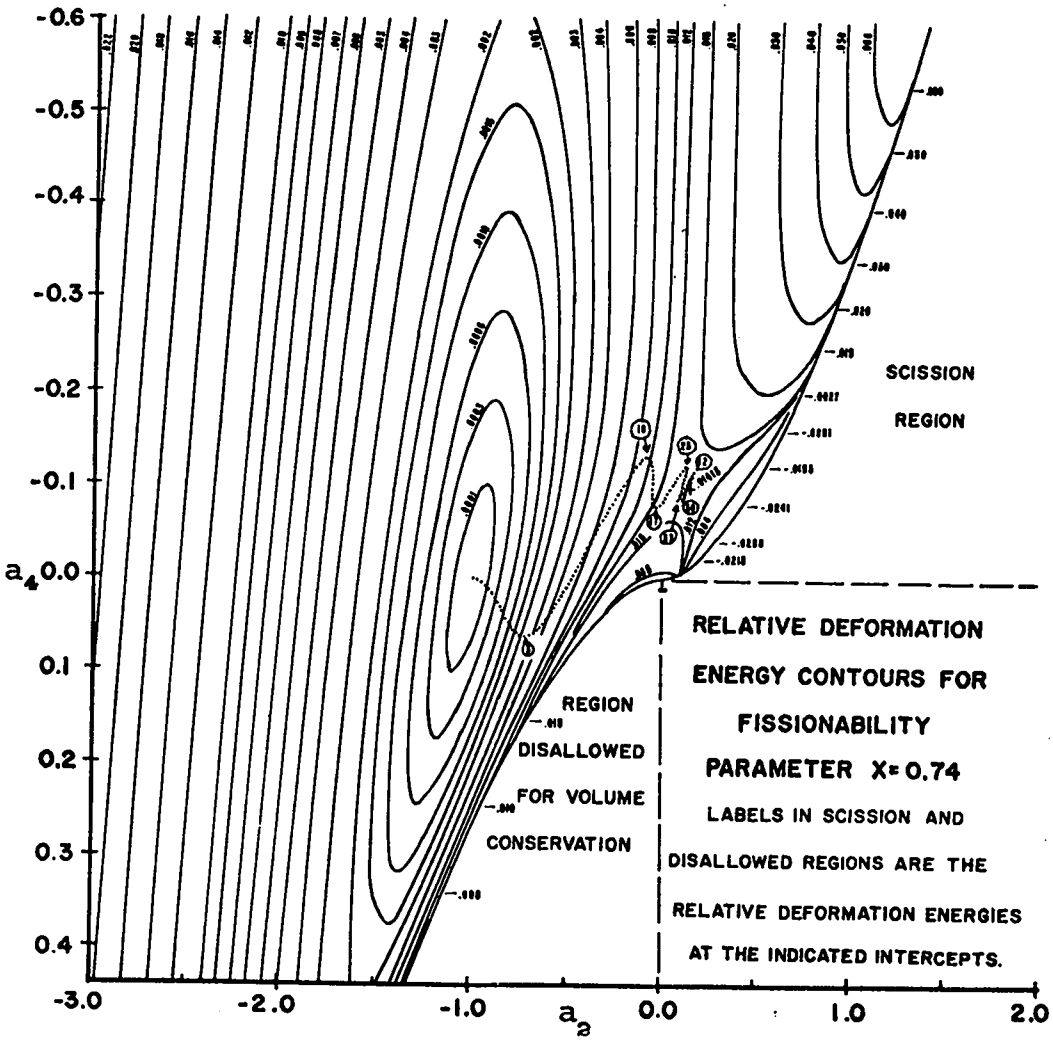

Fig. 28. Dotted curve traces the motion on the deformation energy surface from the spherical configuration. With sufficient initial kinetic energy (0.0142222) to pass over the fission barrier (0.01413), the system failed to scission when the motion became out of phase with crossing the saddle point. After 50 time steps the motion began to approximately retrace its course towards the spherical configuration. Initial conditions were: $a_2=-1.0, a_4=0.0, \dot{a}_2=1.6, \dot{a}_4=0.0$. Small circled numbers indicate the number of time steps required to reach that configuration.

In the motions which proceed to scission the value of the boundary condition integral GSI grew from about 10^{-5} at the saddle to about 10^{-2} just prior to scission. This suggests that a more complicated velocity potential than that used in these numerical calculations could provide a better fit to the boundary conditions as scission is accomplished.

Future Efforts and Conclusions

A considerable effort was made to develop an alternative theoretical treatment along somewhat different principles. Basic to this second approach was the statement of Kelvin's minimum energy theorem[16], as given in the section REVIEW OF FISSION THEORY. For a velocity potential of a form which did not satisfy Laplace's equation:

$$-\varphi = \sum_{\substack{i=0 \\ j=0 \\ 0=i\neq j=0 \\ \varkappa=2,4}}^{\substack{I \\ J}} \dot{a}_{\varkappa}\beta_{i,j,\varkappa}\rho^{2i}z^{2j}$$

the boundary condition (equation (16)) was to be satisfied exactly over the range $-z_o$ to z_o. This condition was not sufficient to determine all of the $\beta_{i,j,\varkappa}$'s. The remaining $\beta_{i,j,\varkappa}$'s were to be determined by the condition of minimization of kinetic energy, in view of Kelvin's minimum energy theorem. Calculations of small amplitude motions about spherical did not agree with the predictions of Rayleigh[48], and Plesset[49]. In analysis this was ascribed to relaxation of the restriction of incompressibility (satisfaction of Laplace's equation). Further work attempting to incorporate the compressibility corrections was deferred to the future.

The immediately obvious continuation of this study is the inclusion of more terms in the velocity potential. The algebraic manipulations (required to obtain the equations of motion) are long and complicated, but use of the IBM experimental programming system FORMAC (FOmula MAnipulation Compiler) would reduce the labor involved. While a more complicated velocity potential should reduce the boundary condition integral at all shape configuration, its effect on the motion is certainly of interest but unpredictable from the general equations.

A two parameter description of the liquid drop shape has been used to calculate the deformation energy and fission barrier shapes of a uniformly charged liquid drop. The calculations compare favorably with other work that used a nine-parameter description of the shape. The agreement was best for values of the fissionability parameter X greater than 0.70.

With the additional assumptions of incompressibility and irrotational fluid flow the equations of motion for such a two parameter liquid drop were developed. Subject to the minimization of the error in the fulfillment of the boundary conditions calculations of the motion of the liquid drop were performed. The calculated motions,even for a simple form of the velocity potential,were in substantial agreement with the predicted motion a fissioning liquid drop.

Consideration was restricted to symmetric shapes and symmetric fission. By including additional parameters in the equation defining the shape of the liquid drop it should be possible within the framework of the developed theory to describe asymmetric fission without taxing the memory capabilities of the currently available computers.

APPENDIX I

In considering small deviations from a spherical drop, the radius may be expressed as

$$r = R\left(1 + \alpha_2 P_2 (\cos\theta)\right) = R\left(1 - \frac{\alpha_2}{2} + \frac{3}{2}\alpha_2 \mu^2\right)$$

where α_2 is a small quantity compared to unity, and

$$\mu = \cos\theta.$$

Imposing the condition that this distorted spheroid has the same volume as the sphere of radius R_0, we set

$$\frac{4\pi}{3} R_0^3 = \int_0^{2\pi} d\varphi \int_0^{\pi} \sin\theta d\theta \int_0^{r(\theta)} r^2 dr$$

$$= \frac{2\pi}{3}\int_0^{\pi} r^3 (\theta) \sin\theta d\theta = \frac{2\pi}{3}\int_{-1}^{1} r^3 (\mu)\, d\mu$$

$$= \frac{2\pi R^3}{3}\int_{-1}^{1}\left(1 - \frac{\alpha_2}{2} + \frac{3}{2}\alpha_2 \mu^2\right)^3 d\mu$$

Neglecting terms of order α_2^3 and higher, we obtain

$$\frac{4\pi}{3}R_0^3 \cong \frac{2\pi R^3}{3}\int_{-1}^{1}\Big(1 - \frac{3}{2}\alpha_2 + \frac{3}{4}\alpha_2^2 + \frac{9}{2}\alpha_2\mu^2 - \frac{9}{2}\alpha_2^2\mu^2 + \frac{27}{4}\alpha_2^2\mu^4\Big)\, d\mu$$

$$\cong \frac{4\pi}{3}R^3\left(1+\frac{3}{5}\alpha_2^2\right)$$

Solving for R, and using the binomial expansion to retain only terms of order α_2^2 or lower, we get

$$R \cong R_0\left(1-\frac{1}{5}\alpha_2^2\right) \tag{A1}$$

To find the surface energy we must evaluate the integral

$$E_s = \Phi\int dS = \Phi\iint r^2\left[1+\left(\frac{dr}{rd\theta}\right)^2\right]^{\frac{1}{2}}\sin\theta d\theta d\varphi$$

Discarding terms in α_2 higher than squared in evaluating $\left[1+\left(\frac{dr}{rd\theta}\right)^2\right]^{\frac{1}{2}}$ by the binomial expansion, and integrating with respect to φ,

$$E_s \cong 2\pi R^2\,\Phi\int_0^{\pi}\left(1+\alpha_2P_2\right)^2\left(1-\frac{9}{2}\alpha_2^2\cos^2\theta\sin^2\theta\right)\sin\theta d\theta$$

$$\cong 2\pi R^2\,\Phi\int_0^{\pi}\left(1+2\alpha_2^2P_2^2+\alpha_2^2P_2^2-\frac{9}{2}\alpha_2^2\cos^2\theta\sin^2\theta\right)\sin\theta d\theta$$

$$\cong 4\pi R^2\,\Phi\left(1+\frac{4}{5}\alpha_2^2\right)$$

Substituting for R by equation A1, expanding, and retaining terms of order α_2^2 or lower, we obtain

$$E_s \cong 4\pi\,\Phi\,R_0^2\left(1+\frac{2}{5}\alpha_2^2\right) = E_s^{\circ}\left(1+\frac{2}{5}\alpha_2^2\right) \tag{A2}$$

To find the Coulomb energy we evaluate

$$E_c = \tfrac{1}{2}\sigma^2\iint\frac{d\tau_1\,d\tau_2}{r_{12}} = \tfrac{1}{2}\sigma^2\int V(r_1,\theta_1)\,d\tau_1$$

where $V(r_1,\theta_1) = \int\frac{d\tau_2}{r_{12}}$ = electrostatic potential

The term $\frac{1}{r_{12}}$ can be expanded in Legendre polynomials as

$$\frac{1}{r_{12}} = \sum_{k=0}^{\infty} \frac{r_2^k}{r_1^{k+1}} P_k (\cos \theta_{12}) \quad \text{for } r_2 < r_1$$

$$= \sum_{k=0}^{\infty} \frac{r_1^k}{r_2^{k+1}} P_k (\cos \theta_{12}) \text{ for } r_2 > r_1$$

where θ_{12} is the angle between the points.

Evaluating $V(r_1, \theta_1)$ first, we write

$$V(r_1, \theta_1) = \iint \sin \theta_2 d\theta_2 d\varphi_2 \int_0^{r_1} \frac{r_2^2}{r_{12}} dr_2 \quad \text{for } r_2 < r_1$$

$$+ \iint \sin \theta_2 d\theta_2 d\varphi_2 \int_{r_1}^{r(\theta_2)} \frac{r_2^2}{r_{12}} dr_2 \text{ for } r_2 > r_1$$

Substituting for $\frac{1}{r_{12}}$ and integrating over r_2, we obtain

$$V(r_1, \theta_1) = \sum_{k=0}^{\infty} \frac{r_1^2}{(k+3)} \iint d\omega_2 P_k (\cos \theta_{12}) +$$

$$\sum_{k \neq 2} \frac{r_1^k}{(-k+2)} \iint d\omega_2 P_k (\cos \theta_{12}) r^{-k+2} -$$

$$\sum_{k \neq 2} \frac{r_1^2}{(-k+2)} \iint d\omega_2 P_k (\cos \theta_{12}) +$$

$$\iint d\omega_2 P_2 (\cos \theta_{12}) r_1^2 \ln \frac{r}{r_1}$$

where $d\omega_2 = \sin \theta_2 d\theta_2 d\varphi_2$.

The integrals involving P_k (cos θ_{12}) are evaluated using the relation

$$P_k \ (\cos \theta_{12}) = \sum_{m=-k}^{k} \frac{(k-m)!}{(k+m)!} P_k^m \ (\cos \theta_1) \ P_k^m \ (\cos \theta_2) \ e^{im(\varphi_1-\varphi_2)}$$

where P_k^m are the associated Legendre functions.

By the orthoginality conditions the integration over φ_2 is zero except for m = 0, which gives an answer of "2π", and the integration over θ_2 is zero except when terms of the form $\int P_k^2 d\theta$ occur and give $\frac{2}{2k+1}$. Upon substituting $r = R\left(1+\alpha_2 P_2 \ (\cos \theta_2)\right)$, performing the integration, and retaining terms of order α_2^2 or less, one obtains

$$V(r_1, \ \theta_1) = -\frac{2}{3} \pi r_1^2 + 2\pi R^2 + \frac{4}{5} \pi r_1^2 \ \alpha_2 P_2 \ (\cos \theta_1) + \pi R^2 \sum_{k=0}^{\infty} \left(\frac{r_1}{R}\right)^k (-k+1) \ \alpha_2^2 \ C_{k22} \ P_k \ (\cos \theta_1)$$

where $C_{k22} = \int_0^{\pi} \sin \theta_2 d\theta_2 \ P_k \ (\cos \theta_2) \ P_2^2 \ (\cos \theta_2)$.

Performing the integration over $d\tau_1 = r_1^2 \sin \theta_1 \ dr_1 d\theta_1 d\varphi_1$, and retaining only those terms of order α_2^2, yields four corresponding terms as

$$\frac{E_c}{\frac{I}{2}\sigma^2} = \int V(r_1, \ \theta_1) \ d\tau_1 = \frac{-8\pi^2 R^5}{15} \left(1+2\alpha_2^2\right) + \frac{8\pi^2 R^5}{3} \left(1+\frac{3}{5}\alpha_2^2\right) + \frac{16}{25} \pi^2 R^5 \ \alpha_2^2 + \frac{8}{15} \pi^2 R^5 \ \alpha_2^2$$

Collecting terms, substituting $\sigma = Ze/\frac{4}{3}\pi R_o^3$ and $R \cong R_o(1-\frac{1}{5}\alpha_2^2)$, and discarding terms of order higher than α_2^2, one finally obtains

$$E_c \cong \frac{3}{5}\frac{Z^2e^2}{R_o}\left(1-\frac{1}{5}\alpha_2^2\right) = E_c^\circ\left(1-\frac{1}{5}\alpha_2^2\right) \qquad \text{(A3)}$$

APPENDIX II

Since in practice the potential surface near the saddle point is a quadratic surface, it is sufficient to discuss the property of quadratic forms. As mentioned in the body of this paper, the necessary condition for a point to represent a saddle point (or a local maximum or minimum or inflection point) is that all the first partial derivatives vanish at that point. Such a point is termed a "critical point". Limiting the discussion to the quadratic form, $f = \sum a_{ij} x_i x_j$, such a critical point can only represent a saddle point, maximum or minimum, but not an inflection point (as this requires surfaces of higher order than quadratic).

Such a quadratic surface is conveniently expressed in matrix form as

$$f = \begin{vmatrix} a_{11} & a_{12} & \cdot & \cdot & \cdot & \cdot & a_{1n} \\ \cdot & a_{22} & & & & & \cdot \\ \cdot & & & & & & \cdot \\ \cdot & & & & & & \cdot \\ a_{n1} & \cdot & \cdot & \cdot & \cdot & \cdot & a_{nn} \end{vmatrix}$$

where we recognize that $a_{ij} = \frac{\partial^2 f}{\partial x_i \partial x_j}$.

We restrict discussion to real symmetric matrices. It can be shown that by a unitary transformation such a matrix can be diagonalized provided the determinant of f is nonzero. A zero matrix would imply that all the elements of the matrix are not independent, and this condition we exclude. It can also be shown that the determinants of the principal minors of the f, i.e., $\left|a_{11}\right|$, $\begin{vmatrix} a_{11} & a_{12} \\ a_{21} & a_{22} \end{vmatrix}$ etc., are invariant under such a transformation.

The transformed matrix is real and diagonal, and the elements along the diagonal are the unmixed second derivatives of the function with respect to the transformed coordinates. Thus, for the unitary matrix T

$$f' = T^{-1} f T = \begin{vmatrix} \frac{\partial^2 f'}{\partial x_1'^2} & & & 0 \\ & \frac{\partial^2 f'}{\partial x_2'^2} & & \\ & & \ddots & \\ 0 & & & \frac{\partial^2 f'}{\partial x_n'^2} \end{vmatrix}$$

Near the critical point $(x_1^\circ, x_2^\circ, \ldots, x_n^\circ)$, f' is a representation of the potential function V. Expanding V about the critical point to second order in a Taylor series yields

$$V-V_0 \cong \frac{\partial^2 V}{\partial x_1'^2}\left(x_1' - x_1^\circ\right)^2 + \frac{\partial^2 V}{\partial x_2'^2}\left(x_2' - x_2^\circ\right)^2 + \ldots + \frac{\partial^2 V}{\partial x_n'^2}\left(x_n' - x_n^\circ\right)^2$$

This expression shows that the critical point is a minimum if the unmixed second derivatives are all positive, a maximum if all are negative, and a saddle point if some are positive and the rest are negative. The equivalent result, stated in terms of the original (nondiagonal) matrix f, is proven by matrix techniques in Watson Fulks, "Advanced Calculus", John Wiley & Son, Inc., New York, 1961.

APPENDIX III

Let the shape of the liquid drop be defined by equation (A4) rotated about the Z-axis:

$$P_o^2 = C+A_2Z^2+A_4Z^4 \tag{A4}$$

where P_o and Z have the dimensions of length, C the dimension of squared length, A_4 of reciprocal squared length and A_2 is dimensionless. Dividing equation (A4) by R_o^2 results in a dimensionless form:

$$\rho_o^2 = c+a_2z^2+a_4z^4 \tag{A5}$$

where

$$\left.\begin{aligned} \rho_o &= P_o/R_o \\ z &= Z/R_o \\ c &= C/R_o^2 \\ a_2 &= A_2 \\ a_4 &= A_4R_o^2 \end{aligned}\right\} \tag{A6}$$

By defining R_o to be the radius of the sphere having the same volume as the multitude of closed shapes given by equation (A4), the quantities ρ_o and z become the coordinates relative to the radius of the spherical configuration.

For simply connected closed shapes the maximum value of Z in equation (A4) occurs when $P_o=0$, and is designated as Z_o. The volume of the surface of rotation is:

$$\text{Volume} = \pi\int_{-Z_o}^{Z_o} P_o^2\,dZ = 2\pi(CZ_o+\tfrac{1}{3}A_2Z_o^3+\tfrac{1}{5}A_4Z_o^5)$$

Equating this to the volume of the sphere of radius, R_o, the condition for volume preservation becomes:

$$\tfrac{4}{3}\pi R_o^3 = 2\pi(CZ_o+\tfrac{1}{3}A_2 Z_o^3+\tfrac{1}{5}A_4 Z_o^5)$$

or in the dimensionless form:

$$-\tfrac{3}{10}a_4 z_o^5-\tfrac{1}{3}a_2 z_o^3-\tfrac{3}{2}cz_o+1 = 0 \qquad \text{(A7)}$$

Combining equation (A7) with the defining equation for z_o, i.e.,

$$\rho_o^2 = 0 = c+a_2 z^2+a_4 z^4 \qquad \text{(A8)}$$

results in the equation for volume preservation given in the text as equation (3):

$$f(z_o) = a_2 z_o^3+\tfrac{6}{5}a_4 z_o^5+ 1 = 0 \qquad \text{(A9)}$$

Equations (A8) and (A9) indicate that $z_o = z_o(a_2, a_4)$ and $c = c(z_o; a_2, a_4) = c(a_2, a_4)$. In such a case the time derivatives of c can be expressed as:

$$\dot{c} = \dot{a}_2 \frac{\partial c}{\partial a_2} + \dot{a}_4 \frac{\partial c}{\partial a_4} \qquad \text{(A10)}$$

The partial derivatives of z_o and c are:

$$\left.\begin{aligned} \frac{\partial z_o}{\partial a_2} &= -\frac{z_o}{3(a_2+2a_4 z_o^2)} \\ \frac{\partial z_o}{\partial a_4} &= -\frac{2z_o}{5(a_2+2a_4 z_o^2)} \\ \frac{\partial c}{\partial a_2} &= -\frac{z_o^3}{3} \\ \frac{\partial c}{\partial a_4} &= -\frac{z_o^4}{5} \end{aligned}\right\} \qquad \text{(A11)}$$

APPENDIX IV

The surface energy E_s of a closed surface may be expressed as:

$$E_s = \vartheta \int dS$$

where ϑ, the surface tension (surface energy per unit area), is assumed constant, and dS is an element of the surface area. For a nucleus of mass A and spherical radius R_o, $\vartheta = \alpha_s A^{\frac{2}{3}}/4\pi R_o^2$, where $\alpha_s = 17.97$ MeV.[A1] A symmetric surface of revolution (about the Z-axis) has the area

$$\int dS = 2\pi \int_{-Z_o}^{Z_o} P_o \left[1 + \left(\frac{dP_o}{dZ}\right)^2\right]^{\frac{1}{2}} dZ$$

where P_o and Z_o are as defined in Appendix III.

Substitution of equation (A4) in the above expression yields:

$$\int dS = 2\pi \int_{-Z_o}^{Z_o} \left\{ 4A_4^2 Z^6 + (4A_2A_4 + A_4) Z^4 + (A_2^2 + A_2) Z^2 + C \right\}^{\frac{1}{2}} dZ$$

Using the change of variables as given by equations (A6),

$$\int dS = 2\pi R_o^2 \int_{-z_o}^{z_o} \left\{ 4a_4^2 z^6 + (4a_2 a_4 + a_4) z^4 + (a_2^2 + a_2) z^2 + c \right\}^{\frac{1}{2}} dz$$

$$= 4\pi R_o^2 \int_{0}^{z_o} \left\{ 4a_4^2 z^6 + (4a_2 a_4 + a_4) z^4 + (a_2^2 + a_2) z^2 + c \right\}^{\frac{1}{2}} dz$$

For numerical integration, it is more convenient to integrate from 0 to 1. This simple change of variable gives:

[A1] A. E. S. Green, Rev. Mod. Phys., 30, 569 (1958)

$$E_s = 4\pi R_o^2 \vartheta z_o \int_0^1 \left\{ 4a_4^2 z_o^6 x^6 + (4a_2 a_4 + a_4) z_o^4 x^4 + (a_2^2 + a_2) z_o^2 x^2 + c \right\}^{\frac{1}{2}} dx$$

A sphere of radius R_o would have a surface energy $E_s^\circ = 4\pi R_o^2 \vartheta = \alpha_s A^{\frac{2}{3}}$. Thus, the surface energy of an arbitrary contour relative to that of a sphere is:

(A12)

$$B_s = \frac{E_s}{E_s^\circ} = z_o \int_0^1 \left\{ 4a_4^2 z_o^6 x^6 + (4a_2 a_4 + a_4) z_o^4 x^4 + (a_2^2 + a_2) z_o^2 x^2 + c \right\}^{\frac{1}{2}} dx$$

In treating the dynamics, expressions for $\frac{\partial B_s}{\partial a_2}$ and $\frac{\partial B_s}{\partial a_4}$ are required. From equation (A12) we obtain:

$$\frac{\partial B_s}{\partial a_2} = \int_0^1 \frac{\left\{ N_{26} z_o^6 x^6 + N_{24} z_o^4 x^4 + N_{22} z_o^2 x^2 + \frac{z_o}{2} \frac{\partial c}{\partial a_2} + c \frac{\partial z_o}{\partial a_2} \right\}}{f(x)} \qquad \text{(A13)}$$

$$\frac{\partial B_s}{\partial a_4} = \int_0^1 \frac{\left\{ N_{46} z_o^6 x^6 + N_{44} z_o^4 x^4 + N_{42} z_o^2 x^2 + \frac{z_o}{2} \frac{\partial c}{\partial a_4} + c \frac{\partial z_o}{\partial a_4} \right\}}{f(x)} dx \qquad \text{(A14)}$$

where

$$N_{26} = 16 a_4^2 \frac{\partial z_o}{\partial a_2}$$

$$N_{24} = 2 a_4 z_o + 3(4 a_2 a_4 + a_4) \frac{\partial z_o}{\partial a_2}$$

$$N_{22} = (a_2 + \tfrac{1}{2}) z_o + 2(a_2^2 + a_2) \frac{\partial z_o}{\partial a_2}$$

$$N_{46} = 4 a_4 z_o + 16 a_4^2 \frac{\partial z_o}{\partial a_4}$$

$$N_{44} = 2 a_2 z_o + \frac{z_o}{2} + 3(4 a_2 a_4 + a_4) \frac{\partial z_o}{\partial a_4}$$

$$N_{42} = 2(a_2^2 + a_2) \frac{\partial z_o}{\partial a_4}$$

$$f(x) = \left\{ 4a_4^2 z_o^6 x^6 + (4a_2 a_4 + a_4) z_o^4 x^4 + (a_2^2 + a_2) z_o^2 x^2 + c \right\}^{\frac{1}{2}}$$

and $\frac{\partial z_o}{\partial a_2}$, $\frac{\partial z_o}{\partial a_4}$, $\frac{\partial c}{\partial a_2}$ and $\frac{\partial c}{\partial a_4}$ are equations (A11).

APPENDIX V

In order to develop an expression for the electrostatic energy E_c of a volume of revolution filled with a uniformly charged medium, consider this volume sliced into many thin disks. Using this model and the diagram in Fig. A1, the integral equations are developed. For convenience, the origin of the coordinate system is selected to be one of zeros of the generating function P(Z). (The subscript "$_o$" in $P_o(Z)$ has been omitted, as it will be necessary to distinguish two generating functions in this treatment).

Consider a thin disk of uniform volume charge density σ and a radius P_A situated with its center on the Z-axis at A. Following the development of A. Gray[A2], an expression in terms of Bessel functions is found for the potential at any point P. Let the thickness of the disk be dZ_A, and the axial distance (along the Z-axis) between the disk and point P be $|Z_A - Z_B|$. Let the distance of the point P from the Z-axis be P_p.

On the thin disk at A, consider a ring with its center at A of radius P and thickness dP. Let E represent a point on this ring and φ_A be the angle AE makes with the radius which lies in the PBA plane. The potential V at P is given by:

$$V = \sigma dZ_A \int_0^{P_A} \int_0^{2\pi} \frac{P dP d\varphi_A}{\{|Z_A - Z_B|^2 + P_p^2 + p^2 - 2PP_p \cos\varphi\}^{\frac{1}{2}}} \qquad \text{(A15)}$$

[A2] A. Gray, Phil. Mag. Series 6, XXXVIII, 201 (1919).

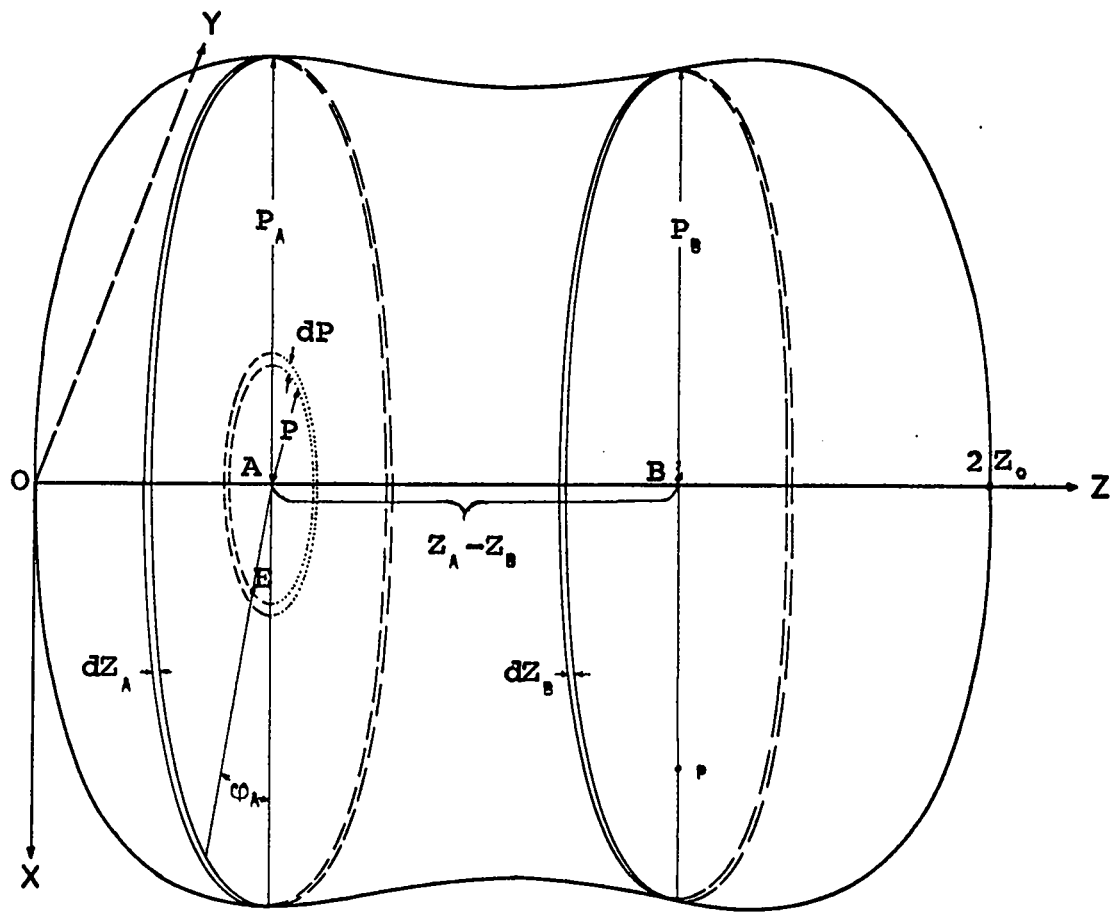

Fig. A1. Diagram of the surface of revolution about the Z-axis

Setting $R^2=P_p{}^2+P^2-2PP_p\cos\varphi_A$ and using the identity[A3]

$$\frac{1}{(a^2+b^2)^{\frac{1}{2}}}=\int_0^\infty e^{-ax}J_0(bx)\,dx$$

we obtain:

$$V = \sigma dZ_A\int_0^{2\pi} d\varphi_A\int_0^{P_A} PdP\int_0^\infty e^{-\lambda|\,Z_A-Z_B|}\,J_0(\lambda R)d\lambda \qquad \text{(A16)}$$

By use of Neumann's multiplication theorem[A4]

$$J_0\left(\sqrt{b^2+2bc\,\cos\alpha+c^2}\right)=J_0(b)J_0(c)+2\sum_{s=1}^{\infty}(-1)^sJ_s(b)J_s(c)\,\cos s\alpha$$

with the substitution $\pi-\varphi_A=\alpha$, $P\lambda=b$, $P_p\lambda=c$, and $n=s$, we obtain:

$$J_0(\lambda R) = J_0(\lambda P)\,J_0(\lambda P_p)+2\sum_{n=1}^{\infty}J_n(\lambda P)J_n(\lambda P_p)\cos n\,\varphi_A \qquad \text{(A17)}$$

Using this expression in equation (A16), and integrating with respect to φ_A,

$$V = 2\pi\sigma dZ_A\int_0^\infty e^{-\lambda|\,Z_A-Z_B|}\left\{\int_0^{P_A}J_0(\lambda P)P\,dP\right\}J_0(\lambda P_p)\,d\lambda \qquad \text{(A18)}$$

since the summation term in the integration of equation (A17) vanishes. To evaluate the integral

$$\int_0^A x\,J_0(\lambda x)dx=\frac{1}{\lambda^2}\int_0^{\lambda A} y\,J_0(y)\,dy$$

[A3] A. Gray, G. Mathews, and T. MacRobert, Bessel Functions (MacMillan and Co.,London, 1922) pp. 64-65.

[A4] Ibid. p. 38

one uses the recursion relation: $yJ_n'(y) = -nJ_n(y) + yJ_{n-1}(y)$ which for n=1 becomes: $yJ_1'(y) = -J_1(y) + yJ_o(y)$. Substitution and integration by parts yields:

$$\int_o^A xJ_o(\lambda x)\, dx = \frac{A}{\lambda} J_1(\lambda A) \qquad \text{(A19)}$$

Inserting equation (A19) in equation (A18), the potential at a point $P(P_P, Z_B, \varphi_P)$ due to a uniformly charged, thin disk of thickness dZ_A, diameter P_A, at point Z_A, on the Z-axis disk is

$$V(P_P, Z_B) = 2\pi\sigma dZ_A \int_o^\infty e^{-\lambda|Z_A - Z_B|} P_A J_1(\lambda P_A) J_o(\lambda P_P)\, \frac{d\lambda}{\lambda} \qquad \text{(A20)}$$

For the coordinate system in Fig. (A1), with the angle φ measured clockwise from the positive X-axis, the electrostatic energy of an element of volume (of charge density σ) located at point $P(P_P, Z_B, \varphi_P)$ would be:

$$dE_c = \tfrac{1}{2}\sigma V(P_P, Z_B)\, P_P\, dP_P\, d\varphi_P\, dZ_B$$

The energy of interaction of a pair of disks is represented by the double integral

$$E_{c_{DISKS}} = \tfrac{1}{2}\sigma \left[\int_o^{2\pi} \left\{ \int_o^{P_B} V(P_P, Z_B) P_P\, dP_P \right\} d\varphi_P \right] dZ_B \qquad \text{(A21)}$$

Since $V(P_P, Z_B)$ is not a function of φ_P, immediate integration in equation (A21) yields:

$$E_{c_{DISKS}} = \pi\sigma \int_o^{P_B} V(P_P, Z_B) P_P\, dP_P\, dZ_B \qquad \text{(A22)}$$

Substituting equation (A20) for $V(P_\rho, Z_B)$, the energy of interaction of the pair of disks a distance $|Z_A - Z_B|$ apart is:

$$E_{c_{DISKS}} = 2\pi^2\sigma^2 dZ_A\, dZ_B \int_0^{P_B} P_\rho\, dP_\rho \int_0^{\infty} e^{-\lambda|Z_A - Z_B|} \times P_A J_1(\lambda P_A) J_0(\lambda P_\rho) \frac{d\lambda}{\lambda} \qquad \text{(A23)}$$

The integral $\int_0^{P_B} P_\rho J_0(\lambda P_\rho)\, dP_\rho$ is evaluated by use of equation (A19). This gives:

$$E_{c_{DISKS}} = 2\pi^2\sigma^2 dZ_A\, dZ_B \int_0^{\infty} e^{-\lambda|Z_A - Z_B|} P_A P_B J_1(\lambda P_A) J_1(\lambda P_B) \frac{d\lambda}{\lambda^2} \qquad \text{(A24)}$$

The total energy of interaction over all such pairs of disks is obtained by integrating both dZ_A and dZ_B over the range of Z, i.e., from 0 to $2Z_0$. Thus,

$$E_c = 2\pi^2\sigma^2 \int_0^{2Z_0} P_A\, dZ_A \int_0^{2Z_0} P_B\, dZ_B \int_0^{\infty} e^{-\lambda|Z_A - Z_B|} J_1(\lambda P_A) J_1(\lambda P_B) \frac{d\lambda}{\lambda^2} \qquad \text{(A25)}$$

where $P_A = P_A(Z_A)$

$P_B = P_B(Z_B)$

Equation (A25) can be transformed into an integral involving only trigonometric functions by use of the identity[A5]:

$$\int_0^{\infty} e^{-at} J_\nu(bt) J_\nu(ct) t^{\mu-1} dt = \frac{(bc)^\nu \Gamma(\mu+2\nu)}{\pi a^{(\mu+2\nu)} \Gamma(2\nu+1)} \times \int_0^{\pi} {}_2F_1\left(\frac{\mu+2\nu}{2}, \frac{\mu+2\nu+1}{2}; \nu+1; \frac{-\omega^2}{a^2}\right) \sin^{2\nu}\varphi\, d\varphi$$

[A5] G. N. Watson, A Treatise on the Theory of Bessel Functions, (University Press, Cambridge, 1944) p. 389.

where $\omega = (b^2+c^2-2bc\cos\varphi)^{\frac{1}{2}}$

${}_2F_1$ = hypergeometric function

if Real $(a \pm ib \pm ic)>0$ and Real $(\mu + 2\nu)>0$

For the values of a, b, c, μ, and ν corresponding to the integral in equation (A25), the conditions for validity of the identity are met, and one obtains:

$$\int_0^\infty e^{-\lambda|Z_A-Z_B|} J_1(\lambda P_A) J_1(\lambda P_B)\,\frac{d\lambda}{\lambda^2}$$

$$= \frac{P_A P_B \Gamma(1)}{\pi|Z_A-Z_B|\Gamma(3)} \int_0^\pi {}_2F_1\left(\tfrac{1}{2},1;2;-\frac{\omega^2}{a^2}\right)\sin^2\varphi\,d\varphi$$

where $\frac{-\omega^2}{a^2} = -\frac{P_A^2+P_B^2-2P_A P_B\cos\varphi}{|Z_A-Z_B|^2}$

$\Gamma(1) = 1$

$\Gamma(3) = 2$

$${}_2F_1(a,b;c;z) = 1 + \frac{ab}{c}\,\frac{z}{1!} + \frac{a(a+1)b(b+1)}{c(c+1)}\,\frac{z^2}{2!} + \cdots.$$

Since the hypergeometric function ${}_2F_1\left(\tfrac{1}{2},1;2;-\frac{\omega^2}{a^2}\right)$ never terminates, it was desirable to find a form which did terminate. The following transformation[A6] accomplishes this:

$$(1+Z)^{2a}\,{}_2F_1(2a,2a+1-c;c;z) = {}_2F_1\left(a,a+\tfrac{1}{2};c;\frac{4Z}{(1+Z)^2}\right)$$

[A6] W. Magnus and F. Oberhettinger, Functions of Mathematical Physics (Chelsa Publishing Co., New York, 1954) p. 9.

In the present case $a=\frac{1}{2}$, $c=2$, such that

$$ {}_2F_1\left(\tfrac{1}{2},1;2;\frac{\omega^2}{a^2}=\frac{4z}{(1+z)^2}\right) = (1+z)\,{}_2F_1(1,0;2;z) = 1+z \qquad \text{(A27)} $$

Solving for $(1+z)$ in terms of P_A, P_B, $\cos\varphi$, and $|Z_A-Z_B|$, one finds:

$$ (1+z) = 2|Z_A-Z_B|\left\{\frac{1}{DEN}\right\} \qquad \text{(A28)} $$

where

$$ DEN = \left\{ |Z_A-Z_B| \pm \sqrt{|Z_A-Z_B|^2+P_A^2+P_B^2-2P_AP_B\cos\varphi} \right\} $$

Combining equations (A28), (A27), and (A26) with (A25), one obtains:

$$ E_c = 2\pi\sigma^2\int_0^{2Z_0} P_A^2\,dZ_A \int_0^{2Z_0} P_B^2\,dZ_B \int_0^{\pi} \frac{\sin^2\varphi\,d\varphi}{DEN} \qquad \text{(A29)} $$

Since the square root in the denominator (DEN) of equation (A29) can never be less than $|Z_A-Z_B|$, only the positive sign has physical meaning. The negative sign could give a negative energy of interaction, which is not physically acceptable.

The triple integral equation (A29) involves two integrations extending over the same physical range of Z. A savings can be accomplished in numerical calculations if we change the range of integration over Z_B to 0 to Z_A and double the value of the integral. This has the further advantage of eliminating the absolute value requirement on the difference in Z_A and Z_B.

In the above development, the generating function P(Z) differs from that for the surface energy integral in the shift of the origin by Z_0. At this point of development

$$P^2 = A_4 Z^4 - 4A_4 Z_o Z^3 + (6A_4 Z_o^2 + A_2) Z^2 - (4A_4 Z_o^3 + 2A_2 Z_o) Z$$

The dimensionality of the integral is removed by making the change of variables given by equations (A6). Thus:

$$E_c = 4\pi\sigma^2 R_o^5 \int_0^{2z_o} \rho_A^2 dz_A \int_0^{z_A} \rho_B^2 dz_B \int_0^{\pi} \frac{\sin^2\varpi d\varpi}{den}$$

where

$$den = \left\{ (z_A - z_B) + \sqrt{(z_A - z_B)^2 + \rho_A^2 + \rho_B^2 - 2\rho_A \rho_B \cos\varpi} \right\}$$

$$\rho^2 = a_4 z^4 - 4a_4 z_o z^3 + (6a_4 z_o^2 + a_2) z^2 - (4a_4 z_o^3 + 2a_2 z_o) z$$

$$z = z_A \text{ or } z_B$$

$$\rho = \rho_A \text{ or } \rho_B$$

By definition the electric charge density σ is the electric charge (eZ, where e is the electron charge and Z is the number of protons in the nucleus) divided by the volume. Normalizing to the volume of a sphere of radius R_o, $\sigma = \frac{3eZ}{4\pi R_o^3}$. The Coulomb energy of such a sphere is $E_c^o = \frac{3(eZ)^2}{5R_o}$. The relative Coulomb energy becomes

$$B_c = \frac{E_c}{E_c^o} = \frac{15}{14\pi} \int_0^{2z_o} \rho_A^2 dz_A \int_0^{z_A} \rho_B^2 dz_B \int_0^{\pi} \frac{\sin^2\varpi d\varpi}{den}$$

The desired form for B_c is obtained by three changes of variable making the range of integration 0 to 1 in all cases. Thus,

$$B_c = 120 z_o^5 \int_0^1 \rho_a^2 dz \int_0^1 z\rho_b^2 dy \int_0^1 \frac{\sin^2\pi x \, dx}{z(1-y) + \sqrt{z^2(1-y)^2 + \rho_a^2 + \rho_b^2 - 2\rho_a \rho_b \cos\pi x}} \qquad \text{(A30)}$$

where

$$\rho_a^2 = 4a_4 z_o^2 z^4 - 8a_4 z_o^2 z^3 + (6a_4 z_o^2 + a_2) z^2 - (2a_4 z_o^2 + a_2) z$$

$$\rho_b^2 = 4a_4 z_o^2 z^4 y^4 - 8a_4 z_o^2 z^3 y^3 + (6a_4 z_o^2 + a_2) z^2 y^2 - (2a_4 z_o^2 + a_2) zy$$

The corresponding expressions for $\frac{\partial B_c}{\partial a_2}$ and $\frac{\partial B_c}{\partial a_4}$, which are required in the dynamics, are obtained from equation (A30), as:

$$\frac{\partial B_c}{\partial a_2} = 60 z_o^4 \int_0^1 z\,dz \int_0^1 dy \int_0^1 G_2 \sin^2 \pi x \, dx \qquad \text{(A31)}$$

where

$$G_2 = \frac{d_2 \rho_b^2 + d_3 \rho_a^2}{z(1-y)+d_1} - \frac{\rho_a^2 \rho_b^2 \left[d_2 \left(1 - \frac{\rho_b}{\rho_a} \cos \pi x\right) + d_3 \left(1 - \frac{\rho_a}{\rho_b} \cos \pi x\right)\right]}{2d_1 \left[z(1-y)+d_1 \right]^2}$$

$$d_1 = \sqrt{z^2 (1-y)^2 + \rho_a^2 + \rho_b^2 - 2\rho_a \rho_b \cos \pi x}$$

$$d_2 = 4d_4 z_o^2 z^3 + 2d_5 z_o z^2 + d_6 z$$

$$d_3 = 4d_4 z_o^2 z^3 y^3 + 2d_5 z_o z^2 y^2 + d_6 zy$$

$$d_4 = -4a_4 \frac{\partial z_o}{\partial a_2}$$

$$d_5 = 12a_4 z_o \frac{\partial z_o}{\partial a_2} + 1$$

$$d_6 = -\left(12a_4 z_o^2 \frac{\partial z_o}{\partial a_2} + 2a_2 \frac{\partial z_o}{\partial a_2} + 2z_o\right)$$

$$\frac{\partial z_o}{\partial a_2} = \frac{-z_o}{3(a_2 + 2a_4 z_o^2)}$$

and

$$\frac{\partial B_c}{\partial a_4} = 60 z_o^4 \int_0^1 z\,dz \int_0^1 dy \int_0^1 G_4 \sin^3 \pi x \, dx \qquad \text{(A32)}$$

where

$$G_4 = \frac{d_7 \rho_b^2 + d_8 \rho_a^2}{z(1-y)+d_1} - \frac{\rho_a^2 \rho_b^2 \left[d_7 \left(1-\frac{\rho_b}{\rho_a}\cos\pi x\right) + d_8 \left(1-\frac{\rho_a}{\rho_b}\cos\pi x\right)\right]}{2 d_1 \left[z(1-y)+d_1 \right]^2}$$

$$d_7 = 8 z_o^3 z^4 + 4 d_9 z_o^2 z^3 + 2 d_{10} z_o z^2 + d_{11} z$$

$$d_8 = 8 z_o^3 z^4 y^4 + 4 d_9 z_o^2 z^3 y^3 + 2 d_{10} z_o z^2 y^2 + d_{11} z y$$

$$d_9 = -\left(4 z_o + 4 a_4 \frac{\partial z_o}{\partial a_4}\right)$$

$$d_{10} = 6 z_o^2 + 12 a_4 z_o \frac{\partial z_o}{\partial a_4}$$

$$d_{11} = -\left(4 z_o^3 + 12 a_4 z_o^2 \frac{\partial z_o}{\partial a_4} + 2 a_4 \frac{\partial z_o}{\partial a_4}\right)$$

$$\frac{dz_o}{\partial a_4} = -\frac{2 z_o^3}{5(a_2 + 2 a_4 z_o^2)}$$

APPENDIX VI

In Cartesian coordinates the moment of inertia about each axis is:

$$I_x = M_{yy}+M_{zz} = \iiint \sigma_m (Y^2+Z^2)\ dX\ dY\ dZ$$

$$I_y = M_{xx}+M_{zz} = \iiint \sigma_m (X^2+Z^2)\ dX\ dY\ dZ$$

$$I_z = M_{xx}+M_{yy} = \iiint \sigma_m (X^2+Y^2)\ dX\ dY\ dZ$$

where σ_m is the mass density and M_{xx}, M_{yy}, M_{zz} are the second moments of inertia with respect to the coordinate planes. To express these equations in cylindrical coordinates the usual substitutions are made, i.e., $X=P\cos\Theta$, $Y=P\sin\Theta$, $Z=Z$, and $dV = dX\ dY\ dZ = PdPd\Theta Z$.

The moment of inertia of a sphere of radius R_o and constant density is $I_{SPHERE} = \frac{8}{15}\pi\sigma_m R_o^5$. Since the axis of symmetry for the liquid drop is the Z-axis, the relative parallel and perpendicular moments of inertia are

$$I_{\parallel} = \frac{I_z}{I_{SPHERE}} \quad \text{and} \quad I_{\perp} = \frac{I_x}{I_{SPHERE}} = \frac{I_y}{I_{SPHERE}}$$

The liquid drop contour is formed by revolving about the Z-axis the curve:

$$P^2 = C + A_2 Z^2 + A_4 Z^4$$

Making the indicated substitutions, one obtains

$$M_{xx} = \sigma_m \int_0^{2\pi} \cos^2\Theta d\Theta \int_{-Z_o}^{Z_o} dZ \int_0^{\sqrt{C+A_2Z^2+A_4Z^4}} P^3 dP = M_{yy}$$

since

$$\int_0^{2\pi} \cos^2\theta\, d\theta = \int_0^{2\pi} \sin^2\theta\, d\theta$$

and

$$M_{zz} = \sigma_e \int_0^{2\pi} d\theta \int_{-Z_0}^{Z_0} Z^2\, dZ \int_0^{\sqrt{C+A_2Z^2+A_4Z^4}} P\, dP$$

where Z_0 is the positive real root of $P(Z_0)=0$.

Combining the results of the indicated operations and converting to dimensionless units by equations (A6) yields:

$$I_{\parallel} = \frac{15}{8}\left\{\frac{a_4^2 z_0^9}{9} + \frac{2a_2a_4 z_0^7}{7} + \frac{(a_2^2+2a_4c)z_0^5}{5} + \frac{2a_2c z_0^3}{3} + c z_0\right\}$$

and

$$I_{\perp} = \frac{15}{8}\left\{\frac{a_4^2 z_0^9}{18} + \frac{(a_2a_4+2a_4)z_0^7}{7} + \frac{(a_2^2+4a_2+2a_4c)z_0^5}{5} + \frac{(a_2c+2c)z_0^3}{3} + \frac{c^2 z_0}{2}\right\}$$

The electric quadrupole moment of a uniformly charged solid is defined to be

$$Q = \frac{1}{e}\int_{vol} \sigma_e (3Z^2-R^2)\, dVol$$

where e is the electron charge

$$\sigma_e = \frac{Ze}{\int_{vol} dVol} = \frac{Ze}{V}$$

V is the volume

Ze is the total charge in multiples of the electron charge e

R is the radius of any point in spherical coordinates

$$R = \sqrt{Z^2+P^2}$$

P is the distance from the Z-axis (cylindrical coordinates)

To obtain results comparable with those of C and S[47], the above definition is modified slightly to be

$$Q = \int_{Vol} (3z^2-r^2)\ dVol$$

In this form dimensionality has been removed.

Substitutions of the appropriate quantities in cylindrical coordinates yield:

$$Q = \int_0^{2\pi} d\theta \int_{-z_0}^{z_0} dz \int \sqrt{c+a_2 z^2+a_4 z^4}\ (2z^2\rho-\rho^3)\,d\rho$$

$$Q = 4\pi\left\{\frac{a_4^2 z_0^9}{36} + \frac{a_4(2-a_2)z_0^7}{14} + \frac{(4a_2-a_2^2-2a_4c)z_0^5}{20} + \frac{c(2-a_2)z_0^3}{6} - \frac{c^2 z_0}{4}\right\}$$

---

[47] S. Cohen and W. J. Swiatecki, Ann. Phys., 22, 406 (1963).

APPENDIX VII

For an axially symmetric liquid drop, defined by equation (A4), a suitable form for the velocity potential which satisfies Laplaces' equation is

$$-\Phi = \sum_{n=1}^{N} B_{2n} R^{2n} P_{2n}(\cos\theta)$$

where B_{2n} are time dependent parameters, R is the radial distance from the origin to the perimeter of the disk of cylindrical radius P located at position Z on the Z-axis, P_{2n} is the Legendre polynomial of order "2n", and θ is the angle between the Z-axis and R. The term for "n=0" is omitted, as it is a constant, not affecting the motion. The dimensional features of this velocity potential become a constant coefficient by change of variables

$$r = R/R_o$$

$$\beta_{2n} = B_{2n} T_o R_o^{2n-2}$$

Thus,

$$-\Phi = -\frac{R_o^2}{T_o}\varphi = \frac{R_o^2}{T_o}\sum_{n=1}^{N} \beta_{2n} r^{2n} P_{2n}(\cos\theta) \qquad \text{(A33)}$$

Furthermore, ϖ may be expressed in terms of z and ρ by the change of variables:

$$r\cos\theta = z$$

$$r^2 = \rho^2 + z^2$$

such that

$$-\varphi = \sum_{n=1}^{N} \beta_{2n} H_n(\rho, z) \qquad \text{(A34)}$$

Since axially symmetric motion is assumed, the two non-zero velocity components (in cylindrical coordinates) are

$$V_z = -\frac{\partial\Phi}{\partial Z}\frac{\partial Z}{\partial z} = \frac{R_o}{T_o}\sum_{n=1}^{N}\beta_{2n}\frac{\partial H_n}{\partial z} = \frac{R_o}{T_o}v_z \tag{A35}$$

$$V_\rho = -\frac{\partial\Phi}{\partial P}\frac{\partial P}{\partial \rho} = \frac{R_o}{T_o}\sum_{n=1}^{N}\beta_{2n}\frac{\partial H_n}{\partial \rho} = \frac{R_o}{T_o}v_\rho \tag{A36}$$

Using these equations and those describing the shape of the drop the desired expressions for the kinetic energy and boundary condition are next derived.

For a liquid drop which simply changes shape the kinetic energy is expressed by the integral:

$$E_K = \frac{\sigma_m}{2}\int_{vol}(\nabla\Phi)^2 dVol = \frac{\sigma_m}{2}\int_{vol}(V_z^2+V_\rho^2)\ dVol$$

where σ_m is the mass density of the liquid ($=3M_o/4\pi R_o^3$), or

$$E_K = \frac{3M_o R_o^2}{4T_o^2}\int_{-z_o}^{z_o} dz\int_{0}^{\rho_o}(v_z^2+v_\rho^2)\ \rho d\rho$$

where ρ_o is obtained from equation (A5), and v_z^2 and v_ρ^2 are double summations of equations (A35) and (A36). Integration over ρ and z yields

$$E_K = \frac{3M_o R_o^2}{T_o^2}\sum_{\substack{i=1\\j=1}}^{J}\sum^{J}\beta_{2i}\beta_{2j}I_{2i,2j} \tag{A37}$$

where

$$I_{a_i,a_j} = \frac{1}{4}\int_{-z_o}^{z_o} dz \int_{0}^{\rho_o} \left\{ \frac{\partial H_i}{\partial z}\frac{\partial H_j}{\partial z} + \frac{\partial H_i}{\partial \rho}\frac{\partial H_j}{\partial \rho} \right\} \rho d\rho \qquad (A38)$$

Dividing equation (A37) by the fundamental energy unit $E_s^{\circ}(=\alpha_s A^{\frac{2}{3}})$ gives the relative kinetic energy B_K:

$$B_K = \frac{3m_o A r_o^2}{\alpha_s T_o^2} \sum_{\substack{i=1 \\ j=1}}^{J,J} \beta_{a_i}\beta_{a_j} I_{a_i,a_j}$$

Setting the coefficient of the summation to unity provides the relation defining T_o, as given in the discussion of units, i.e.,

$$T_o = r_o\sqrt{\frac{3m_o A}{\alpha_s}} = 0.482_4 \times 10^{-22} A^{\frac{1}{2}} \text{seconds} \qquad (A39)$$

Thus, the final expression for the relative kinetic energy is:

$$B_K = \sum_{\substack{i=1 \\ j=1}}^{J,J} \beta_{a_i}\beta_{a_j} I_{a_i,a_j} \qquad (A40)$$

The implicit (dimensional) equation for the surface of the drop may be written as

$$F(P,Z) = P - P_o(Z) = 0 \qquad (A41)$$

where the entire time dependence is contained in P_o (i.e., neither P nor Z are considered functions of time). The special boundary condition to which the equations of continuity degenerated at the surface is:

$$\frac{DF}{DT} = \frac{\partial F}{\partial T} + \underline{V} \cdot \nabla F = 0$$

where $\underline{V}$ is the vector velocity of the fluid on the surface. Applying this condition to equation (A41), and multiplying by

P_o (to simplify future numerical calculations) the boundary condition becomes:

$$G' = P_o V_\rho - P_o P_o' V_z - P_o \dot{P}_o = 0 \qquad \text{(A42)}$$

where V_ρ and V_z are the velocity components on the surface, $P_o' = \frac{\partial P_o}{\partial Z}$ and $\dot{P} = \frac{\partial P_o}{\partial T}$. By use of equations (A6), (A35), (A36), and $\dot{\rho}_o = \dot{P}_o T_o / R_o$, the boundary condition becomes:

$$G' = \frac{R_o^2}{T_o} G = 0$$

where

$$G = \rho_o v_\rho - \rho_o \rho_o' v_z - \rho_o \dot{\rho}_o = 0 \qquad \text{(A43)}$$

and v_ρ and v_z are evaluated on the surface.

The boundary condition is used to determine the functional relations of the β_{2n}'s (to be used in equation (A34)). Since the dimensional coefficient R_o^2/T_o is a constant, it will be omitted from further discussion, and equation (A43) will be considered the boundary condition.

Only for a velocity potential with an infinity of terms would it be possible to exactly satisfy equation (A43) over the range $-z_o$ to z_o. Since a mathematically tractable method of following the motion of the liquid drop is desired, it is necessary to compromise and use a finite number of terms in the velocity potential, which will only approximately satisfy equation (A43).

Consider the integral: $GSI = \int_{-z_o}^{z_o} G^2 dz$

If equation (A43) were satisfied exactly, the integral would vanish. The technique for determining a finite number of β_{2n}'s is to minimize this integral with respect to the β_{2n}'s by forming:

$$\frac{\partial}{\partial \beta_{2n}} \left\{ \int_{-z_o}^{z_o} G^2 dz \right\} = 0 \qquad \text{(A44)}$$

Since GSI is quadratic in the β_{2n}'s, equation (A44) becomes a linear set of "n" equations in the "n" β_{2n}'s.

From the shape defining equation (A5) expressions for $\rho_o \rho_o'$ and $\rho_o \dot{\rho}_o$ are

$$\rho_o \rho_o' = a_2 z + 2a_4 z^3$$

$$\rho_o \dot{\rho}_o = \tfrac{1}{2}\dot{c} + \tfrac{1}{2}\dot{a}_2 z^2 + \tfrac{1}{2}\dot{a}_4 z^4$$

Combining these equations and (A10), (A35), (A36), and (A43), equation (A44) becomes:

$$\frac{\partial}{\partial \beta_{2n}} \int_{-z_o}^{z_o} G^2 dz = 2 \sum_{j=1}^{J} \beta_{2j} G_{jn} + G_n = 0 \qquad \text{(A45)}$$

where

$$G_{jn} = \int_{-z_o}^{z_o} \left\{ \rho_o^2 \frac{\partial H_j}{\partial \rho} \frac{\partial H_n}{\partial \rho} - 2\rho_o (a_2 z + 2a_4 z^3) \frac{\partial H_j}{\partial \rho} \frac{\partial H_n}{\partial \rho} \right.$$

$$\left. + (a_2 z + 2a_4 z^3)^2 \frac{\partial H_j}{\partial z} \frac{\partial H_n}{\partial z} \right\} dz$$

$$G_n = \int_{-z_o}^{z_o} \left\{ \dot{a}_4 \left(z^4 + \frac{\partial c}{\partial a_4} \right) + \dot{a}_2 \left(z^2 + \frac{\partial c}{\partial a_2} \right) \right\} \left\{ -\rho_o \frac{\partial H_n}{\partial \rho} + (a_2 z + 2a_4 z^3) \frac{\partial H_n}{\partial z} \right\} dz$$

Solution of equation (A45) yields the β_{2n}'s as explicit functions with linear dependence on $\dot{a}_2$ and $\dot{a}_4$.

In terms of G_{jn} and G_n, the boundary condition integral is:

$$GSI = \sum_{\substack{n=1 \\ j=1}}^{J} \beta_{2n}\beta_{2j}G_{nj} + \sum_{n=1}^{J} \beta_{2n}G_n + G_o$$

where

$$G_o = \frac{1}{4}\int_{-z_o}^{z_o} \left\{ \dot{a}_4\left(z^4 + \frac{\partial c}{\partial a_4}\right) + \dot{a}_2\left(z^2 + \frac{\partial c}{\partial a_2}\right)\right\}^2 dz \qquad \text{(A46)}$$

While the meaning of the actual values of GSI for a particular velocity is uncertain, the smaller the value of GSI the closer the boundary conditions are being met.

Having obtained the β_{2n}'s in this manner the equations of motion are determined from the Lagrangian $L(=B_K - \xi$, where $\xi = (B_s - 1) + 2X(B_c - 1))$ as:

$$\frac{d}{\partial t}\left(\frac{\partial L}{\partial \dot{a}_\kappa}\right) - \frac{\partial L}{\partial a_\kappa} = \frac{d}{dt}\left(\frac{\partial B_K}{\partial \dot{a}_\kappa}\right) - \frac{\partial B_K}{\partial a_\kappa} + \frac{\partial \xi}{\partial a_\kappa} = 0 \qquad \text{(A47)}$$

The term $\frac{d}{dt}\left(\frac{\partial \xi}{\partial \dot{a}_\kappa}\right)$ vanished, because B_c and B_s had no explicit dependence on $\dot{a}_2$ or $\dot{a}_4$.

Since the kinetic energy B_K does not explicitly depend on time, the total time derivitive becomes:

$$\frac{d}{dt} = \sum_{\eta=2,4} \ddot{a}_\eta \frac{\partial}{\partial \dot{a}_\eta} + \sum_{\eta=2,4} \dot{a}_\eta \frac{\partial}{\partial a_\eta}$$

Recalling that the β_{2n}'s are functions of the shape coordinates (a_2 and a_4) and linear in $\dot{a}_2$ and $\dot{a}_4$, and using equation (A40) for B_κ, the complete equations of motion are:

$$\sum_{\substack{i=1\\j=1\\\eta=2,4}}^{J\,J} \ddot{a}_\eta \frac{\partial\beta_{2i}}{\partial\dot{a}_\kappa}\frac{\partial\beta_{2j}}{\partial\dot{a}_\eta} I_{2i,2j}$$

$$+\sum_{\substack{i=1\\j=1\\\eta=2,4}}^{J\,J} \dot{a}_\eta\left\{\left(\frac{\partial^2\beta_{2i}}{\partial\dot{a}_\kappa\partial a_\eta}\beta_{2j}+\frac{\partial\beta_{2i}}{\partial\dot{a}_\kappa}\frac{\partial\beta_{2j}}{\partial a_\eta}\right) I_{2i,2j}+\frac{\partial\beta_{2i}}{\partial\dot{a}_\kappa}\beta_{2j}\frac{\partial I_{2i,2j}}{\partial a_\eta}\right\}$$

$$-\sum_{\substack{i=1\\j=1}}^{J\,J}\left\{\frac{\partial\beta_{2i}}{\partial a_\kappa}\beta_{2j}I_{2i,2j}+\tfrac{1}{2}\beta_{2i}\beta_{2j}\frac{\partial I_{2i,2j}}{\partial a_\kappa}\right\}+\tfrac{1}{2}\frac{\partial\xi}{\partial\dot{a}_\kappa}=0 \qquad \text{(A48)}$$

The fact that $I_{2j,2i}$ is symmetric in "i" and "j" has been used to simplify this equation.

Equation (A48) is a coupled set of differential equations linear in $\ddot{a}_\eta$ of the form:

$$\left.\begin{aligned} C_{22}\ddot{a}_2+C_{24}\ddot{a}_4 &= f_1+f_2\\ C_{42}\ddot{a}_2+C_{44}\ddot{a}_4 &= f_3+f_4\end{aligned}\right\} \qquad \text{(A49)}$$

where C_{22}, C_{24}, C_{42}, C_{44}, f_1, f_2, f_3, and f_4 are functions of the coordinates (a_2, a_4) and in addition f_1 and f_3 are quadratic in $\dot{a}_2$ and $\dot{a}_4$. When initial conditions on the coordinates and their time derivatives are specified, this set of equations

may be numerically integrated with respect to time, thereby determining successive values of a_2, a_4, $\dot{a}_2$, and $\dot{a}_4$. At each time step the various properties of the motion are readily calculable from the equations given.

While the methods described are quite general, one limitation deserves mentioning. The shape defining equation (A5) is too general for the description of motion defined by a single term velocity potential. For such a simple velocity potential one of the coordinates (a_2 or a_4) must be restricted to the value zero (and never change), because the set of equations (A49) otherwise became linearly dependent.

APPENDIX VIII

In extending Plesset's treatment of small oscillations of a uniformly charged liquid drop about the spherical shape[A 8], consideration is restricted to a single shape defining parameter α_2. Following Plesset's nomenclature, the surface is defined by the relation:

$$r = R_0 (1+\alpha_0+\alpha_2 P_2) \tag{A50}$$

where α_0 is fixed by volume preservation and P_2 is the second order Legendre polynomial.

For small oscillations the maximum excursion of α_2 and its time derivatives are very small. The surface and Coulomb energies will be calculated to order α_2^4. To fourth order in α_2 conservation of volume fixes α_0 at

$$\alpha_0 = \tfrac{1}{5}\alpha_2^2 - \tfrac{2}{105}\alpha_2^3 + o\alpha_2^4$$

The relative surface energy may be expressed

$$B_s = \frac{1}{4\pi R_0^2}\int_0^{2\pi} d\varphi \int_0^{\pi} r^2 \left[1 + \left(\frac{1}{r}\frac{dr}{d\theta}\right)^2\right]^{\frac{1}{2}} \sin\theta d\theta \tag{A51}$$

Retaining terms of order α_2^4, equation (A51) after integration over φ becomes:

$$B_c = \tfrac{1}{2}\int_0^{\pi} \left\{\left(1 - \tfrac{1}{5}\alpha_2^2 - \tfrac{2}{105}\alpha_2^3 + \alpha_2 P_2\right)^2 + \tfrac{1}{2}\alpha_2^2\left(\frac{\partial P_2}{\partial\theta}\right)^2 - \tfrac{1}{8}\alpha_2^4\left(\frac{\partial P_2}{\partial\theta}\right)^4\right\} \sin\theta d\theta$$

[A 8] M. S. Plesset, Am. Journal of Physics, 9,1 (1941).

Straight forward integration using the orthoginality properties of Legendre functions yields

$$B_s = 1 + \tfrac{2}{5}\alpha_2^2 - \tfrac{4}{105}\alpha_2^3 - \tfrac{83}{175}\alpha_2^4 \qquad \text{(A52)}$$

The relative Coulomb energy may be expressed as

$$B_c = \frac{15}{32\pi^2 R_o^5}\int_0^{2\pi}\int_0^{\pi}\int_0^{r(\Theta)} V(r_1,\Theta_1)\; r_1 dr_1 \sin\Theta_1 d\Theta_1 d\varphi_1$$

where

$$V(r_1,\Theta_1) = \int_0^{2\pi}\int_0^{\pi}\int_0^{r_1(\Theta_1)} \frac{r_2 dr_2 \sin\Theta_2 d\Theta_2 d\varphi_2}{r_{12}}$$

$$\frac{1}{r_{12}} = \sum_{K=0}^{\infty} \frac{r_2^K}{r_1^{K+1}} P_K(\cos\Theta_{12}) \qquad r_2 < r_1$$

$$= \sum_{K=0}^{\infty} \frac{r_1^K}{r_2^{K+1}} P_K(\cos\Theta_{12}) \qquad r_2 > r_1$$

Θ_{12} is the angle between the vectors $\underline{r}_1$ and $\underline{r}_2$.

The indicated integrations are tedious, requiring use of the orthoginality and other properties of the Legendre polynomials, and finally yield to order α_2^4:

$$B_c = 1 - \tfrac{1}{5}\alpha_2^2 - \tfrac{4}{105}\alpha_2^3 - \tfrac{334}{1225}\alpha_2^4 \qquad \text{(A53)}$$

The expression for B_s equation (A52), and B_c equation (A53), agree through order α_2^2 with Plesset[18] and through

order α_2^3 with those obtained by Nix[A9] (who did not include terms of higher order). The relative deformation energy is:

$$\xi = \tfrac{2}{5}\alpha_2^2 - \tfrac{4}{105}\alpha_2^3 - \tfrac{83}{175}\alpha_2^4 + 2X\left\{ - \tfrac{1}{5}\alpha_2^2 - \tfrac{4}{105}\alpha_2^3 + \tfrac{334}{1225}\alpha_2^4 \right\} \qquad \text{(A54)}$$

Because the handling of the expression for kinetic energy differs appreciably from that of Plesset[A8], more detail will be given. Again, the expression will be developed to order α_2^4 (actually $\dot{\alpha}_2^2\alpha_2^2$).

The implicit equation of the surface may be written as:

$$f = r - R_o\left(1 - \tfrac{1}{5}\alpha_2^2 - \tfrac{2}{105}\alpha_2^3 + \alpha_2 P_2\right) = 0 \qquad \text{(A55)}$$

The assumed form of the velocity potential is

$$-\varphi = \dot{\alpha}_2\left\{\beta_2 r^2 P_2 + \beta_4 \frac{r^4}{R_o^2} P_4 + \beta_6 \frac{r^6}{R_o^4} P_6\right\}$$

where the "$\dot{\alpha}_2$" dependence is explicitly stated and β_2, β_4, and β_6 are to be expressed to order 2 in α_2. The velocity becomes

$$\underline{v} = -\text{grad}\varphi = \dot{\alpha}_2\left\{\left(2r\beta_2 P_2 + 4\frac{r^3}{R_o^2}\beta_4 P_4 + 6\frac{r^5}{R^4}\beta_6 P_6\right)\underline{i}_r\right.$$

$$\left. + \left(r\frac{\partial P_2}{\partial\Theta}\beta_2 + \frac{r^3}{R_o^2}\frac{\partial P_4}{\partial\Theta}\beta_4 + \frac{r^5}{R_o^4}\frac{\partial P_6}{\partial\Theta}\beta_6\right)\underline{i}_\Theta\right\} \qquad \text{(A56)}$$

In applying the boundary condition:

$$\frac{Df}{Dt} = \frac{\partial f}{\partial t} + \underline{v}\cdot\text{grad } f = 0$$

[A9] J. R. Nix, "The Normal Mode of Oscillation of a Uniformly Charged Drop About Its Saddle-Point Shape", UCRL-16786 (1966), unpublished.

a common factor "$\dot{\alpha}_2 R_0$" appears in all terms and is factored out. Performing the indicated operations on equations (A55) and (A56), with appropriate substitutions for "r" from equation (A50), an expression with only angular dependence (from the P_2, P_4, and P_6) is obtained. Correct through order α_2^2 the resulting boundary condition equation can be satisfied by assuming β's of the form:

$$\beta_2 = A + B\alpha_2 + C\alpha_2^2$$

$$\beta_4 = D\alpha_2 + E\alpha_2^2$$

$$\beta_6 = F\alpha_2^2$$

This algebra yields:

$$\beta_2 = \tfrac{1}{2} + \tfrac{1}{14}\alpha_2 + \tfrac{54}{245}\alpha_2^2$$

$$\beta_4 = -\tfrac{27}{70}\alpha_2 + \tfrac{459}{2695}\alpha_2^2$$

$$\beta_6 = \tfrac{45}{77}\alpha_2^2$$

The relative kinetic energy is

$$B_K = \frac{1}{8\pi R_0^5}\int_0^{2\pi} d\varphi \int_0^{\pi} \sin\theta d\theta \int_0^{r(\theta)} v^2 r^2 dr$$

where the time dependence in α_2 is expressed in terms of T_0 (equation (A39)). Inserting the expressions for v^2 from equation (A56) and the expression for $r(\theta)$ from (A50), the integration gives, to order $\dot{\alpha}_2^2\alpha_2^2$:

$$B_K = \tfrac{1}{4}\dot{\alpha}_2^2\left\{\beta_2^2\left(\tfrac{4}{5} + \tfrac{4}{5}\alpha_2 + \tfrac{44}{35}\alpha_2^2\right) + \tfrac{144}{35}\alpha_2\beta_2\beta_4 + \tfrac{8}{9}\beta_4^2\right\}$$

Inserting the relations for β_2 and β_4, the kinetic energy to order $\dot{\alpha}_2^2\alpha_2^2$ is:

$$B_K = \dot{\alpha}_2^2 \left\{ \frac{1}{20} + \frac{9}{140}\alpha_2 - \frac{87}{2450}\alpha_2^2 \right\} \qquad \text{(A57)}$$

Plesset's expression[4,8] for the kinetic energy contains only the first term in the brackets because of his assumption that the drop shape could be assumed undeformed (in his kinetic energy treatment).

For the derived expressions for the deformation energy and kinetic energy the equations of motion would be

$$\frac{d}{dt}\frac{\partial B_K}{\partial \dot{\alpha}_2} - \frac{\partial B_K}{\partial \alpha_2} + \frac{\partial \xi}{\partial \alpha_2} =$$

$$\ddot{\alpha}_2 \left\{ \frac{1}{10} + \frac{9}{70}\alpha_2 - \frac{87}{1225}\alpha_2^2 \right\} + \dot{\alpha}_2^2 \left\{ \frac{9}{140} - \frac{87}{1225}\alpha_2 \right\}$$

$$+ \left\{ \frac{4}{5}\alpha_2 - \frac{4}{35}\alpha_2^2 - \frac{332}{175}\alpha_2^3 \right\} + 2X \left\{ -\frac{2}{5}\alpha_2 - \frac{4}{35}\alpha_2^2 + \frac{1336}{1225}\alpha_2^3 \right\} = 0 \qquad \text{(A58)}$$

For motion sufficiently near spherical such that terms of order α_2^3 (or $\dot{\alpha}_2^2\alpha_2$) are neglible compared to terms of order α_2^2 (or $\dot{\alpha}_2^2$), the expressions for the kinetic and deformation energies are simply quadratic in $\dot{\alpha}_2^2$ and α_2^2, respectively. In this case the equation of motion is that of a simple harmonic oscillator, i. e.,

$$\frac{1}{10}\ddot{\alpha}_2 + \frac{4}{5}(1-X)\,\alpha_2 = 0$$

For such a motion the period of the sinusoidal oscillation of a_2 ($\dot{a}_2$ and $\ddot{a}_2$) will be

$$\tau_{SHM} = \frac{2\pi}{\sqrt{8(1-X)}}\,T_o \qquad \text{(A59)}$$

where T_0 is the "basic" time unit ($=0.482_4 \times 10^{-22} A^{\frac{1}{3}}$ seconds).

In the small oscillation limitation a simple relation exists between the coordinates α_2 used in this Appendix and the coordinate a_2 used in the main text. Equation (A50) may be expressed in terms of z and ρ_0 and compared with the corresponding equation in terms of a_2 ($a_4=0$), i.e., $\rho_0^2 = a_2 z^2 + c$. Equating the coefficients of the z^2 terms gives

$$\alpha_2 = \frac{a_2+1}{3} \tag{A60}$$

which has a first time derivative:

$$\dot{\alpha}_2 = \tfrac{1}{3}\, \dot{a}_2 \tag{A61}$$

These approximate relations are valid only when α_2^3 is negligible compared to α_2^2. Under this restriction the motion will still be sinusoidal in terms of a_2 with the same period as given by equation (A59). The kinetic energy will be:

$$B_K = \tfrac{1}{180}\, \dot{a}_2^2 \tag{A62}$$

For larger amplitude excursions the motion will differ from simple harmonic motion, and be described by equation (A58). The second term of equation (A58) contains a feature which is seldom encountered in oscillator problems. For the liquid drop problem the spherical configuration is the equilibrium position. At this position there is no force generated by the potential energy, and in the commonly encountered oscillator problems there would be zero acceleration. However, in the present case because the "mass" appearing in the kinetic energy expression is dependent linearly on the position coordinate, there appears a force in the equation of

motion which is proportional to the velocity squared. In the standard treatments of small oscillations, the mass is independent of the position coordinate and such non-vanishing terms do not arise for the equilibrium position.

This property of the liquid drop should also appear in the more general description where the two coordinates a_2 and a_4 are used to define the shape. That is, there should exist an acceleration for non-vanishing velocities at the spherical shape in the a_2-a_4 description of the problem. The situation is somewhat more complicated because the equations of motion (equation (21) in main text) are a coupled set involving both $\ddot{a}_2$ and $\ddot{a}_4$, and a non-vanishing $\dot{a}_2$ with $\dot{a}_4=0$ should cause both accelerations to be non-zero (even at spherical).

APPENDIX IX

For purposes of numerically checking the theory a two term velocity potential was used. Let this velocity potential be written:

$$-\varphi = \beta_2 r^2 P_2(\cos\theta) + \beta_4 r^4 P_4(\cos\theta)$$

$$= \beta_2 r^2\left(\tfrac{3}{2}\cos^2\theta - \tfrac{1}{2}\right) + \beta_4 r^4\left(\tfrac{35}{8}\cos^4\theta - \tfrac{15}{4}\cos^2\theta + \tfrac{3}{8}\right)$$

$$= \beta_2\left\{\tfrac{3}{2}z^2 - \tfrac{1}{2}(\rho^2+z^2)\right\} + \beta_4\left\{\tfrac{35}{8}z^4 - \tfrac{15}{4}z^2(\rho^2+z^2) + \tfrac{3}{8}(\rho^2+z^2)^2\right\}$$

$$= \beta_2\left\{z^2 - \tfrac{1}{2}\rho^2\right\} + \beta_4\left\{z^4 - 3z^2\rho^2 + \tfrac{3}{8}\rho^4\right\}$$

Thus in the notation of the main text

$$H_1 = z^2 - \tfrac{1}{2}\rho^2$$

$$H_2 = z^4 - 3z^2\rho^2 + \tfrac{3}{8}\rho^4$$

The components of the vector velocity are

$$v_z = \sum_{n=1}^{2} \beta_n \frac{\partial H_n}{\partial z} = 2z\beta_2 + (4z^3 - 6z\rho^2)\,\beta_4 \qquad \text{(A63)}$$

and

$$v_\rho = \sum_{n=1}^{2} \beta_n \frac{\partial H_n}{\partial \rho} = -\rho\beta_2 + \left(-6z^2\rho + \tfrac{3}{2}\rho^3\right)\beta_4 \qquad \text{(A64)}$$

The expressions for $\frac{\partial H_n}{\partial z}$ and $\frac{\partial H_n}{\partial \rho}$ are evaluated at the surface (i.e., set $\rho=\rho_0$) before insertion in the equation for GSI

(equation (17) of the main text), giving,

$$GSI = G_{11}\beta_2^2+(G_{12}+G_{21})\beta_2\beta_4+G_{22}\beta_4^2+G_1\beta_2+G_2\beta_4+G_0 \qquad (A65)$$

where

$$G_{11} = \int_{-z_0}^{z_0}\left\{\rho_0^2\left(\frac{\partial H_1}{\partial\rho}\right)^2-2\rho_0(a_2z+2a_4z^3)\frac{\partial H_1}{\partial\rho}\frac{\partial H_1}{\partial z}+(a_2z+2a_4z^3)^2\left(\frac{\partial H_1}{\partial z}\right)^2\right\}dz$$

$$= 2\left\{c^2z_0+2a_2cz_0^3+\tfrac{1}{5}(9a_2^2+10a_4c)z_0^5+\tfrac{30}{7}a_2a_4z_0^7+\tfrac{25}{9}a_4^2z_0^9\right\}$$

$$G_{12} = 2\left\{-\tfrac{3}{2}c^3z_0+\left(2c^2-\tfrac{11}{2}a_2c^2\right)z_0^3+\tfrac{1}{5}\left(20a_2c-\tfrac{57}{2}a_4c^2-\tfrac{81}{2}a_2^2c\right)z_0^5\right.$$
$$+\tfrac{1}{7}\left(28a_4c-129a_2a_4c+22a_2^2-\tfrac{51}{2}a_2^3\right)z_0^7$$
$$+\tfrac{1}{9}\left(-\tfrac{201}{2}a_4^2c+68a_2a_4-\tfrac{225}{2}a_2^2a_4\right)z_0^9$$
$$\left.+\tfrac{1}{11}\left(-\tfrac{321}{2}a_2a_4^2+54a_4^2\right)z_0^{11}-\tfrac{147}{26}a_4^3z_0^{13}\right\}$$

$$G_{21} = 2\left\{-\tfrac{3}{2}c^3z_0+\left(2c^2-\tfrac{7}{2}a_2c^2\right)z_0^3+\tfrac{1}{5}\left(36a_2c-\tfrac{33}{2}a_4c^2-\tfrac{57}{2}a_2^2c\right)z_0^5\right.$$
$$+\tfrac{1}{7}\left(60a_4c-93a_2a_4c+38a_2^2-\tfrac{39}{2}a_2^3\right)z_0^7$$
$$+\tfrac{1}{9}\left(-\tfrac{153}{2}a_4^2c+116a_2a_4-\tfrac{177}{2}a_2^2a_4\right)z_0^9$$
$$\left.+\tfrac{1}{11}\left(-\tfrac{261}{2}a_2a_4^2+86a_4^2\right)z_0^{11}-\tfrac{123}{26}a_4^3z_0^{13}\right\}$$

$$G_{22} = 2\left\{\tfrac{9}{4}c^4z_0+(9a_2c^3-6c^3)z_0^3+\tfrac{1}{5}\left(45a_4c^3-138a_2c^2+\tfrac{207}{2}a_2^2c^2+36c^2\right)z_0^5\right.$$
$$+\tfrac{1}{7}\left(-222a_4c^2+333a_2a_4c^2-270a_2^2c+120a_2c+135a_2^3c\right)z_0^7$$
$$+\tfrac{1}{9}\left(\tfrac{531}{8}a_4^2c^2-804a_2a_4c+168a_4c+603a_2^2a_4c+100a_2^2-150a_2^3+\tfrac{225}{2}a_2^4\right)z_0^9$$
$$+\tfrac{1}{11}\left(873a_2a_4^2c-582a_4^2c+280a_2a_4-630a_2^2a_4+315a_2^3a_4\right)z_0^{11}$$
$$+\tfrac{1}{13}\left(405a_4^3c-858a_2a_4^2+\tfrac{1287}{2}a_2^2a_4^2+196a_4^2\right)z_0^{13}$$
$$\left.+\tfrac{1}{8}\left(-126a_4^3+189a_2a_4^3\right)z_0^{15}+\tfrac{729}{88}a_4^4z_0^{17}\right\}$$

$$G_1 = \int_{-z_0}^{z_0} \left\{ \dot{a}_4 \left(z^4 + \frac{\partial c}{\partial a_4} \right) + \dot{a}_2 \left(z^2 + \frac{\partial c}{\partial a_4} \right) \right\} \left\{ -\rho_0 \frac{\partial H_1}{\partial \rho} + (a_2 z + 2a_4 z^3) \frac{\partial H_1}{\partial z} \right\} dz$$

$$= 2\dot{a}_4 \left\{ c \frac{\partial c}{\partial a_4} z_0 + a_2 \frac{\partial c}{\partial a_4} z_0^3 + \left(a_4 \frac{\partial c}{\partial a_4} + \frac{1}{5} c \right) z_0^5 + \frac{3}{7} a_2 z_0^7 + \frac{5}{9} a_4 z_0^9 \right\}$$

$$+ 2\dot{a}_2 \left\{ c \frac{\partial c}{\partial a_2} z_0 + \left(a_2 \frac{\partial c}{\partial a_4} + \frac{1}{3} c \right) z_0^3 + \left(a_4 \frac{\partial c}{\partial a_2} + \frac{3}{5} a_2 \right) z_0^5 + \frac{5}{7} a_4 z_0^7 \right\}$$

$$G_2 = 2\dot{a}_4 \left\{ -\frac{3}{2} c^2 \frac{\partial c}{\partial a_4} z_0 + (-3a_2 + 2) c \frac{\partial c}{\partial a_4} z_0^3 \right.$$

$$+ \left(-5a_4 c \frac{\partial c}{\partial a_4} + 2a_2 \frac{\partial c}{\partial a_4} - \frac{3}{2} a_2^2 \frac{\partial c}{\partial a_4} - \frac{3}{10} c^2 \right) z_0^5$$

$$+ \left(2a_4 \frac{\partial c}{\partial a_4} - 3a_2 a_4 \frac{\partial c}{\partial a_4} - \frac{9}{7} a_2 c + \frac{6}{7} c \right) z_0^7$$

$$+ \left(-\frac{3}{2} a_4^2 \frac{\partial c}{\partial a_4} - \frac{5}{3} a_4 c + \frac{10}{9} a_2 - \frac{5}{6} a_2^2 \right) z_0^9$$

$$\left. + \frac{1}{11} \left(14a_4 - 21 a_2 a_4 \right) z_0^{11} - \frac{27}{26} a_4^2 z_0^{13} \right\}$$

$$+ 2\dot{a}_2 \left\{ -\frac{3}{2} c^2 \frac{\partial c}{\partial a_2} z_0 + \left(-3a_2 c \frac{\partial c}{\partial a_2} + 2c \frac{\partial c}{\partial a_2} - \frac{1}{2} c^2 \right) z_0^3 \right.$$

$$+ \left(-3a_4 c \frac{\partial c}{\partial a_2} + 2a_2 \frac{\partial c}{\partial a_2} - \frac{9}{2} a_2^2 \frac{\partial c}{\partial a_2} - \frac{9}{5} a_2 c + \frac{6}{5} c \right) z_0^5$$

$$+ \left(2a_4 \frac{\partial c}{\partial a_2} - 3a_2 a_4 \frac{\partial c}{\partial a_2} - \frac{15}{7} a_4 c + \frac{10}{7} a_2 - \frac{15}{14} a_2^2 \right) z_0^7$$

$$\left. + \left(-\frac{3}{2} a_4^2 \frac{\partial c}{\partial a_2} + \frac{14}{9} a_4 - \frac{7}{3} a_2 a_4 \right) z_0^9 - \frac{27}{22} a_4^2 z_0^{11} \right\}$$

$$G_0 = 2\left\{\left[\frac{\dot{a}_4^2}{4}\left(\frac{\partial c}{\partial a_4}\right)^2 + \frac{\dot{a}_2\dot{a}_4}{2}\frac{\partial c}{\partial a_2}\frac{\partial c}{\partial a_4} + \frac{\dot{a}_2^2}{4}\left(\frac{\partial c}{\partial a_2}\right)^2\right]z_0\right.$$

$$+ \frac{1}{8}\left(\dot{a}_2\dot{a}_4\frac{\partial c}{\partial a_4} + \dot{a}_2^2\frac{\partial c}{\partial a_2}\right)z_0^3$$

$$\left. + \frac{1}{20}\left(\dot{a}_2^2 + 2\dot{a}_2\dot{a}_4\frac{\partial c}{\partial a_2} + 2\dot{a}_4^2\frac{\partial c}{\partial a_4}\right)z_0^5 + \frac{1}{14}\dot{a}_2\dot{a}_4 z_0^7 + \frac{1}{36}\dot{a}_4^2 z_0^9\right\}$$

After taking the partial derivatives of equation (A65), the resulting set of equations are solved for β_2 and β_4 in terms of G_{11}, G_{12}, G_{21}, G_{22}, G_1, and G_2, yielding:

$$\beta_2 = \frac{2G_1G_{22} - G_2(G_{12} + G_{21})}{(G_{12}+G_{21})^2 - 4G_{11}G_{22}} \qquad \text{(A66)}$$

$$\beta_4 = \frac{2G_2G_{11} - G_1(G_{12}+G_{21})}{(G_{12}+G_{12})^2 - 4G_{11}G_{22}} \qquad \text{(A67)}$$

Equations (A66) and (A67) are the functional forms of the β's which are now used in the kinetic energy and equations of motion. The partial derivatives of the β's with respect to $\dot{a}_2$, $\dot{a}_4$, a_2 and a_4 are obtained from equations (A66) and (A67), using the expressions given above for G_{11}, G_{12}, G_{21}, G_{22}, G_1, and G_2, and equations (A11) for

$$\frac{\partial c}{\partial a_2}, \frac{\partial c}{\partial a_4}, \frac{\partial z_0}{\partial a_2} \text{ and } \frac{\partial z_0}{\partial a_4}.$$

The functional expressions for the three $I_{2_i,2_j}$ integrals which appear in the kinetic energy and equations of motion are also extracted in the routine manner, yielding:

$$I_{22} = \tfrac{1}{8}c^2 z_o + \tfrac{1}{3}\left(c + \tfrac{1}{4}a_2 c\right) z_o^3 + \tfrac{1}{5}\left(a_2 + \tfrac{1}{4}a_4 c + \tfrac{1}{8}a_2^2\right) z_o^5$$

$$+ \tfrac{1}{7}\left(a_4 + \tfrac{1}{4}a_2 a_4\right) z_o^7 + \tfrac{1}{72}a_4^2 z_o^9$$

$$I_{24} = \tfrac{1}{4}c^3 z_o + \tfrac{1}{4}\left(a_2 c^2 - 6c^2\right) z_o^3 + \tfrac{1}{5}\left(\tfrac{3}{4}a_4 c^2 + \tfrac{3}{4}a_2^2 c - 9a_2 c + 4c\right) z_o^5$$

$$+ \tfrac{1}{7}\left(\tfrac{1}{4}a_2^3 + \tfrac{3}{8}a_2 a_4 c - 9a_4 c - \tfrac{9}{2}a_2^2 + 4a_2\right) z_o^7$$

$$+ \tfrac{1}{9}\left(\tfrac{3}{4}a_2^2 a_4 + \tfrac{3}{4}a_4^2 c - 9a_2 a_4 + 4a_4\right) z_o^9$$

$$+ \tfrac{1}{11}\left(\tfrac{3}{4}a_2 a_4^2 - \tfrac{9}{2}a_4^2\right) z_o^{11} + \tfrac{1}{52}a_4^3 z_o^{13}$$

$$I_{44} = \tfrac{9}{64}c^4 z_o + \left(\tfrac{3}{16}a_2 c^3 + \tfrac{1}{2}c^3\right) z_o^3 + \tfrac{1}{5}\left(\tfrac{9}{16}a_4 c^3 + \tfrac{27}{32}a_2^2 c^2 + \tfrac{9}{2}a_2 c^2 - \tfrac{3}{2}c^2\right) z_o^5$$

$$+ \tfrac{1}{7}\left(\tfrac{9}{16}a_2^3 c + \tfrac{27}{16}a_2 a_4 c^2 + \tfrac{9}{2}a_2^2 c - \tfrac{9}{2}a_4 c^2 - 3a_2 c + 4c\right) z_o^7$$

$$+ \tfrac{1}{9}\left(\tfrac{9}{64}a_2^4 + \tfrac{27}{16}a_2^2 a_4 c + \tfrac{27}{32}a_4^2 c^2 + \tfrac{3}{2}a_2^3 + 9a_2 a_4 c - 3a_4 c - \tfrac{3}{2}a_2^2 + 4a_2\right) z_o^9$$

$$+ \tfrac{1}{11}\left(\tfrac{9}{16}a_2^3 a_4 + \tfrac{27}{16}a_2 a_4^2 c + \tfrac{9}{2}a_2^2 a_4 + \tfrac{9}{2}a_4^2 c - 3a_2 a_4 + 4a_4\right) z_o^{11}$$

$$+ \tfrac{1}{13}\left(\tfrac{27}{32}a_2^2 a_4^2 + \tfrac{9}{16}a_4^3 c + \tfrac{9}{2}a_2 a_4^2 - \tfrac{3}{2}a_4^2\right) z_o^{13}$$

$$+ \tfrac{1}{5}\left(\tfrac{3}{16}a_2 a_4^3 + \tfrac{1}{2}a_4^3\right) z_o^{15} \quad \tfrac{9}{1088}a_4^4 z_o^{17}$$

The required partial derivatives were obtained from these expressions in the usual manner.

APPENDIX X

The interval determining and self testing features of the Runge-Kutta subroutine provide a balance between the desired accuracy and time required for an integration. The user provides an initial and final value of the independent variable (time); an initial interval size; and an accuracy specification (ACC). Integration is performed twice over the same time interval; the first time in a single step, and the second time in two steps. The difference (DIF) in the two integrations (for each dependent variable) is compared with the accuracy specification (ACC). If DIF $< \frac{ACC}{4}$, then the integration is considered successful, and the time interval doubled before the next integration. If $\frac{ACC}{4} \leq DIF \leq ACC$, the integration is also successful, but the time interval is unchanged. If DIF > ACC, the integration failed, the time interval is cut in half, and an integration attempt is repeated for the shorter time interval. In using the subroutine no difficulties were encountered by unlimited cutting of the time interval. After each successful integration the independent variable is increased by the amount of the time interval. Should the difference in the final and current value of the independent variable be less than the time interval, the time interval is reduced to exactly this difference (so that the final integration is completed at the value specified as "final" for the independent variable).